2014

Holographic Sensors: Three-Dimensional Analyte-Sensitive Nanostructures and Their Applications

Ali K. Yetisen
University of Cambridge

Izabela Naydenova
Technological University Dublin, izabela.naydenova@tudublin.ie

Fernando da Cruz Vasconcellos
University of Cambridge

Jeffrey Blyth
University of Cambridge

Christopher R. R. Lowe
University of Cambridge

Recommended Citation

Ali K Yetisen, Izabela Naydenova, Fernando da Cruz Vasconcellos, Jeffrey Blyth, Christopher R Lowe, Holographic sensors: three-dimensional analyte-sensitive nanostructures and their applications, *Chemical Reviews* 2014 Oct 11;114(20):10654-96.

CHEMICAL REVIEWS

Review

pubs.acs.org/CR

Holographic Sensors: Three-Dimensional Analyte-Sensitive Nanostructures and Their Applications

Ali K. Yetisen,*[,†] Izabela Naydenova,[‡] Fernando da Cruz Vasconcellos,[†] Jeffrey Blyth,[†] and Christopher R. Lowe[†]

[†]Department of Chemical Engineering and Biotechnology, University of Cambridge, Tennis Court Road, Cambridge CB2 1QT, United Kingdom

[‡]Centre for Industrial and Engineering Optics, School of Physics, College of Sciences and Health, Dublin Institute of Technology, Dublin 8, Ireland

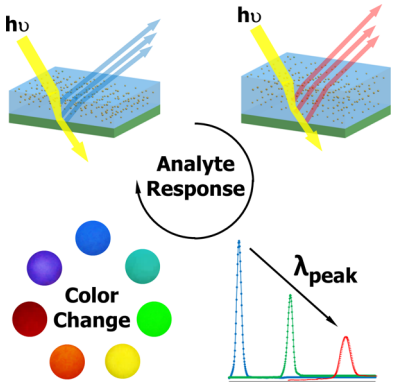

CONTENTS

1. INTRODUCTION

Holographic sensors are analytical devices that systematically diffract narrow-band light in the ultraviolet to near-infrared range for application in the detection and quantification of analytes and/or physical parameters.[1] They can be functionalized with analyte-responsive materials to construct highly

Received: February 26, 2014

   dx.doi.org/10.1021/cr500116a | Chem. Rev. XXXX, XXX, XXX−XXX

sensitive optical sensors for use in testing, where a visual readout, fast turnaround time, and reversibility are needed.[2] Holography allows fabrication of disposable sensors that are lightweight for miniaturization and multiplexing purposes.[3] Holographic sensors offer three capabilities on a single analytical device: (i) label-free analyte-responsive polymer, (ii) real-time, reversible quantification of the external stimuli, and (iii) three-dimensional visual image display. Their potential applications range from in vitro diagnostics to optical security devices (Figure 1).

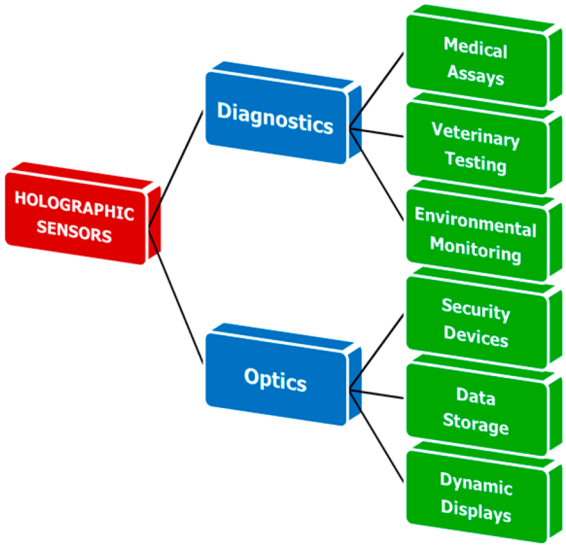

Figure 1. Potential applications of holographic sensors.

The purpose of this Review is to (1) establish a theoretical framework for holographic sensing, (2) define terminology in holographic sensing, (3) demonstrate how holographic sensing fits into the existing body of sensing mechanisms, and (4) highlight gaps in the previous research. The goals of this Review include integrating and summarizing what is known in holographic sensing, identifying where the major questions remain, and enabling others in the field to be able to replicate the existing experimental setups for fabricating and interrogating holographic sensors. The scope of this Review consists of the state-of-the-art techniques for producing holographic sensors, and their potential applications in research, industrial settings, and among the public. This Review mainly covers holographic sensor research from 1990 to 2014, but also refers to earlier literature for historical developments and fundamentals. It also discusses the need for optical sensing, the fundamentals of holography, the origins of holographic sensors, holographic media and materials, fabrication techniques, sensing capabilities, readouts, and relevant theoretical studies. This Review concludes with a discussion of gaps within the field and how to overcome the perceived limitations of holographic sensors. Fundamentally different technologies, often confused with holography, such as stereo photography, Victorian "Pepper's Ghost" effect,[4] and liquid crystal display,[5] are not covered in this Review.

In this work, "diffraction" refers to scattering of the light wave propagating through a 3D periodic structure with alternating layers of differing refractive index (RI). The term specular "reflection" refers to the change in direction of a wavefront (laser or white light) at an interface between two different media, resulting in return of the wavefront into the medium from which it originated without changing its spectral characteristics, where the angle of incidence equals the angle of reflection. The term "refraction" refers to the change in direction of a wave due to a variation in the refractive index of its transmission medium, where the phase velocity of the wave is altered, while the frequency remains constant.

1.1. The Need for Responsive Optical Devices

Optical sensors with characteristics that respond to external stimuli can provide fast, quantitative, visual colorimetric readouts in real-time and in a reversible manner.[6] They may consist of bioactive recognition elements that can transmit the signal through a transducer, preferably embedded within the system. Such responsive photonic structures may have applications in chemical, biological, and physical sensors incorporating 3D images, dynamic displays, inks, paints, and optically active components for security applications.[7]

Optical devices can be used in medical diagnostics, veterinary screening, environmental monitoring, pharmaceutical bioassays, optomechanical sensing, and security applications.[8] An application area of importance is medical diagnostics and biochemical sensing such as detection and/or quantitation of chemical analytes and cells.[9] Applications in biology and biochemistry include sensitive biomolecular detection, real-time monitoring of enzyme activity, and cell morphology research.[8] Additionally, due to their immunity from electromagnetic interference and capability of remote sensing, optical sensors have advantages over established laboratory techniques such as electrochemical sensing. Optical sensors can also find applications in implantable devices that are required to stay in the body for a long time, where continuous monitoring and biocompatibility are required.

Optical sensors can play a substantial role in environmental monitoring by detection and/or quantification of environmental stressors. Worldwide appreciation of the importance of the environmental monitoring has been increasing in recent years. To control air and water quality, the main contaminants have been identified, and strict regulations on their concentrations have been imposed.[10] However, most of the existing methods of environmental monitoring are costly and time-consuming. Moreover, sampling and analytical techniques are limited. There is a need for accurate, long-term monitoring of environmental contaminants using sensors that can be operated on site.[11] For each contaminant, a portable sensor is sought that can provide rapid response, ease of operation for field use, and a sufficiently sensitive detection limit.

Responsive optical sensors can potentially be used for the advanced authentication of original documents, banknotes, and high-value products. However, the existing static methods involving the use of embossed holograms offer limited protection against fake labels or patterns because they can be easily copied, although exact copies are difficult to produce.[12] Recent investigations have indicated that counterfeited goods worldwide accounted for sales of $651 bn, as of 2013, where the drugs and electronics markets combined constituted 56% of this amount.[13] For example, an important problem is counterfeit medications. In an investigation carried out in Southeast Asia, 38% of artesunate (an antimalarial drug) purchased were found to be fake, containing no active ingredient.[14] Similarly, 41% of the drugs in the Nigerian market were found to be fake.[15] Counterfeited antibiotics also play a significant role in the increase of bacterial resistance.[16]

dx.doi.org/10.1021/cr500116a | *Chem. Rev.* XXXX, XXX, XXX−XXX

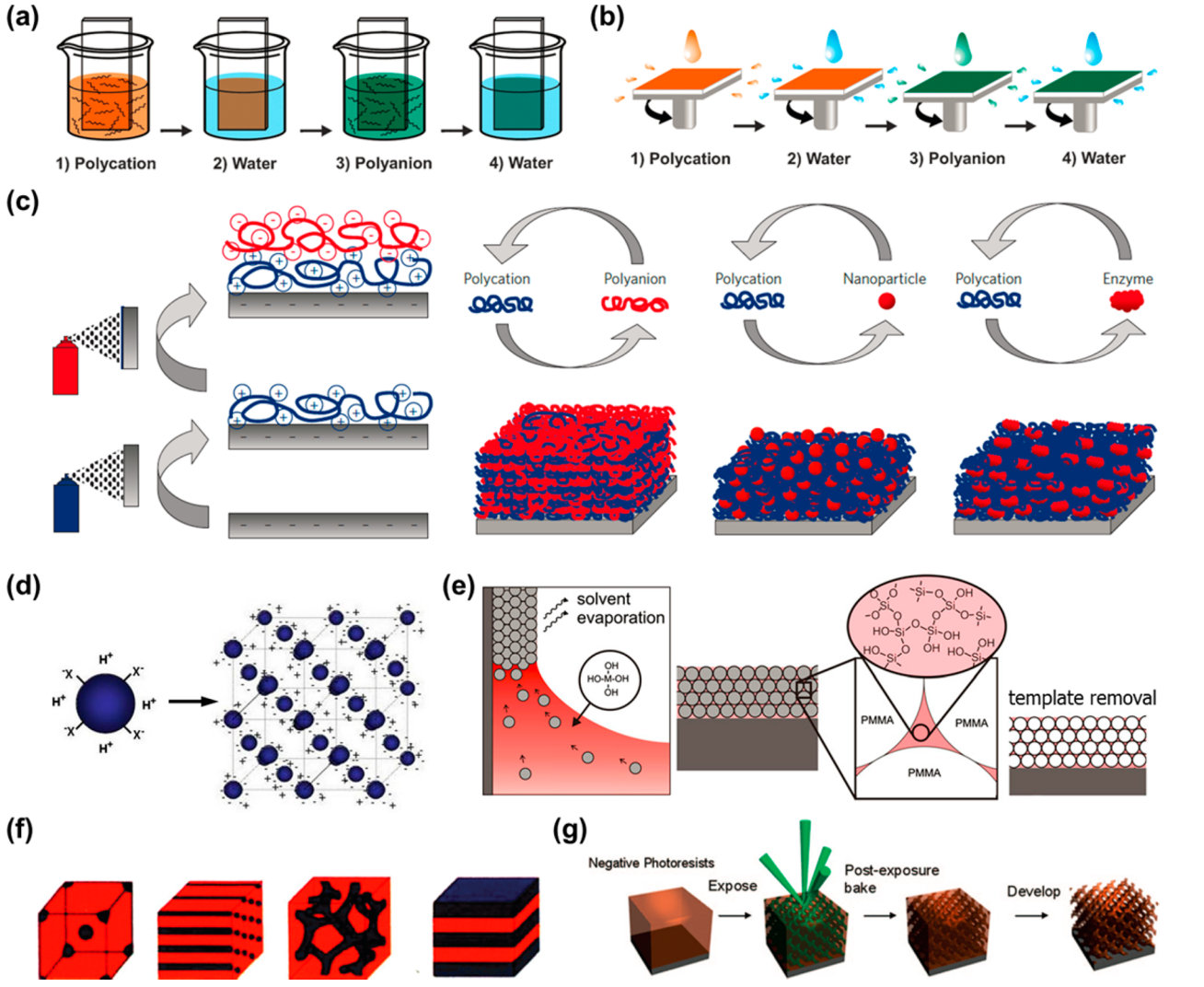

Figure 2. Fabrication of photonic sensing materials. (a) Dipping layer-by-layer assembly. (b) Spin-assisted layer-by-layer assembly. Reprinted with permission from ref 21a. Copyright 2012 Royal Society of Chemistry. (c) Layer-by-layer deposition by alternating spray coating of polyanions and -cations. The films may incorporate functional materials such as nanoparticles and enyzmes. Reprinted with permission from ref 32. Copyright 2009 Macmillan Publishers Ltd. (d) Electrostatic repulsion-driven self-assembly of monodisperse, charged polystyrene particles into crystalline colloidal arrays (CCAs) with face-centered cubic (FCC) or body-centered cubic (BCC) lattices. Reprinted with permission from ref 33. Copyright 2002 Springer. (e) Fabrication of inverse opal thin films. This process involves colloidal self-assembly, matrix infiltration, and template removal. Reprinted with permission from ref 34. Copyright 2010 National Academy of Sciences of the U.S.A. (f) Self-assembly of diblock copolymers into spherical, cylindrical, gyroid, and lamellar geometries. Reprinted with permission from ref 35. Copyright 1995 American Chemical Society. (g) Interference lithography involves an optical setup with four interfering beams, forming diamond-like interference patterns. Reprinted with permission from ref 36. Copyright 2010 American Chemical Society.

For example, adulterated low-potency drugs prevent a patient completing a course of treatment, resulting in microorganisms that are immune to antibiotic treatment. If a low-potency counterfeit drug is involved, completion of a course of treatment cannot be fully effective. To prevent such counterfeit products, technically advanced recognition mechanisms are required. Optically responsive sensors can provide solutions in the identification of genuine products. For example, the information can be invisible to the user until a chemical stimulant, pressure, or heat is applied to the optical sensor, which in turn displays a verifying image.

Another potential application area of optical devices is display technologies and wavelength filters. Such optical elements can be used in active color units of flexible display media and video displays for use in 3D teleconferencing.[17] In taking advantage of their wavelength tunability, optical sensors can be used in smart windows that can change color and/or transparency when subjected to a specific wavelength or electric field, resulting in significant reduction of energy consumption in buildings.[18] Alternatively, such optical devices can find military applications, involving camouflage of military vehicles or personnel using dynamically changing color and patterns adapted to the surroundings. Responsive photonic structures can also contribute to rewritable electronic paper and E-ink technology, which require the use of electrophoresis of absorbing or scattering materials in suspension between electrode panels that limits the production of colored images to switchable bichromic states.[19] The incorporation of responsive photonic structures can improve the color range and the resolution of the images.

dx.doi.org/10.1021/cr500116a | *Chem. Rev.* XXXX, XXX, XXX−XXX

1.2. Responsive Photonic Structures

Photonic band gap materials work through the periodic modulation of the refractive index in a dielectric material, which allows filtering out and diffracting specific wavelengths. These optical nanostructures allow the control and the manipulation of the propagation of light. Their applications include reflective coatings on lenses, pigments in paints and inks, waveguides, reflective mirrors in laser cavities, and other optical components.[20] Over the last two decades, several top-down and bottom-up fabrication techniques have been developed: layer-by-layer stacking,[21] electrochemical etching,[22] electron-beam lithography,[23] laser beam scanning chemical vapor deposition,[24] as well as the self-assembly of crystalline colloidal arrays (CCAs),[6−8,25] inverse opals,[26] block copolymers,[27] and nanocomposites[28] (Figure 2). Bottom-up approaches involve self-assembly of preformed building blocks such as monodisperse colloidal particles into periodic gratings. Such building blocks may be silica (SiO_2), polystyrene microspheres, or block copolymers. The symmetry, lattice constant of the crystal, and the index of refraction contrast can be finely controlled to fabricate ordered photonic structures. To achieve visible-light Bragg diffraction, colloidal particles with diameters from 100 nm to 1 μm may be used to form one-, two-, and three-dimensional photonic structures.[29] Additionally, block copolymers can also self-assemble into periodic regions through phase separation of chemically different polymer blocks.[30] Other attractive materials for constructing photonic nanostructures might include plasmonic nanoparticles, graphene, graphite, carbon nanotubes, and silicon nanopillars.[31]

Sensors that combined the optical properties of photonic crystals and quantum dots were also developed.[37] These hybrid sensors were fabricated from two-dimensional photonic crystal slabs that operated at visible wavelengths, and their leaky modes were overlapped with the absorption and emission wavelengths of the quantum dots. An enhancement in fluorescent emission was produced due to a combination of high-intensity near fields and coherent scattering based on leaky eigenmodes of the photonic crystal. This approach allowed the enhancement of the fluorescence intensity by a factor of up to 108 as compared to quantum dots on an unpatterned surface.[37] Another approach involved the fabrication of slotted photonic crystal waveguides and cavities to support resonant modes in air.[38] The geometry of the photonic crystal allowed detection of refractive index changes in a given analyte due to an overlap between the optical mode and the analyte. This study reported photonic crystal sensors with a sensitivity of 1500 nm/refractive index units and a *Q*-factor of up to 50 000.[38]

Label-free optical sensors based on asymmetric Fano resonances in plasmonic nanoholes have also been developed.[39] This sensing mechanism utilized extraordinary light transmission phenomena through high-quality factor (~200) subradiant dark modes. The detection of a single monolayer of biomolecules (antibody capture) by eye was possible. The improved sensitivity was attributed to suppression of the radiative losses due to the structural quality of the devices and the subradiant nature of the resonances. The sensor had a figure of merit (FOM) of 162 in wavelength units for the (+1,0) subradiant dark mode as compared to the theoretically estimated upper limits (FOM = 108) of the prism coupled surface plasmon sensors.[39] Plasmonic metamaterials were also proposed for the label-free detection of single molecules.[40] For example, the feasibility of singular visible-light nano-optics, which employed the attributes of plasmonic field enhancement and peculiarities of the phase light, has been demonstrated. The plasmonic metamaterials exhibited topologically protected zero reflection yielding nearby phase changes, which were employed to improve the sensitivity of detectors based on plasmon resonances.[40]

Self-assembled photonic structures allow higher efficiencies and lower costs in comparison to microfabricated photonic devices. Stimulus-responsive materials were often incorporated into these photonic devices to induce a change in their lattice constants or spatial symmetry of the crystalline array, or refractive index contrast. For example, refractive index tunable oxide materials such as WO_3, VO_2, and $BaTiO_3$ have been used in these matrixes to produce photonic structures that are sensitive to electric fields or temperature.[41] When the colloidal arrays were infiltrated with liquid crystals, they also showed responsive photonic characteristics upon applying an external electric field or increasing the temperature of the device.[42] There are numerous fabrication strategies and materials developed to build responsive photonic structures for applications in sensing chemical stimuli, temperature variation, light, electrical and magnetic fields, and mechanical forces.[43] However, the challenges included limited tunability, slow turnaround times, and hysteresis. Another critical challenge in the field has been the narrow response range due to the limited external stimuli-induced changes in the lattice spacing or the index of refraction. However, to overcome these challenges, polymer chemistries, new building blocks, and new tuning mechanisms constantly evolve to create practical devices.

These methods offer potential feasibility for producing optical devices. However, there is limited control over the material selection, patterning ability, angle of diffraction, three-dimensional organization of diffracting elements, and manufacturing. To overcome these limitations, alternative generic approaches are explored with capabilities of incorporating 3D imaging and flexibility in fabrication.[6−8]

1.3. Holography

Holography is a technique that allows three-dimensional imaging of an object or digital information through the use of a light-sensitive material and laser light, or micro- or nanofabrication techniques.[1b,44] In 1865, James Clerk Maxwell had proposed theoretically that light is an electromagnetic wave, which led to the conclusion that light is an electromagnetic disturbance propagated through the field according to electromagnetic laws.[45] In 1869, Wilhelm Zenker theoretically showed that an incident light wave propagating toward a mirror produces a reflected wave, which combines with the incident wave to form an interference pattern with a half-wavelength separation between fringes.[46] In 1887, Heinrich Hertz experimentally demonstrated the existence of electromagnetic waves by showing that radio waves were consistent with Maxwell's theory.[47] He produced radio standing waves by reflection from a zinc plate. When a monochromatic wave is reflected at a surface, the reflected wave and the incident wave combine to form standing waves, which oscillate up and down without propagation (Figure 3a). The distance between successive nodes or antinodes is equal to one-half of the wavelength (Figure 3b). Within the standing wave, there is no oscillation at the nodes, while at the antinodes, the oscillations are of maximum amplitude.

It was not until the 1890s that Zenker's idea to record standing waves of light was experimentally demonstrated by

dx.doi.org/10.1021/cr500116a | *Chem. Rev.* XXXX, XXX, XXX−XXX

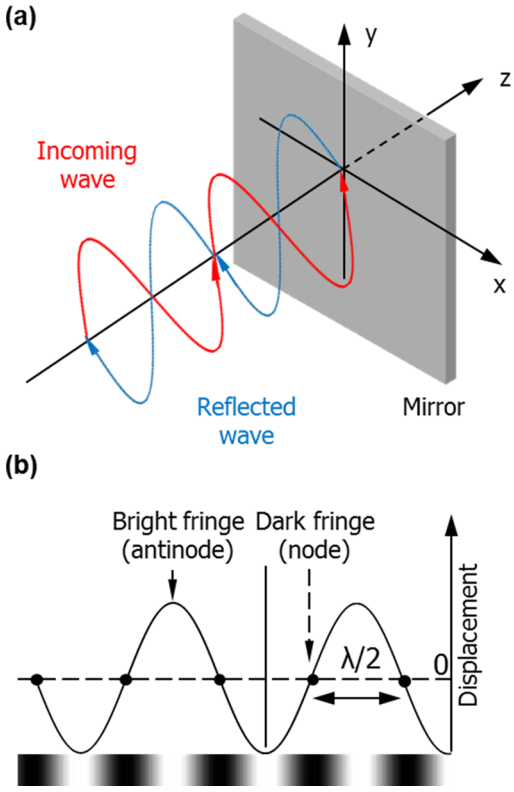

Figure 3. Principle of a (a) standing wave and (b) its corresponding interference pattern.

Otto Wiener.[48] In his experimental setup, a carbon arc light, entering a darkroom through a slit, was passed through a prism to filter out the red region of the spectrum. Using a lens, the orthochromatic light was focused and directed perpendicularly to a 2° tilted 20 nm-thick collodion-process-based photographic plate backed by a leveled silver mirror. After the photographic plate was developed and printed, a periodic standing wave pattern was observed under high magnification. While the antinodes appear bright, the nodes, containing no light, look dark (Figure 3b). Additionally, the wave might change phase upon reflection and influence the absolute position of the nodes and antinodes. In 1891, Gabriel Lippmann developed a method of reproducing colors photographically based on the phenomenon of interference.[49] In his experiment, he projected an image onto a photographic recording medium. The image was produced by shining light through a photographic plate backed by a mirror of liquid mercury, which reflected the light back through the medium to create standing waves. Lippmann was able to obtain a latent image (defined as an invisible image before development) produced by the standing waves that are characterized by a series of interference maxima and minima. After the recording medium was developed, fixed, and dried through the traditional photographic methods, planes of reduced silver particles, whose spacing was a function of the wavelength of the light used during recording, were obtained. Upon illumination with white light source, the diffracted light from the silver planes gave rise to a colored projection of the recorded image.[50] In the 1910s, X-ray microscopy for recreating the image from the diffraction pattern of a crystal lattice structure was studied by a number of scientists, including W. L. Bragg, H. Broersch, and F. Zernike.[44a,51] In the 1920s, Mieczysław Wolfke reported that if an X-ray diffraction pattern is illuminated with a monochromatic light, a new diffraction pattern, which is identical to the image of the object, is formed.[52] In the late 1940s, Dennis Gabor (1900−1979), while trying to improve the resolution of the electron microscope by overcoming the spherical aberration of the lenses, found that by adding a coherent background as a phase reference, the original object wave was contained in an interferogram, which he later called a hologram.[53] By establishing the principle of holography, he received the Nobel Prize in Physics in 1971. The term hologram was coined from the Greek words *holos*, meaning "whole", and *gramma*, meaning "message". However, the stability of the interference required (i) mechanical and thermal stability of the interferometer used in the holographic recording, and (ii) the coherence of the light source.

Another milestone in the realization of holography was the invention of laser (light amplification by stimulated emission of radiation). The foundations of laser theory were established in the early years of the twentieth century by Planck and Einstein.[54] In the early 1960s, lasers (optical oscillators) were developed to produce monochromatic light.[55] After the development of the laser, Yuri Denisyuk of the former Soviet Union, and Emmett Leith and Juris Upatnieks in the United States recorded independently the first optical holograms in 1962.[56] These early holograms were based on silver−halide chemistry. Transmission holograms, originally made by Leith and Upatnieks, require monochromatic light (usually a laser) to view the image, otherwise viewing in white light causes severe chromatic aberrations, whereas holograms produced by Denisyuk's method can be viewed in light of a broad spectral range.[44b] Denisyuk was originally inspired by the method of color photography developed by Lippmann. In particular, Denisyuk holograms have been applied in a wide variety of fields including artistic displays, optical elements, holographic data storage, and analytical devices. Later, in 1969, Stephen Benton, then working for Polaroid Inc., invented a method of avoiding chromatic aberration in transmission holograms.[57] Such holograms are known as Benton or Rainbow holograms. Because these holograms could be the templates for the production of stampable or embossable holograms, the Benton hologram has become the foundation of more than 99% of all of the hologram industry worldwide, particularly for security applications, for example, credit cards and bank notes, as well as the cheapest end of the market as diffractive foils for decoration. Embossable holograms diffract a rainbow of colors upon illumination with white light, but it is obviously not possible to emboss monochromatic reflection gratings that run inside the polymer matrix approximately parallel with the plane of the film. However, monochromatic reflection gratings can be embossed by patterning the film surface with a microscopic structure reminiscent of an array of Aztec pyramids.[58] Figure 4a illustrates the theoretical profile of the Aztec grating, and Figure 4b shows the SEM image of an actual grating in photoresist produced by the interference of three coherent laser beams.

Holographic gratings can be fabricated using various geometries, which involve the use of multiple collimated laser beams. The first step in recording holograms involves passing a single laser beam through a beam splitter, which divides the beam into two beams. The first beam is expanded by a lens, and redirected by mirrors (front surface) onto an object. The light that is scattered back falls onto a recording medium. Meanwhile, the second beam, expanded by a lens, travels directly onto the recording medium. The interference of the two mutually coherent beams creates constructive (antinodes)

dx.doi.org/10.1021/cr500116a | *Chem. Rev.* XXXX, XXX, XXX−XXX

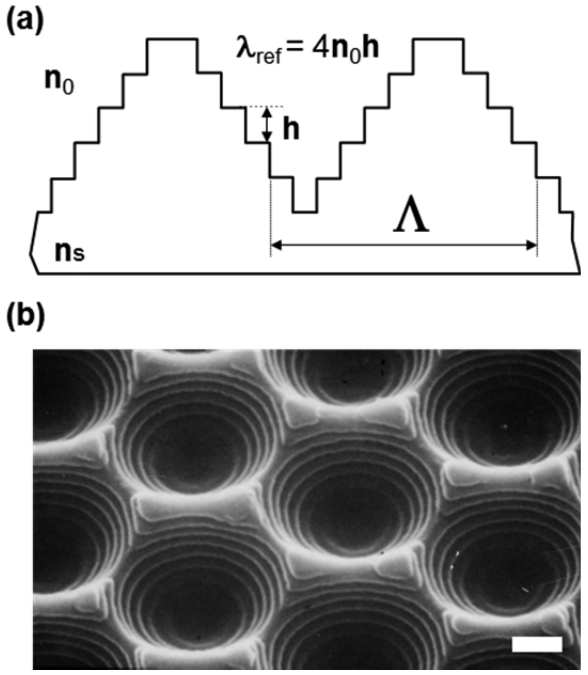

Figure 4. Aztec gratings diffract monochromatic color. (a) The principle of operation. The diffracted light (λ_{ref}) is governed by the step height (h) and the refractive index of the incident medium (n_0). (b) SEM image of the grating. Scale bar = 1 μm. Reprinted with permission from ref 58c. Copyright 2008 Society of Photo Optical Instrumentation Engineers.

and destructive (nodes) interferences, which are recorded in the photosensitive medium, and thus all optical information about the object is coded in the diffraction field produced by the hologram at the reconstruction stage.[59] The contrast of these fringes is determined by the coherence length of the laser light, the state of polarization of the two recording beams, and the ratio of their intensities. The coherence length is the propagation distance l over which a wave maintains a degree of coherence, and it is defined as $L = \lambda_0^2/\Delta\lambda$, where λ_0 is the mean wavelength and $\Delta\lambda$ the bandwidth of the radiation. High-contrast interference fringes, with fringe visibility (V), are required to record efficient holograms. To obtain interference fringes with good visibility, the optical path difference between the object and the reference beams must be small as compared to the coherence length of the radiation.[60]

The visibility of the fringes in an interferometer with an optical path difference less than the coherence length is determined by the spatial coherence μ, which depends on the size of the light source, the angle φ between the planes of polarization (orientation of the wave oscillations) of the two interfering waves, and the ratio (R) of the intensities of the reference (I_R) and the object (I_O) waves $R = I_O/I_R$.[61] The plane of polarization of the wave is defined as the plane containing the propagation vector and the electric field vector. It is the plane of oscillation of the electric field. The visibility of the interference fringes is given by

$$V = \mu\frac{2\sqrt{I_R I_O}}{I_R + I_O}\cos\varphi = 2\mu\frac{\sqrt{R}}{1+R}\cos\varphi \quad (1)$$

The maximum contrast of 1 is achieved when the intensities of the two recording beams are equal (the parameter R is equal to 1) and the two beams have the same linear polarization (cos φ is equal to 1). This equation states that the intensities of the reference and the object beams must be balanced to get good visibility of the fringes, and the state of polarization of the two recording beams must be considered. In Denisyuk reflection mode, the reference to object beam ratio is typically 4:3; however, this ratio is 3:1 in transmission hologram recording.[44b] The distance between the recorded interference fringes is normally smaller than the wavelength of visible light. Holographic recording introduces changes in the optical properties of the recording material. An amplitude hologram is recorded when the interference pattern created by the object and the reference beams is recorded as variation of the absorption coefficient of the recording material. A phase hologram is created when the holographic recording leads to variation of the refractive index or the thickness of the hologram. Holographic gratings can also be recorded in Denisyuk reflection mode. Reflection holograms are typically formed by passing an expanded beam of laser light through the recording plate to illuminate an object on the other side of the plate. Light from the object is then reflected back through the plate and interferes with the light passing through the plate for the first time, thus forming standing waves of light, which are recorded as "holographic nanoparticle spacings" running roughly parallel with the plane of the recording medium (Figure 5a).[44b,62] Reflection holograms allow the image to be viewed by the observer on the same side as the one from which the hologram is illuminated. However, a transmission hologram is viewed by the observer from the side opposite to the one of the illuminating light. In practice, virtually all commercial transmission holograms such as those used on bank cards, bank notes, and security labels have a reflective metallic backing, which allows viewing transmission holograms on the same side of the observer. Holographers, however, exclude these types of holograms from their meaning of the term "reflection" hologram.

When the hologram is illuminated with a white light source, the recorded nanoparticle spacings act as Bragg mirrors. The diffracted light forms an image of the original object used during laser exposure. This diffracted light from the periodic gratings results in a narrow-band spectral peak determined by the wavelength of the laser light and the angle between the two recording beams. The holographic diffraction is governed by Bragg's law (Figure 5b):

$$\lambda_{peak} = 2n_0\Lambda\sin(\theta) \quad (2)$$

where λ_{peak} is the wavelength of the first-order diffracted light at the maximum intensity in vacuo, n_0 is the effective index of refraction of the recording medium, Λ is the spacing between the two consecutive recorded nanoparticle-based layers (constant parameter), and θ is the Bragg angle, which is determined by the recording geometry.

1.4. The Origins of Holographic Sensors and Their Advantages

During the 1970s, those practicing the art of making reflection or "Denisyuk" holograms found that they always had one particular problem. While this type of hologram was able to give a reconstructed image using just a point source of white light, the color of the fully processed image was always in a shorter wavelength than that from the original laser used to make it.[64] Typically, the laser wavelength would be red at 632.8 nm (HeNe laser) and the reconstructed image would be green (~500−570 nm). The recording plates and films (gelatin and

dx.doi.org/10.1021/cr500116a | Chem. Rev. XXXX, XXX, XXX−XXX

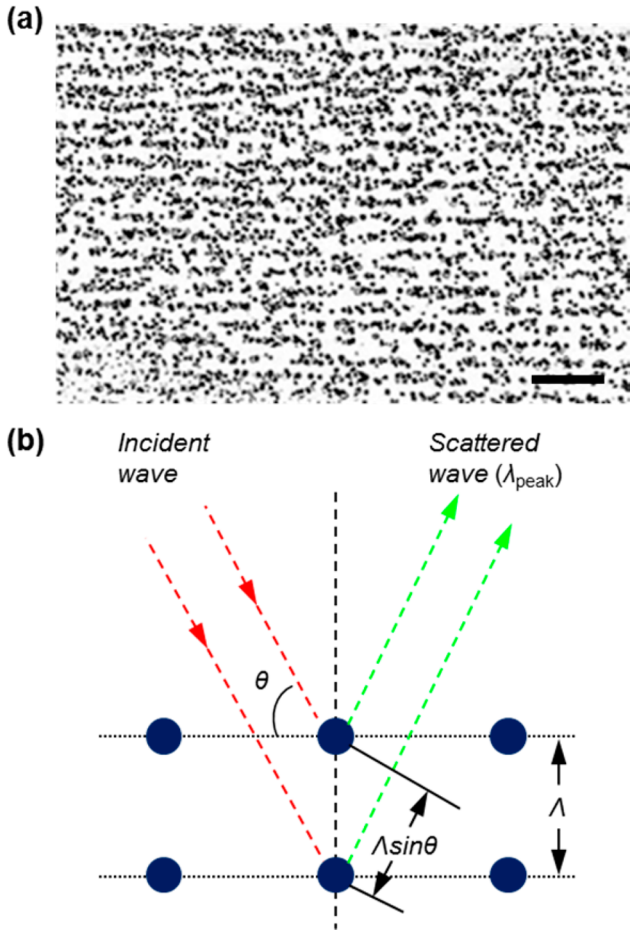

Figure 5. Electron micrographs of hologram cross sections and satisfaction of Bragg condition. (a) A Lippmann phase hologram recorded in a Holotest 8E75HD plate using a HeNe laser operated at 632.8 nm. Hologram diffraction efficiency is ~50%. Scale bar = 1 μm. Reprinted with permission from ref 63. Copyright 1988 The Optical Society of America. (b) The two electromagnetic waves are scattered off two different atoms in a crystalline structure and undergo constructive interference in accordance with Bragg's law.

silver halide (AgBr) emulsions) used to make such holograms at that time were based on the same principles as those employed in traditional photography. However, the conventional method used in photography was to remove all of the unexposed AgBr grains and to leave a photographic image consisting only of developed silver metal (Ag^0) grains (nanoparticles). Using this technique to develop the hologram meant that the bright fringes were recorded as Ag^0 grains while the undeveloped AgBr grains in the dark fringe areas were removed using conventional "hypo" (sodium thiosulfate) solution. In this process, the gelatin that once held the undeveloped AgBr shrank as it dried, and the remaining Ag^0 nanoparticle spacings moved closer together. Thus, the nanoparticle spacings in the finished hologram selected out a shorter wavelength from the white light source to reconstruct the image.

From the earliest holography experiments, it was appreciated that greater diffraction efficiency was obtained by turning the Ag^0 nanoparticles back into transparent AgBr or AgI crystals. Therefore, in a process known as bleaching, various oxidizing agents were used with bromide or iodide ions in solution or alternatively dilute alcoholic solutions of iodine, or less frequently bromine was used. However, a breakthrough occurred when it was discovered that still greater diffraction efficiency was obtained by not actually removing the AgBr crystals in the dark fringes with the traditional hypo solution in the first place.[65] The reason for this may seem initially counterintuitive, but it is thought that the unexposed AgBr crystals in the dark fringes act as seeding centers for the newly formed AgBr to settle on. In effect, as the Ag^0 nanoparticle in the bright fringes is reoxidized to AgBr, it is more energetically favorable for it to move over onto the neighboring AgBr in the dark fringes than to form a new AgBr crystal.[65] This then had the major advantage of not only using all of the original AgBr present in the plate, but also of preventing most of the shrinkage, which had been causing the "blue shift" in the reconstruction wavelengths.

In the late 1970s, it was also then realized by those preparing art holograms that so-called "pseudo-color" effects could be obtained by using several exposures of one scene with the 633 nm beam from a helium−neon (HeNe) laser with each exposure only illuminating different sections of that scene. Notably, before each exposure, the moisture level (and pH) of the whole gelatin emulsion was changed by removing the plate and treating it in a triethanolamine (3−35%, v/v) bath. This resulted in having a color range from orange to violet when the finished hologram was replayed under a white spotlight.[66] Specifically, the thickness of the emulsion can be varied through preswelling or preshrinking before laser exposure. The fact that a gelatin film's thickness is greatly affected by its moisture content led to the first use of moisture control techniques.[66c,67] In the 1980s, systematic studies were reported to optimize emulsion pretreatment to obtain a range of display wavelengths using a fixed exposure wavelength.[64,68] This was accomplished by varying the emulsion thickness, tuned through imbibition with multiple solutions that either swelled or contracted the emulsion, during the various fixed wavelength exposures. These studies investigated tuning the degree of swelling of the polymer through the use of solvents (e.g., water and propan-2-ol) and proteolytic enzymes (e.g., collagenase, maxatase, trypsin, and papain) to cleave various bonds in the emulsion structure.[69]

It was not until the 1990s that the tuning technique in holography led to the realization that reflection holograms could be used as sensors to quantify humidity and chemical substances.[1a,70] Any physical or chemical stimulant that changes the lattice spacing (recorded nanoparticle spacings) (Λ) or the effective index of refraction (n_0) of the film will cause observable changes in the wavelength (λ_{peak}) or its profile (color distribution), or the intensity (brightness) of the hologram. The intensity output by the hologram depends on the modulation depth of the recorded refractive index pattern (dark and bright fringes), as well as the number of cycles of refractive index change present in the polymer matrix. Swelling in the polymer matrix increases the distance between nanoparticle spacings and produces a shift of the diffracted light to longer wavelengths, whereas shrinkage in the matrix shifts the diffracted light to shorter wavelengths. The diffraction grating acts as a reporter, whose characteristics are determined by the physical changes of the polymer matrix. For example, when the polymer matrix is functionalized with a receptor comonomer that has the ability to draw or expel aqueous solution from the system upon binding, the degree of swelling indirectly represents the concentration of the target analyte. The resulting change in the wavelength can be monitored by

dx.doi.org/10.1021/cr500116a | Chem. Rev. XXXX, XXX, XXX−XXX

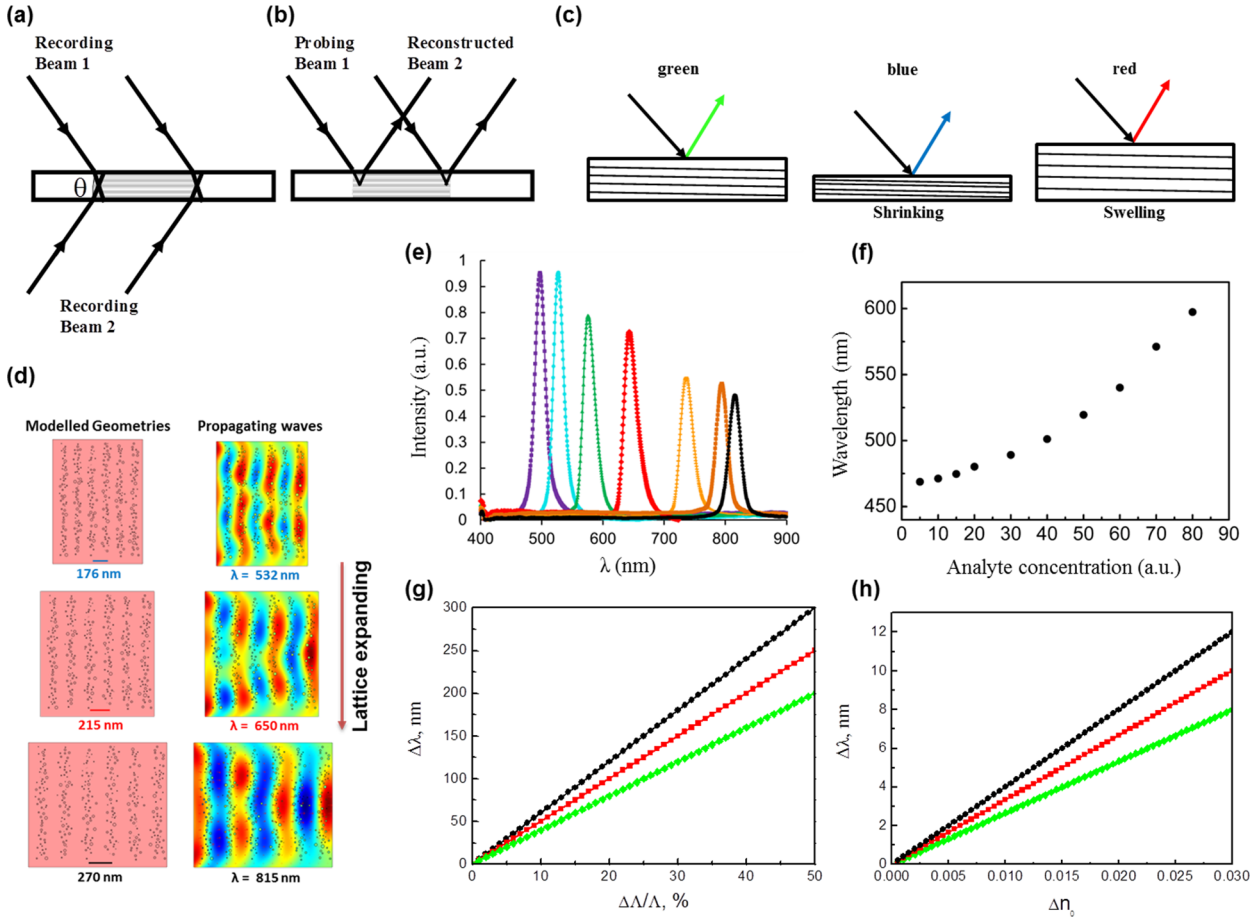

Figure 6. Principle of operation of a sensor based on a "Denisyuk" reflection hologram. (a) Recording and (b) probing of a reflection holographic grating. Reprinted with permission from ref 71. Copyright 2011 Nova Science Publishers, Inc. (c) A dimensional alteration such as shrinkage or swelling of the photopolymer layer leads to a change of the recorded lattice spacing and a change of the wavelength of the diffracted light in a specific direction. (d) Model geometries and the simulated transmission spectra for different holographic sensors with lattice constants of 176, 215, and 270 nm. Reprinted with permission from ref 72. Copyright 2014 Royal Society of Chemistry. (e) A typical analyte response of a reflection hologram. Reprinted with permission from ref 73. Copyright 2014 Wiley-VCH Verlag GmbH&Co. KGaA, Weinheim. (f) Bragg shift due to a change in the concentration of an analyte. Reprinted with permission from ref 74. Copyright 2009 Elsevier. (g) Dependence of the peak wavelength shift on the relative dimensional change. The initial wavelength is 600 nm (●), 500 nm (red ■), 400 nm (green ◆). Reprinted with permission from ref 71. Copyright 2011 Nova Science Publishers, Inc. (h) Dependence of the peak wavelength shift on the average refractive index change. Reprinted with permission from ref 71. Copyright 2011 Nova Science Publishers, Inc.

eye or a spectrophotometer, and the sensor can be calibrated on the basis of the inputted physical or chemical change. The same sensor can be visually or optically interpreted to quantify the tested analytes or physical changes of interest. This is in contrast to the case of the transmission hologram, where the holographic nanoparticle spacings run roughly perpendicular to the plane of the plate, and therefore any thickness changes will not greatly change the replay wavelengths. In transmission holograms, the changes resulting from the exposure to the target analyte have to be registered by a photodetector. These are changes in the brightness of the hologram and the direction of the diffracted beam.

1.5. Fundamentals of Holographic Sensors

A holographic sensor is capable of changing its optical characteristics when it is exposed to a target analyte. For example, as a result of interacting with the analyte, the sensor could change its diffraction efficiency and/or its spectral response, which in visual terms translates into a change of its brightness and/or color. The diffraction efficiency of a hologram is defined as the ratio of the intensities of the diffracted beam divided by the incident beam. It is a quantitative measure of the brightness of the hologram. Depending on the recording geometry and what optical property of the material is changed during holographic recording, different holograms can be produced and used in the design of the sensor; these are volume or surface relief holograms, transmission or reflection holograms, and phase or amplitude holograms.[61] In the following section, analysis of volume phase transmission and reflection holograms for use as holographic sensors is provided.[71]

1.5.1. Sensors Based on Reflection Holograms. The main advantage of the sensors based on reflection holograms is that they can be used as visual indicators as they can operate in normal room light. Figure 6a,b shows the recording and probing of a "Denisyuk" reflection hologram. In this geometry of recording, two coherent beams are incident from the opposite sides of the recording medium. For recording of a simple diffraction grating, two plane waves are normally used, and the spatial period of the grating is determined by Bragg's law (eq 2).

dx.doi.org/10.1021/cr500116a | Chem. Rev. XXXX, XXX, XXX−XXX

When the beams have the same incident angles, the interference fringes are parallel to the surface of the recording medium, and an unslanted reflection grating is recorded. The incident angles of the two recording beams can also be different, and, in this case, the fringes will be at an angle with respect to the recording medium surface, and the recorded grating will be slanted. In either case, the fringes always run along the bisector line of the angle between the two beams.

In reflection holograms, the most conveniently observed optical characteristic in the presence of an analyte is the change in wavelength of the diffracted light. When illuminated with a light source that has a broad spectral range, a reflection hologram diffracts selectively, and operates as a wavelength filter. The maximum diffraction efficiency occurs at a wavelength that satisfies eq 2.

As can be seen from eq 2, an alteration in either the average refractive index or the lattice spacing will cause a change in the diffracted light wavelength. It is assumed that the hologram is a thick volume hologram and the angle of observation is constant. To quantify how the different factors will influence the spectral peak position in diffracted light, we differentiate eq 2:

$$\frac{\Delta\lambda}{\lambda} = \frac{\Delta n_0}{n_0} + \frac{\Delta\Lambda}{\Lambda} + \cot\theta\Delta\theta \tag{3}$$

where $\Delta\lambda$, Δn_0, $\Delta\Lambda$, and $\Delta\theta$ are the changes in wavelength, effective refractive index, grating period, and the Bragg angle, respectively. Using eq 3, the influence of these changes on the wavelength of the diffracted light can be modeled.

1.5.1.a. Swelling/Shrinking Dynamics. Any dimensional change of the layer in which the hologram is recorded, such as swelling or shrinking, leads to a change of the recorded lattice spacing, and thus alters the spectral response of the hologram (Figure 6c,d). A typical spectral response of a holographic sensor is seen in Figure 6e, and its shift with the change of analyte concentration is shown in Figure 6f. A simulation assuming that the average refractive index and probe angle remain constant reveals that practically achievable alterations in dimensions could produce large changes in the peak wavelength (Figure 6g). For example, a dimensional change of 30%, which is normally achieved in an acrylamide-based photopolymer hologram, would produce over a 100 nm shift depending on the initial peak wavelength.

1.5.1.b. Effective Refractive Index. The effective refractive index of the layer, in which the hologram is recorded, can change due to absorption of the target analyte. Assuming that the only property that is changing is the effective refractive index, the resulting change in the diffracted light peak wavelength can be calculated using eq 2. Figure 6h illustrates that a significant change in effective refractive index is required to spectroscopically measure a change in the peak wavelength. The initial effective refractive index in these simulations was 1.5. For example, an effective refractive index change of 15×10^{-3} is required to achieve a 6 nm shift in wavelength for a sensor originally operating at 600 nm wavelength. With the grating period and probe angle remaining constant, it is preferable to record the hologram at a longer wavelength. The absolute change in the peak wavelength ($\Delta\lambda$) can be increased by choosing materials with lower initial effective refractive index (n). Materials with higher porosity will have lower effective refractive index. Moreover, for detection of larger size analytes, it would be preferable to use materials with larger pore size, which will allow the analyte to diffuse easily into the polymer layer.

Both a dimensional change and an effective refractive index change can simultaneously contribute to the alteration in the spectral response of the hologram. For example, in gelatin-based sensors, the effective refractive index decreases as the sensor absorbs water and swells; thus the two factors make opposing contributions to the spectral shift. However, one of the factors is generally the main contributor. For example, in humidity sensors recorded in acrylamide-based photopolymer studied at relative humidity up to 80%, the main factor is the swelling of the polymer due to absorption of moisture.[74]

1.5.2. Sensors Based on Transmission Holograms. Holographic sensors based on transmission holograms require a spectrometer or an optical power meter for readouts. After exposure to the target analyte, both the diffraction efficiency and the wavelength of maximum diffraction efficiency can change at constant angle of interrogation. Figure 7a illustrates the beam geometry for recording of a simple transmission hologram. For simplicity, the two recording beams are assumed to be plane waves. In this case, the recorded hologram is a transmission diffraction grating.

The recorded holographic grating will reconstruct one of the recording beams when it is probed by the other (Figure 7b). The period of the diffraction grating, Λ, is determined by the angle between the two recording beams, θ, and the recording wavelength, λ, by

$$2\Lambda \sin\theta = \lambda \tag{4}$$

The diffraction efficiency (η), defined as the ratio of the diffracted and the incident beam intensities,[75] of a volume phase transmission hologram is determined by

$$\eta = \sin^2\left(\frac{\pi n_1 d}{\lambda \cos\theta}\right) \tag{5}$$

where n_1 is the refractive index modulation (the difference between the refractive indices in exposed and unexposed areas), d is the thickness of the hologram, λ is the wavelength of the probe beam that is used to measure the diffraction efficiency, and θ is the Bragg angle. To analyze the effect of the different parameters on the sensitivity of the holographic sensor, we differentiate eq 5:

$$\frac{\Delta\eta}{\eta} = \left|\frac{2}{\tan\left(\frac{\pi n_1 d}{\lambda\cos\theta}\right)}\frac{\pi n_1 d}{\lambda\cos\theta}\right|\left(\frac{\Delta n_1}{n_1} + \frac{\Delta d}{d} - \frac{\Delta\lambda}{\lambda} + \tan\theta\Delta\theta\right) \tag{6}$$

The two physical parameters of the hologram that are influenced by the presence of the analyte are the refractive index modulation and the thickness of the hologram. A change in either of these two parameters will cause a change in the diffraction efficiency of the grating. In addition, a dimensional change of the layer such as swelling/shrinking could change the Bragg angle and the wavelength at which maximum diffraction efficiency is observed.

1.5.2.a. Refractive Index Modulation. To understand the influence of the change in refractive index on sensor's response, it is assumed that the thickness of the hologram, the probe wavelength, and the Bragg angle remain constant. The probe

dx.doi.org/10.1021/cr500116a | Chem. Rev. XXXX, XXX, XXX−XXX

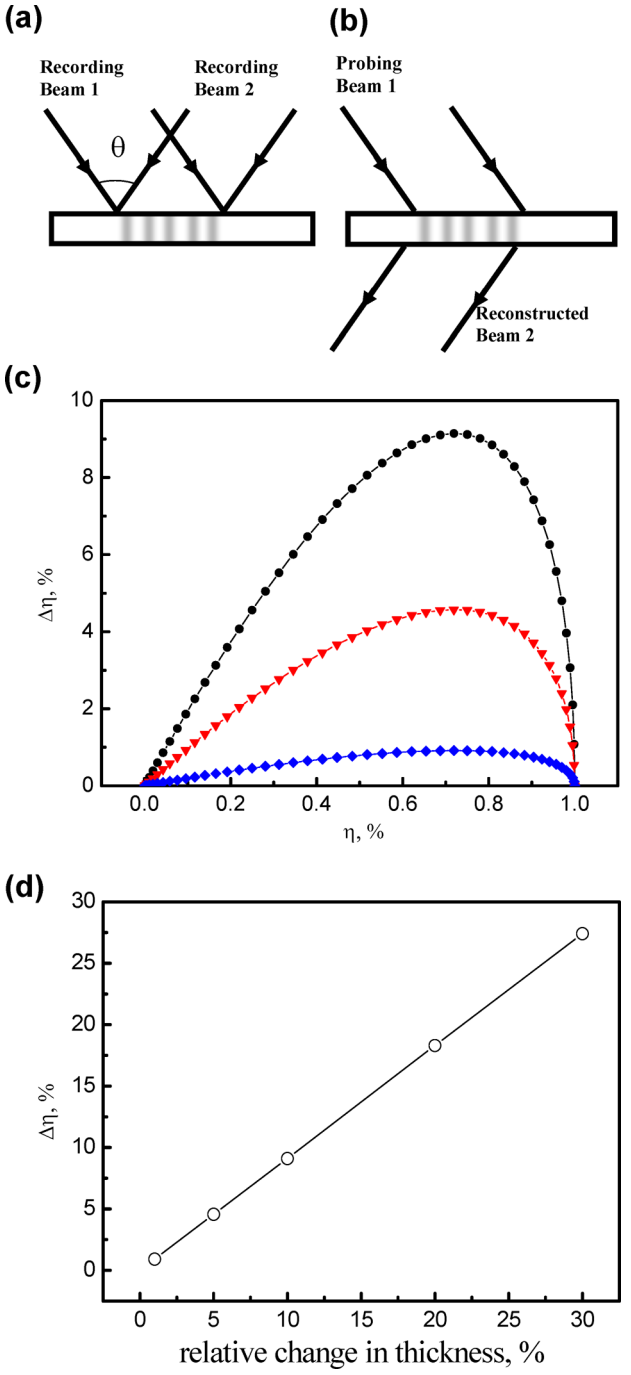

Figure 7. Transmission holograms. (a) Recording and (b) probing of a transmission holographic grating. (c) Absolute change of the diffraction efficiency ($\Delta\eta$) due to a change of the refractive index modulation (n_1): 1% (blue ◆), 5% (red ▼), 10% (●). (d) Change of the diffraction efficiency ($\Delta\eta$) due to an alteration of the layer thickness caused by the analyte. Initial diffraction efficiency is 70%. Reprinted with permission from ref 71. Copyright 2011 Nova Science Publishers, Inc.

wavelength and angle can be controlled externally, and they depend on the design of the interrogation system.

A transmission hologram recorded in a material is characterized by different properties (density, porosity, chemical affinity, charge density, solubility) in the bright and dark regions. If the two regions experience different changes when exposed to the target analyte, this causes a change in the refractive index modulation n_1.[76] Figure 7c shows the dependence of the absolute change of the diffraction efficiency ($\Delta\eta$) on the initial diffraction efficiency (η) for different relative changes of the refractive index modulation. The refractive index modulation, commonly achieved during holographic recording in most photopolymer materials, is of the order of 5×10^{-3}. It can be seen from the graphs that a change in the refractive index modulation 10^{-5} to 10^{-4} will lead to a change in the diffraction efficiency from 0.1% to 9.0%.

1.5.2.b. Swelling/Shrinking of the Layer. To understand the influence of the change in layer's thickness on sensor's response, it is assumed that the refractive index modulation, probe wavelength, and interrogation angle are fixed. Figure 7d shows that thickness change due to shrinking or swelling of the hologram will influence its diffraction efficiency. Generally the relative changes in the thickness of the hologram are larger than the relative changes in refractive index. A thickness alteration of order of 30% will cause a diffraction efficiency change of around 25% (Figure 7d).

1.5.2.c. Probe Beam Wavelength. If a light source with broad spectral range is used to probe a slanted transmission grating, a spectral shift of the maximum diffraction efficiency, caused by shrinking or swelling in the presence of an analyte, will be detected.[75] A slanted grating consists of lattice spacings that are slanted at an angle with respect to the layer's surface, and any dimensional change of the layer could lead to effective change of the lattice spacing and thus will influence the wavelength at which the diffraction efficiency will peak (see eq 6). For unslanted transmission gratings, such shift in the diffraction efficiency peak wavelength can only be observed in the presence of lateral shrinking/swelling of the layer.

1.5.2.d. Probe Beam Incident Angle. If a monochromatic beam of light is used to interrogate the sensor and the layer containing the hologram shrinks or swells in the presence of an analyte, a change in the Bragg angle and thus the angular position of the maximum diffraction efficiency is expected in slanted holographic gratings. As it can be seen from eq 6, the sensitivity of the sensors can be increased by using a grating with a smaller period. No change of the Bragg angle is expected in unslanted holographic gratings unless lateral shrinking/swelling of the layer takes place.

2. THE PROSPECTS FOR HOLOGRAPHIC SENSORS

2.1. Recording Materials

An ideal photosensitive material should be sensitive to laser light with spectral sensitivity and spatial resolution suitable for recording interference patterns. The recording materials should possess linearity in response and produce high image quality with minimum noise, while being low-cost, thereby rendering them amenable to mass manufacturing. To minimize light scatter, nanoparticles, if present in the recording material, should be preferably <10 nm in diameter. The recording materials should be mechanically stable over a supporting substrate. The medium after recording should be permeable to target analyte, and its physical and chemical characteristics such as lattice spacing and/or index of refraction contrast should change based on its interaction with target analytes. The recorded images should be preferably stable during the readout of data and have long shelf life.[1b,44b] Additionally, they should preferably pose no or little risk to health or the environment.

2.1.1. Substrates. A holographic film base is a transparent, mechanically stable supporting medium for the photosensitive

dx.doi.org/10.1021/cr500116a | *Chem. Rev.* XXXX, XXX, XXX−XXX

emulsion. In Denisyuk reflection mode, holographic film base materials should be transparent and nonpolarizing to allow the light to pass through and permit the object beam to return. Hence, optically active and birefringent materials that alter the polarization of light passing through cannot be used as a substrate. If the supporting substrate is anisotropic, it typically causes striations across the image, where each stripe has reduced diffraction efficiency. This is usually due to some of the returning light from the object having its polarization plane rotated, so that it is in a different plane from that of the beam when it first entered the emulsion. Such effects are usually caused by differing degrees of mechanical strain occurring across or along the substrate during the manufacturing process such as extrusion. Another ideal characteristic of the substrate is that its surface should be hydrophobic, but easily functionalized to coat the emulsion. Traditional holographic base materials include glass and cellulose triacetate. Additionally, plastics such as poly(methyl methacrylate) (PMMA, also known as Plexiglas or Perspex) manufactured by the casting can be used as substrates.

2.1.1.a. Glass and Silane Coupling. When a holographic sensor is used in systems containing liquids, it is essential that the polymeric matrix containing the hologram withstands any repeated cycles of swelling and shrinking without becoming detached from its glass or plastic support. This requires a so-called "subbing" or unimolecular sublayer to be fixed to the underlying substrate before coating it with an emulsion.

Silane coupling is a surface modification technique that allows forming bonds between organic and inorganic materials.[77] Silane coupling agent ($R-(CH_2)_n-Si-X_3$) typically exhibits two classes of functionality. Organosilanes generally comprise one organic substituent (R) and three hydrolyzable substituents (X) such as alkoxy, acyloxy, or halogen. For surface treatment applications, for example, the alkoxy groups of the trialkoxysilanes are hydrolyzed to form silanol-containing species. The reaction of the silanes requires four steps. First, hydrolysis of the three labile groups takes place. This is followed by condensation of oligomers. Next, these oligomers form hydrogen bonds with OH groups of the substrate. When the system is dried, a covalent linkage is formed with the substrate due to concomitant loss of water. At the interface of the silicon of the organosilane and the surface of substrate, generally one bond is formed. The two remaining silanol groups may be present in condensed or free form. However, the R group remains available for covalent reaction or physical interaction with other phases.[77]

For gelatin coatings, generally (3-aminopropyl)-triethoxysilane and acetone 1:100 (v/v) are used.[78] Clean glass substrates are wetted with the solution and are dried in a ventilated area. As the acetone evaporates, moisture condenses onto the silane, and this hydrolyzes it, leading to SiO bonding to the glass and amino groups available to interact with the gelatin layer when it is coated later. For acrylic polymers such as poly(2-hydroxyethyl methacrylate) (pHEMA), an initial subbing of 3-(trimethoxysilyl)propyl methacrylate is used in a manner similar to the aminosilane; however, in this case, the subbed glass substrates need to be stored in darkness until they are overcoated with polymer.[79] Otherwise, ambient lighting may damage the double bond in the methacrylate group.

2.1.1.b. Plastics and Oxygen Plasma Treatment. Although polymers on glass surfaces are suitable for sensor design, plastic substrates may be preferable for applications in medical diagnostics that demand disposability and flexibility. For these, plastic substrates with minimal or no birefringence are preferable. Most of the plastic substrates exhibit hydrophobic surfaces, and therefore to deposit the emulsion layer, their surface needs to be rendered hydrophilic. For example, poly(methyl methacrylate) (PMMA) has an index of refraction of 1.49 (578 nm, 20 °C),[80] and it can be treated with oxygen plasma (e.g., 30 s, 1 Torr) to render its surface hydrophilic, which allows the emulsion to adhere to the surface.[73]

2.1.2. Recording Media. The photosensitive recording layer, often referred to as the emulsion layer, comprises a laser light-sensitive material, which can capture and store information from light as a latent image or a complete image. Depending on the fabrication technique, the emulsion layer might require a development process to form a visible image. A typical emulsion consists of silver halide salts dispersed in a polymer matrix, coated onto a support backing (substrate). The emulsion layer can be sensitized to blue, green, red light, or other wavelengths. Over the last two decades, various hydrophilic and hydrophobic polymers have been adopted for constructing the recording media including gelatin, poly(2-hydroxyethyl methacrylate) (pHEMA), poly(acrylamide) (pAAm), and poly(vinyl alcohol) (PVA).

2.1.2.a. Gelatin. The use of gelatin in holography dates back to its roots in late 19th century photography. In the early days, the collodion process was used in photography.[81] The collodion wet plate process required that the plates needed to be sensitized with a solution of pyroxylin in alcohol and ether, followed by immediate exposure to the light while still in wet conditions. However, due to its wet processing requirement and chemical hazards, the collodion process was replaced by gelatin as a photographic emulsion by Richard L. Maddox in 1871.[82] Traditionally, gelatin was the most widely used gelling agent to construct recording media because it is a translucent and colorless material, sourced from collagen, with index of refraction 1.54. Gelatin for holography usually consists of type B alkaline processed gelatin for emulsion preparation. Type B holographic grade gelatin is made from ossein derived from beef bones.[83] It also consists of various peptides and proteins, and it is obtained through partial hydrolysis of collagen. For holography, gelatin has large and flexible pores that can accommodate silver halide crystals and silver nanoparticles. In holographic emulsions, gelatin acts as a protective membrane, which also may desirably restrict the grain growth during the precipitation of silver halides. It consists of a mixture of peptides and proteins, and its hydrophilic nature allows the rapid diffusion of developers into the matrix.

A holographic recording medium is generally prepared through the emulsification of gelatin, involving dissolution in water, followed by the addition of halide salts. A solution of silver nitrate ($AgNO_3$) is added with at a specific rate and with constant agitation. The temperature of the solution is increased normally up to 50 °C for a set time. After the gelatin containing silver halide is precipitated by coagulation, the salts are removed from the system through decantation and washing. The distribution of silver halide crystal size can be controlled by varying nucleation and concentration during precipitation. Finally, the system is heated to 50 °C or above to achieve final ripening and sensitization. The gelatin is hardened by treatment with chromium acetate solution (1%, w/v), followed by incubation at 60 °C for 12 h and DI water rinse. Gelatin itself can possess natural ingredients that can serve as photosensitivity enhancers and act like mild developers and can cause fogging over a long period of time. Other ingredients in gelatin

dx.doi.org/10.1021/cr500116a | *Chem. Rev.* XXXX, XXX, XXX−XXX

can act as AgBr grain growth restrainers, but this can vary considerably from batch to batch depending on the diet of the animal from which it was derived.[83] However, due to gelatin's proteinaceous nature, it produces complex responses to pH and ions, limiting its use as an inert recording media in biological sample sources such as blood, tear fluid, and urine.[84]

2.1.2.b. Poly(2-hydroxyethyl methacrylate) (pHEMA). This polymer can expand in the presence of water to act as a hydrogel, which is widely used in soft contact lenses. Its molecular structure is flexible because it can rotate around its central carbon. For example, in water, the polar hydroxyethyl side turns outward rendering pHEMA flexible. The polymer film is produced usually by pipetting down HEMA and its comonomers onto a sheet of aluminized polyester. The monomer HEMA can be copolymerized with cross-linkers such as ethylene dimethacrylate (EDMA), which is a diester used in the free radical copolymer cross-linking reaction of HEMA. Photoinitiators such as 2,2-dimethoxy-2-phenylacetophenone can be used to start free radical UV polymerization.[79] This emulsion can be flattened into a thin film by a glass or a plastic substrate laid on top of the monomer solution. This sandwich is then given a controlled exposure to UV light to create a free radical chain reaction, involving both the methacrylate groups in the HEMA and those in the subbing layer. The aluminised polyester is needed to allow ease of release from the polymer, and it also both reflects back UV lighting and provides a smooth surface to the pHEMA.[79,85] Alternatively, *N*,*N*,*N*′,*N*′-tetramethylethylenediamine (TEMED) may be used as a co-initiator to a thermal initiator, such as ammonium persulfate, to catalyze the polymerization of the recording medium.

2.1.2.c. Poly(acrylamide) (pAAm). This is a hydrophilic polymer, which is commonly used as the primary material in the fabrication of soft contact lenses and gel electrophoresis media. pAAm can be synthesized by cross-linking acrylamide and *N*,*N*′-methylenebis(acrylamide) (MBA) through UV light-initiated free radical polymerization or thermal curing. pAAM has been used in the fabrication of glucose and lactate-responsive holographic sensors.[86] However, cross-linkers such as MBA cause background staining due to the interaction of the free amides with silver.[87] It was shown that bis(acryloyl)-piperazine (BAP), which is a tertiary amide, did not bind to silver ions. This was attributed to the nitrogens present in BAP being unable to interact with silver ions. On the basis of this study, to avoid background staining in holographic recording media, an acrylamide-based recording medium was cross-linked with a bis(tertiary amide) such as 1,4-bis(acryloyl)piperazine.[88]

2.1.2.d. Poly(vinyl alcohol) (PVA). It is a water-soluble synthetic polymer that exhibits atactic properties. PVA is manufactured through hydrolysis of polyvinyl acetate and is commonly used as a binding agent in papermaking, textile, and coatings. It has suitable properties for recording media due to its resistance to most oils and solvents while exhibiting high tensile strength and flexibility. Although its physical properties are subject to change due to variation in humidity, it found some use in holography, and different compositions of it have been prepared to improve the diffraction efficiency.[89] Holographic PVA-based matrixes have been cross-linked with Cr(III) ions, which allowed maintaining adequate porosity and elasticity for sensing applications.[90] Additionally, PVA-based recording materials, where an anisotropic dye is dispersed within the PVA matrix, have also been successfully used as recording material in polarization holography.[91]

2.1.2.e. Poly(dimethylsiloxane) (PDMS). Although hydrophilic polymers are suitable matrixes for analytes in liquids, polymer matrixes that are impermeable to liquids, but permeable to gases, can also find applications in holographic sensing.[92] PDMS is a polymeric nonbiodegradable organosilicon compound, commonly known as silicone. It is optically clear, inert, and nontoxic. After polymerization, PDMS exhibits an external hydrophobic surface, and its surface chemistry does not allow polar solvents to penetrate the matrix. It is suitable for use with aqueous solvents without material deformation. However, organic solvents such as chloroform, ether, and tetrahydrofuran can diffuse into PDMS and result in matrix swelling. It has been widely used in soft lithography, rendering it a suitable stamp resin for the fabrication of microfluidic devices.[93] It is a highly flexible and transparent polymer, which is exceptionally hydrophobic. It swells strongly in petroleum spirits and its vapors, but is not affected by water vapor. It can be used to quantify effectively concentrations of petroleum vapor in air and also butane and propane.[94]

2.1.2.f. Silk Protein. While many materials are suitable for in vitro diagnostics, biocompatible materials are also needed for holographic sensors. For example, in the realization of such devices, implantable degradable systems may circumvent surgically removing the device postfunctional lifetime. Additionally, biodegradable sensors are amenable to mass distribution in the environment without contamination. Natural biopolymers can offer further advantages, which may allow the inclusion of biological dopants during biopolymer processing and cross-linking without the use of harsh chemistry or UV exposure. Silk fibroin has been investigated to explore the integration of optical and biological function in a single element by offering all-aqueous processing as well as the formation of ultrathin films with a variety of fiber diameters.[95] For example, silks spun by spiders and silkworms represent the strongest and toughest natural fibers known and offer many advantages over conventional polymers.

Silk solution was obtained by boiling *Bombyx mori* cocoons for 30 min in an aqueous solution of Na_2CO_3 (0.02 M), followed by rinsing thoroughly with water to extract the glue-like sericin proteins.[96] This mixture was dissolved in LiBr (9.3 M) at room temperature (24 °C), yielding a 20 wt % solution. Next, the solution was dialyzed in water using a dialysis cassette with a cutoff molecular weight of 3500 Da for 48 h. The resulting material can be poured onto a plastic (e.g., PDMS) substrate or a mold with negative surface hologram. Finally, the solution was left to dry 1−2 days until the solvent had evaporated to give solid fibroin protein silk films. The thin film or the holographic grating then was peeled off from the mold. Such biodegradable materials such as silk fibroin, chitosan, alginate, cellulose, gelatin, and starch may find applications in biocompatible implantable sensors.

2.1.2.g. Hybrid Polymers. The versatility of the holographic medium can be improved by copolymerizing multiple monomer species.[97] Such hybrid polymers can exhibit mechanical stability and analyte sensitivity that may not be attainable with conventional recording medium. For example, the hologram can be recorded in gelatin, and the analyte sensitivity can be provided by an additional interpenetrating polymer. In an investigation, the hologram was recorded in a commercially available gelatin holographic plate. Next, a solution comprising a suitable cross-linker (e.g., bis-acryolyl-piperazine), a functional group (e.g., acrylic acid), and a photoinitiator was perfused into the prefabricated gelatin

dx.doi.org/10.1021/cr500116a | *Chem. Rev.* XXXX, XXX, XXX−XXX

hologram, followed by polymerization in situ. The resulting hologram exhibited the optical properties and pH-selectivity of both gelatin and carboxyl groups present in acrylic acid.[97]

Hybrid pAAm-PVA recording media have also been explored for humidity sensing applications. Polyacrylamide photopolymers used for fabrication of holographic sensors normally contain two monomers, acrylamide and *N*,*N*′-methylenebis-(acrylamide) (MBA),[98] together with a dye sensitizer and an initiator dispersed in a polyvinyl alchohol (PVA) matrix to form a dry photopolymer layer. Illumination by light of appropriate wavelength triggers free radical polymerization and a change in the refractive index of the layer. Holograms with diffraction efficiency of above 90% can be recorded in this type of material. Because of the highly hygroscopic nature of both polyacrylamide and PVA, the resulting layer can easily absorb/desorb water. This leads to swelling/shrinking of the layer and causes dimensional changes in the prerecorded holographic structure.

2.1.2.h. Multilayer Recording Media. The recording and processing steps in holography may interfere with enzyme-based assays.[99] For such devices, multilayer recording media may be preferred. Maintaining the activity of the enzyme and causing a sufficiently large wavelength change in a single holographic medium is desirable for quantification purposes or for the detection of the presence of an analyte or inhibitors at useful concentrations. Immobilization of the enzyme in the polymer matrix, followed by producing holograms using silver halide chemistry, was found not to be practical due to a substantial decrease in the enzyme activity.[99] However, immobilization of the enzyme in a secondary layer of a hydrogel, situated between the hologram medium and the solution phase, allowed the maintenance of the enzyme activity in the secondary layer.[100]

2.1.2.i. Control of Polymer Thickness. To obtain consistent diffraction efficiency, the thickness of the recording medium must be controlled accurately.[101] There are numerous techniques for depositing an emulsion onto a substrate based on polymer type, its viscosity, and cross-linking strategy. Techniques such as spin coating, roll-to-roll coating, stamping, spray deposition, or silica and glass bead spacers can be used to control the thickness of the polymer film. At the mass manufacturing level, the thickness of the recording medium can be controlled by doctor blading, which allows a fine control over the thickness.[102]

At laboratory scale, simpler deposition techniques may be preferable. For example, a practical way is to deposit the monomer solution as an elongated blob on a leveled hydrophobic inert substrate. This material should have a flat nonsticky surface, which can facilitate peeling off easily after curing. Such materials include hydrophobic polymers and aluminized sheets. The substrate can be placed on top of the elongated blob, resulting in spread of the monomer solution throughout the substrate surface by capillary action and the weight of the substrate. Because this method allows full enclosure of the monomer solution, it limits contact with oxygen in the environment with the monomer solution, which is desirable for free radical polymerization. Silica and latex beads of diameter ∼10−30 nm may be mixed into the monomer solution to control the thickness.

Another practical way of depositing emulsions on substrates is the Mayer bar coating, which involves the use a stainless steel rod that is wound with a tight spiral of wire.[78,103] The grooves between the wire coil dictate the precise amount of liquid emulsion that will be deposited on the substrate. The final thickness of the emulsion is directly proportional to the diameter of the wire. At first, the initial shape of the coating appears in a series of stripes, and then the surface tension of the liquid film pulls these stripes together, forming a smooth, leveled surface. This process is followed by a drying and curing process through heating or UV exposure.

Printing of recording media is an unexplored way of depositing the polymer matrix and photosensitive materials on substrates. It has practicality, miniaturization capacity, and scalability in printing different functional polymers that can allow the construction of holographic arrays. For example, various polymers can be loaded into a cartridge that supplies a noncontact, contact, or airjet dispenser. As the monomers or materials immobilize on the surface of the substrate through drying at room temperature or through UV exposure, polymer matrixes with different analyte-sensitive materials can be constructed with controlled size and diameter. Because printing minimizes the required volume of the monomer solution, it has the potential to enable mass production.

2.1.2.j. Preparation of Microporous Polymer Matrixes. The analytes must perfuse into the polymer matrix and successfully bind to the receptors with a reasonably short time. To accelerate the diffusion of analytes into hydrogel matrixes, pore forming agents have been utilized.[104] The incorporation of large pores in the hydrogel matrix allows rapid diffusion of the analytes throughout the support medium, thus making the response of the holographic sensor faster.[105] For example, matrixes consisting of HEMA monomers polymerized in water containing methanol (4−8%, w/v) were prepared. The presence of water in the monomer mixture resulted in a microporous polymer structure that displayed faster response to analytes.[104]

2.1.3. Nanoparticles. Nanoparticles can be added to a holographic recording medium to improve its recording properties and to achieve sensitivity of the created photonic structure to target analytes. When choosing the nanoparticles for a specific application, it is important to consider their size, refractive index, their stability in the host material, and their affinity to the target analyte.[106]

Nanoparticles with diameters of 10−30 nm are normally used to reduce the amount of scattered light. Low-scattering recording material is crucial for achieving high contrast of the recorded interference fringes, and high diffraction efficiency of the recorded photonic structure. Nanoparticles with refractive index significantly different from that of the host polymer can be used for improving the dynamic range of the material. The dynamic range is related to the maximum refractive index modulation achievable in the recording material. Large dynamic range is particularly important when multiple holograms are recorded in the same region of the layer. By using appropriate dynamic range and choice of geometry of recording, multiple holograms can be recorded at different exposure conditions.[107]

2.1.3.a. Silver. Silver is the historical choice of recording material for holography.[44b] Silver is available in many forms such as silver nitrate ($AgNO_3$), silver perchlorate ($AgClO_4$), or silver pentafluoropropionate ($C_2F_5CO_2Ag$). Silver nitrate is the least expensive and the most used source of silver in holography. In the solid form of silver nitrate, Ag^+ ions are three-coordinated in a trigonal planar arrangement. Silver nitrate can be dissolved in water, and it exhibits nonhygroscopic properties and stability under light, in contrast to silver perchlorate, silver tetrafluoroborate, or silver pentafluoropropionate. In the formation of emulsions, silver nitrate can be

dx.doi.org/10.1021/cr500116a | *Chem. Rev.* XXXX, XXX, XXX−XXX

Table 1. Selected Lasers Used in Holography To Record a Diffraction Grating

type	laser	principal wavelength[a] (nm)	output
gas	helium−neon[44c,114]	632.8, 543.5, 594, 612	CW up to 70 mW
	argon ion[44c,115]	514.5	CW up to 20 W
	krypton ion[44c]	647.1, 413.1	CW up to 10 W
	helium−cadmium[116]	441.6, 325	CW up to 130 mW
	exciplex,[117] e.g., ArF, KrF, XeCl, XeF	193, 248, 308, 351	CW up to 100 mW
liquid dye	dye, e.g., rhodamine, fluorescein[118]	300−1800	pulsed up to 2.5 J CW up to 5 W
solid state	ruby[1b]	694.3	pulsed up to 40 J
	titanium sapphire[1b]	650−1100	pulsed up to 1 W
	neopdymium yttrium aluminum garnet (Nd:YAG)[119]	1064, 532, 355, 266	pulsed or CW up to TW, 100 W average CW
	semiconductor diode, e.g., GaN/AlGaN, ZnCdSe, InGaAs/GaAs, InGaAs/InP[1b,44c]	430−550, 490−525, 870−1100, 1100−1650	CW (some pulsed) up to 35 W
fiber	yterbium (Yb)[44c]	532	50 W

[a]Most commonly used, CW (continuous wave).

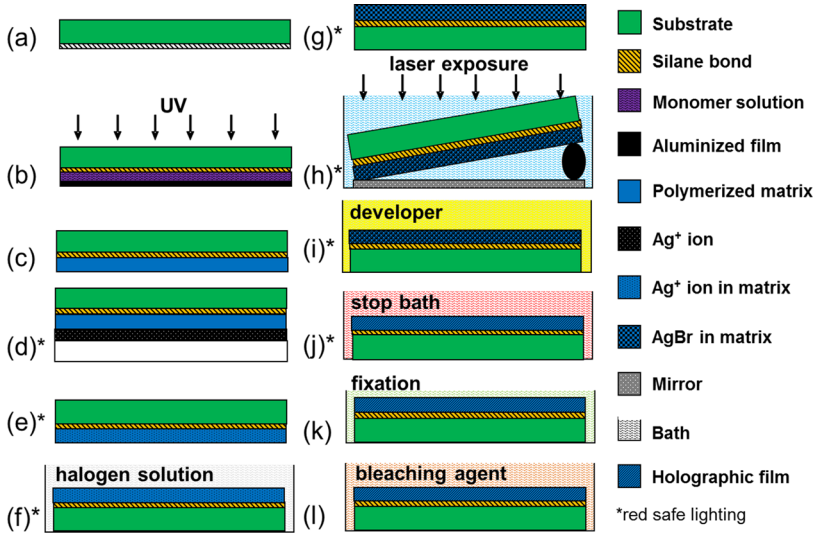

Figure 8. Holographic image formation through the silver halide system. (a) The surface of a substrate is functionalized to allow the polymer layer to attach to the substrate. (b) The monomer solution is polymerized on the substrate. (c) The polymer−substrate system after polymerization. (d) The diffusion of silver salt solution into the polymer matrix. (e) The excessive silver salt solution is wiped off the surface and the polymer layer is dried under a tepid air current. (f) The polymer layer−substrate system is placed in a halide ion solution to form a silver halide (AgBr). (g) The polymer layer−substrate system after silver halide formation. (h) Exposure to laser light with an object at the rear of the polymer layer. (i) Nanoparticle formation. (j) Stop bath. (k) Fixation. (l) Bleaching.

treated with halide salts (e.g., LiBr) to form insoluble silver halide, which may be used with gelatin to form an emulsion. Silver perchlorate is another precursor to form silver halide and silver nanoparticles. It can be dissolved in organic solvents making it suitable for use in hydrophobic matrixes; however, the perchlorate salts are explosive and should be handled with care. Silver pentafluoropropionate can be dissolved in organic solvents (e.g., tetrahydrofuran) to impregnate highly hydrophobic materials (e.g., PDMS).[92] Other silver halide abstraction agents include silver tetrafluoroborate ($AgBF_4$) and silver hexafluorophosphate ($AgPF_6$).

2.1.3.b. Zeolite. Zeolites are defined as crystalline materials with 3D framework structures that form pores with highly regular and uniform sizes of molecular dimensions.[108] Structurally, the zeolites are aluminosilicates based on an infinitely extending connected framework of SiO_4 and AlO_4 tetrahedra that are linked to each other by shared oxygen atoms.[109] Zeolites and zeolite-type materials are classified according to their framework type, pore dimension, and Si/Al or Al/P ratios. The pore volume of a zeolite is related to the framework density defined as the number of tetrahedral atoms (T = Al, Si) per 1000 Å.[110] The tetrahedra are linked together to form cages connected by pore openings of defined size. Depending on the structural type, the pore sizes range from 0.3 to 2 nm.[111] The well-defined porous structure of zeolites consists of true shape-selective molecular sieves with wide ranging applications in catalysis, ion exchange, and adsorption processes.[112] In addition to the variety of pore sizes and shapes, due to the hydrophilic/hydrophobic nature of zeolites, they are selective sorbents and hosts for guest organic or inorganic molecules stable in gas and liquid phases.[76] For example, zeolites have been used as layers in responsive Bragg stacks for applications in sensing solvents.[113]

2.2. Lasers

In hologram recording, lasers are of importance due to their ability to produce monochromatic light. To construct a holographic sensor, generally a single laser source is required. Table 1 shows commonly used lasers in holography. The choice

dx.doi.org/10.1021/cr500116a | Chem. Rev. XXXX, XXX, XXX−XXX

of a laser source for application in holography is based on its coherence length (the propagation distance over which a wave maintains a degree of coherence), the stability of the output power, the stability of the state of polarization, and the emission wavelength. Operation in a single longitudinal mode that is naturally free of mode-hopping (sudden jumps of optical frequency) provides for a long coherence length, and because the coherence length determines the maximum difference in the optical path of the reference and object beam, it governs the achievable optical depth of the holographic image. The stability of the laser output power is important because this ensures that the holographic recording will be controllable within parameters of the recording material. Typically, a study of the optical response of the material versus intensity of recording light and total exposure is carried out initially. This study determines the region of linear response of the material. The state of polarization of the two recording beams is critical for achieving high visibility of the interference fringes; thus a laser with a stable state of polarization is required. Normally, the preferred state of polarization of the two recording beams is s-polarization (perpendicular to the plane of incidence). Finally, the emission wavelength must match the wavelength sensitivity range of the recording material to achieve optimum results.

2.3. Fabrication Techniques

2.3.1. Silver Halide System. Silver halides have been the most consistently successful material used in holography.[44b] A typical silver halide system involves (i) diffusion of silver ions into the analyte-sensitive polymer matrix, (ii) formation of silver halide, (iii) laser exposure to form the latent image, (iv) amplification of the latent image to form a visible image through development, and (v) post processing steps to improve the diffraction efficiency. Figure 8 shows the overview of a generic photochemical processing used in the silver halide system.

2.3.1.a. Diffusion of Silver Ions into the Polymer Matrix. To create a range of sensors, methods of producing photosensitive "emulsions" in substrates other than gelatin were needed. This investigation led to the formation of photosensitive nanoparticles in a variety of precoated polymer films. The preliminary investigations involved experimenting on films of pure gelatin hardened with a small proportion of either gluteraldehyde or chrome alum.[78] Silver nitrate solution (0.3 M) was then diffused into the film, followed by drying under a tepid air current. Working under safelighting, the film or plate was placed in a bath of lithium bromide solution and sensitizing dye for a carefully controlled time, followed by a rapid rinsing under running water. A final bath of mild reducing agent such as a 2% (w/v) solution of ascorbic acid (~pH 6) was then used to enhance greatly the photosensitivity. Finally, the resulting recording medium was exposed to the laser light and developed, followed by bleaching. Transmission electron micrographs showed that ultrafine AgBr grains were produced by this method comparable in terms of grain size to conventional methods of producing the ultrafine grain or Lippmann emulsions (Figure 9).[78] This so-called "diffusion" method was found to be transferable practically to less hydrophilic coated films such as polymerized hydroxyethyl methacrylate (pHEMA).[85,120] However, the increased diffraction that could be obtained from bleaching or turning developed silver metal back into silver halide for holograms in gelatin was not usually obtained in other polymers. Furthermore, it soon became clear that leaving the developed silver unbleached gave it stability under the intense white light source required for spectrophotometry to monitor the hologram's behavior as a sensor.

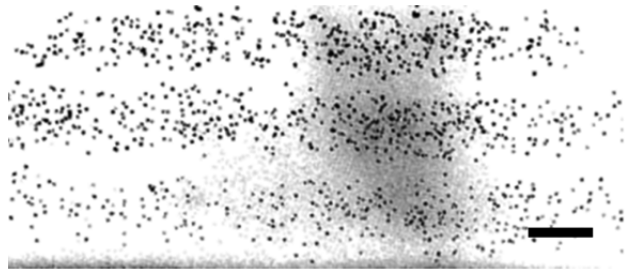

Figure 9. A transmission electron micrograph of the recorded nanoparticle spacings made from developed and fixed silver grains originally formed by the diffusion method, after exposure with a HeNe laser operated at 632.8 nm in Denisyuk reflection mode. Scale bar = 250 nm. Reprinted with permission from ref 78. Copyright 1999 The Royal Photographic Society.

2.3.1.b. Silver Halides. Silver halides are compounds that can be formed between silver and a halogen. These include silver bromide (AgBr), chloride (AgCl), and iodide (AgI). Silver bromide is the most commonly used silver halide in holography, and grains of AgBr are primary light capturing materials suspended in the recording medium.[44a] These small grains minimize light scatter during laser exposure. Silver halides can create high spatial resolutions and high diffraction efficiencies that allow high-resolution 3D images with wide viewing angles. AgCl does not have as high of a refractive index as AgBr and AgI, and therefore does not produce such high diffraction efficiencies. AgCl is also very prone to "printout" or darkening in ambient lighting. Professionally prepared silver halide emulsions for holography usually have around 5% AgI in with the AgBr because that mixture produces a higher sensitivity than just AgBr.[121]

2.3.1.c. Photosensitization. Silver halide crystals are only sensitive to light in the UV and violet regions of the spectrum. The energy absorbed by the silver halide must be sufficient to remove an electron from the Br^- ion. However, for light at longer wavelengths, the energy of photons is not high enough to remove an electron directly in this way. For this reason, to record at longer wavelengths, the photosensitizing dye and Ag^+ complex within the emulsion must absorb the radiation and transfer the energy to the silver–halide crystal. Hence, dye molecules that can absorb the laser light at different wavelengths are incorporated into the emulsion to increase the sensitivity of silver halides to the laser light.[44a] Spectral sensitization involves rendering silver halide grains sensitive to light in a region of a spectrum where they would normally not absorb the light. The dyes used for the sensitization are generally cyanine dyes. For example, for Nd:YAG (λ = 532 nm) pulsed lasers or helium–neon (HeNe) (λ = 633 nm), photosensitizing dyes such as Quinaldine Red or Quinaldine Blue can be used, respectively. Table 2 summarizes commonly used sensitizing dyes in silver halide chemistry.

2.3.1.d. Partial Removal of Photosensitizing Dye from the Polymer Matrix. At the end of the steps needed before exposure, excess dye should be removed to prevent unnecessary light absorption. The excess dye is easily removed by agitating the slide or film in an alcohol/water bath under safelighting; usually ~70% (v/v) ethanol or methanol is used. The dye essential for photosensitization will not be removed by the

dx.doi.org/10.1021/cr500116a | Chem. Rev. XXXX, XXX, XXX–XXX

Table 2. Sensitizing Dyes for Silver−Halide Emulsions

dye	systematic name	absorption, λ_{max} (nm)
auramine O (basic yellow 2)[a]	4,4′-(imidocarbonyl)bis(*N*,*N*-dimethylaniline) monohydrochloride	370, 434 (second)
acridine orange[a]	3,6-bis(dimethylamino)acridine hydrochloride	492
eosin Y (eosin yellowish)[a]	2′,4′,5′,7′-tetrabromofluorescein disodium salt	524
pseudocyanine iodide[a]	1,1′-diethyl-2,2′-cyanine iodide	524
quinaldine red	2-(4-dimethylaminostyryl)-1-ethylquinolinium iodide	528
erythrosin B (iodesine)[a]	2′,4′,5′,7′-tetraiodofluorescein disodium salt	533
rhodamine B[a]	*N*,*N*,*N*′,*N*′-tetra ethylrhodamine hydrochloride	543
isocyanine iodide[a]	1,1′-diethyl-2,4′-cyanine iodide	558
pinaverdol (sensitol green)[a]	1,1′,6-trimethylisocyanine iodide	558
orthochrom T[a]	1,1′-diethyl-6,6′-dimethlisocyanine	564
pinacyanol chloride (quinaldine blue)[a]	1,1′-diethyl-2,2′-carbocyanine chloride	604, 560 (second)
pinacyanol bromide[a]	1,1′-diethyl-2,2′-carbocyanine bromide	607
pinacyanol iodide (sensitol red)[a]	1,1′-diethyl-2,2′-carbocyanine iodide	614
kryptocyanine (rubrocyanine)[a]	1,1′-diethyl-4,4′-carbocyanine iodide	648, 703 (second)
dithiazanine iodide[a]	3,3′-diethylthiadicarbocyanine iodide	655

[a]The dye and systematic name are listed in ref 44a.

alcohol/water bath because it is chemically locked into the silver halide grain. It is only easily released after the grain is developed into Ag^0 metal. This does, however, leave the undeveloped grains in the unexposed areas still holding on to their dye, causing a strong "print-out" effect under the spectrophotometer lighting during readouts, causing the diffraction to gradually weaken. Another problem from this residual dye is that during readouts, it causes the diffracted light to have a pink bias, leading to an artifactual blip in the spectrum (~530 nm). Therefore, these grains need to be removed from the emulsion. However, removing them from the polymer matrix causes shrinkage and a blue shift as already explained. One way around this shrinkage problem is to oxidize and decolorize the dye, so that the grain can be left in place without causing severe "print-out". This may be achieved soaking the slide only briefly in a solution of potassium dichromate (~2%), followed by a deionized water rinse to render the emulsion fairly insensitive to print-out. Such a brief treatment with dichromate does not usually affect the functionality of the hologram in, for example, glucose or pH monitoring.

2.3.1.e. Laser Exposure. Holographic sensors can be recorded in various geometries of the recording beams. The simplest recording mode is Denisyuk reflection holography.[62] To record a hologram with the desired response range and optical characteristics, the conditions during exposure play a critical role. These parameters include the size of the laser beam, the exposure conditions, and the tilt angle of the emulsion plane with respect to the incident beam(s) and the reflective properties of the object to be copied. Traditionally, in artistic holography, the hologram is recorded in dry conditions. This is preferable if the holograms are read in dry conditions. However, in holographic sensing, the emulsion is exposed to wet conditions to enable readouts in aqueous solutions. An important step to produce a holographic sensor is to prepare an exposure bath, which may contain buffers or agents to control the chemical and physical properties of the recording medium during laser exposure. If the hologram is exposed while it is swollen in an aqueous solution, the final wavelength of the dry hologram will be shorter than the wavelength of the laser light.[68] On the other hand, if the exposure bath shrinks the emulsion, the final wavelength of the diffracted light from the dry hologram will be of a longer wavelength than the laser light used during exposure. The next critical step before laser light exposure is the placement of the emulsion−substrate system over the object (e.g., mirror, coin) with an inclination of ~5° with respect to the plane of the film while being immersed in the exposure bath. Tilting the slide prevents the normal specular reflections of white light off the surfaces from drowning out the holographically diffracted light, and smaller angles are preferable to reduce internal reflection. The emulsion should preferably be placed face down to minimize the internal reflection from the substrate, which would otherwise occur because the laser light would have traveled through the substrate on its way back from the reflected object before forming the standing wave in the emulsion. The last step before the laser exposure is to allow the optical setup to settle (~20 min) to minimize creep effects when using continuous wave (CW) lasers. In the case of pulsed lasers, such movements are not a problem, but a settling time of ~1 min is required to allow the emulsion to reach equilibrium in the buffer solution. Finally, the emulsion−substrate system can be exposed to the laser light to form the latent image. In addition to Denisyuk reflection holography, other multibeam interference techniques can be employed to form the latent image.[122]

2.3.1.f. Latent Image. The spatial light intensity distribution formed by interference between the object and reference waves can be recorded as a spatial variation of emulsion transmissivity.[59,123] When the photosensitive film is exposed to the laser light, an invisible latent image is formed. This latent image is laser radiation-induced change in a silver halide crystal that renders the system susceptible to reduction action of a developer. Although the formation of the silver halide-based photochemistry (the Daguerreotype process) was proposed in 1839, it was not until 1938 that the principles of latent image were laid by R. W. Gurney and N. F. Mott.[124] A crystal of silver bromide consists of a regular cubical array of silver and bromide ions. However, this crystal comprises defects in the form of interstitial silver ions occupying spaces between the lattice positions. Additionally, distortions or dislocations are present within or on the crystal, also known as latent image sites.

The Gurney−Mott principle involves two-step formation of a latent image.[124,125] When an incoming photon of laser light is absorbed by a silver bromide crystal, an electron is released from a bromide (Br^-) ion (Figure 10a), and a free bromine atom is formed ($Ag^+Br^- + h\nu \rightarrow Ag^+ + Br + e^-$). Next, the liberated electron, also called photoelectron, migrates to a shallow electron trap site, providing a negative electrical charge to the latent image site (Figure 10b). This stage of the latent image formation is known as the electronic conduction stage. Because the latent image site is negatively charged, it has a tendency to attract interstitial positively charged silver ions (Figure 10c). When an interstitial ion arrives at the latent image site, its charge is counteracted and the silver atom thus is deposited at the trap (Figure 10d), $Ag^+ + e^- \rightarrow Ag^0$. The second stage of the Gurney−Mott mechanism, also known as the ionic stage condition, involves repetition of the whole cycle

dx.doi.org/10.1021/cr500116a | *Chem. Rev.* XXXX, XXX, XXX−XXX

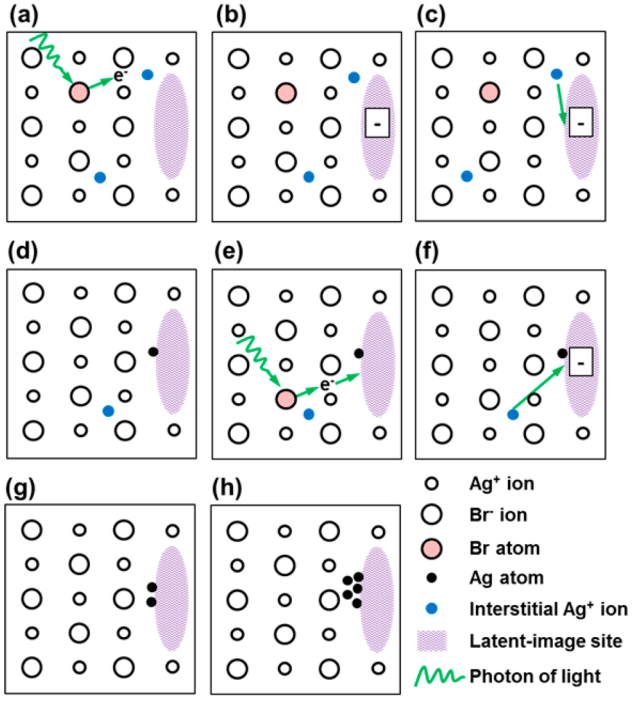

Figure 10. Formation of a latent image.[124] (a) Absorption of a photon and liberation of an electron. (b) Formation of a charged electron trap zone. (c) Migration of an interstitial Ag^+ ion to the electron trap zone. (d) Reduction of the Ag^+ ion to Ag^0. (e–g) Formation of another Ag^0 atom. (h) Ag^0 speck representing the latent image.

of silver atom deposition at the trap site (Figure 10e–g), forming an aggregate (Figure 10h). These photolytic silver clusters (specks) constitute the latent image, which can be later amplified when the emulsion is developed to form a visible image.

2.3.1.g. Nanoparticle Formation. A developer consists of a chemical mixture that amplifies the latent image and produces a visible image.[126] It attacks and reduces the laser light-exposed silver halide crystals to metallic silver. The longer the emulsion remains in the developer, the greater is the degree of reduction of silver halide crystals to metallic silver. Generally, the emulsion is kept in the developer until it is about one-half the optical density of a totally developed piece of the same material as judged under safelight, followed by a rinse in deionized water and/or direct immersion in a stop bath. If the emulsion is rinsed with deionized water, it continues to develop at a lower rate during rinsing. The composition of the developer may include metol (4-(methylamino)phenol hemisulfate) salt, phenidone (1-phenyl-3-pyrazolidinone), dimezone S (4-(hydroxymethyl)-4-methyl-1-phenyl-3-pyrazolidinone), and hydroquinone (1,4-benzenediol) (Figure 11). These developing agents can be prepared in aqueous solutions in

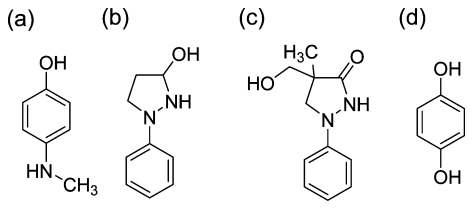

Figure 11. Constituents of a photographic developer. (a) Metol, (b) phenidone, (c) dimezone S, and (d) hydroquinone.

the presence of alkaline agents such as sodium hydroxide, sodium carbonate, and borax. Other chemicals such as hydroquinone can be used as superadditives together with metol to recharge the oxidized metol during reduction. Sulfite in the developer prevents aerial oxidation of the developing agent, and it facilitates the regeneration of metol by hydroquinone. The developer may also contain small quantities of potassium bromide to control the strength of the developer to minimize chemical fogging. To achieve high contrast, the developer requires high concentrations of metol at high pH (~11–12) by adding NaOH. In the preparation of the developer, metol may take longer to dissolve in the presence of a high salt content, and therefore it may be preferable to dissolve the metol first. Protective gloves and goggles should be worn due to high alkalinity of the developers, which may cause skin irritation. Alternative reducing agents such as ascorbic acid (vitamin C) can also be used. In addition, neutral developers are desirable for sensitive biological systems that could be damaged by the high pH of traditional developers. Neutral developers contain 2,4-diaminophenol dihydrochloride (amidol), sodium sulfite, and sodium carbonate.

In silver halide-based holography, JD-4, also known as JARB, is the most widely used developer, which comprises 4-methylaminophenol sulfate (0.3%, w/v), ascorbic acid (2%, w/v), sodium carbonate (5%, w/v), and sodium hydroxide (1.5%, w/v) dissolved in deionized water.[127] To increase the shelf life by up to 3 weeks, this developer can be prepared in two separate mixtures; the first one has metol and ascorbic acid, while the second mixture consists of sodium carbonate and sodium hydroxide.

2.3.1.h. Stop Bath. The stop bath is used in holographic processing after the nanoparticle development process.[128] Submerging (15–30 s) the emulsion into the stop bath halts the development of the silver nanoparticles. The stop bath consists of an acidic solution (e.g., acetic acid (1–5%, v/v)) to immediately decrease the pH in the emulsion, and stop the development process instantly. It also reduces the overall processing time, as opposed to the time required for a substantial water rinse. The stop solution should be replenished when producing holographic sensors in batches because the bases carried over from the developer exhaust the stop bath, causing it to be alkaline. A pH indicator, bromothymol violet, can be used in the stop bath as an indication of high alkalinity. Citric acid or sodium bisulfite may be preferred over acetic acid to reduce the odor of the stop bath.

2.3.1.i. Fixation. A fixer consists of a mix of chemicals that remove the unexposed silver–halide crystals from the emulsion to stabilize the image.[126] After fixation, only the reduced metallic silver (Ag^0) that forms the image is left in the final emulsion, which is then insensitive to light. When the fixers are not used, the remaining silver halide is subject to development over time and fogs the image. Sodium thiosulfate, also known as hypo, and ammonium thiosulfate are the most commonly used salts in the fixer formulas. Aqueous sodium thiosulfate binds to chemically soft metals with high affinity, and dissolves the excessive silver halide within the emulsion. After the fixation, the emulsion should be rinsed with deionized water to remove the exhausted chemicals from the polymer matrix. 10% (w/v) sodium thiosulfate is effective in removing the excess silver halide over 15 min in hydrophilic recording media (e.g., gelatin, polyacrylamide). For less hydrophilic polymers such as pHEMA, sodium thiosulfate (10%, w/v) may be mixed with a

dx.doi.org/10.1021/cr500116a | *Chem. Rev.* XXXX, XXX, XXX–XXX

solvent (e.g., ethanol) (1:1, v/v) to swell the polymer matrix during fixation.

2.3.1.j. Bleaching. This process converts the variation in transmission to a variation in refractive index to increase the diffraction efficiency.[44a] Bleaching transforms the metallic silver grains of an image to a transparent silver salt. Although silver is an inert metal, it can be oxidized directly by elemental halogens such as bromine (Br_2), chlorine (Cl_2), and iodine (I_2). For example, Br_2 reacts with silver particles in the emulsion of an amplitude hologram to form phase holograms with high diffraction efficiency. Bleaching by using I_2 solution in alcohol/water is more practical and less harmful than Br_2. Although bleaching is applicable to display holography, these elements are highly damaging to holographic sensors incorporating delicate enzymes.

The grain size in a bleached hologram has been shown to be ~1.5 times larger than that in an unbleached one (Figure 12).[129] This enlargement in the grain size provided an explanation for the increase in the thickness of the emulsion layer after bleaching. The degree of expansion can be expressed as the following:

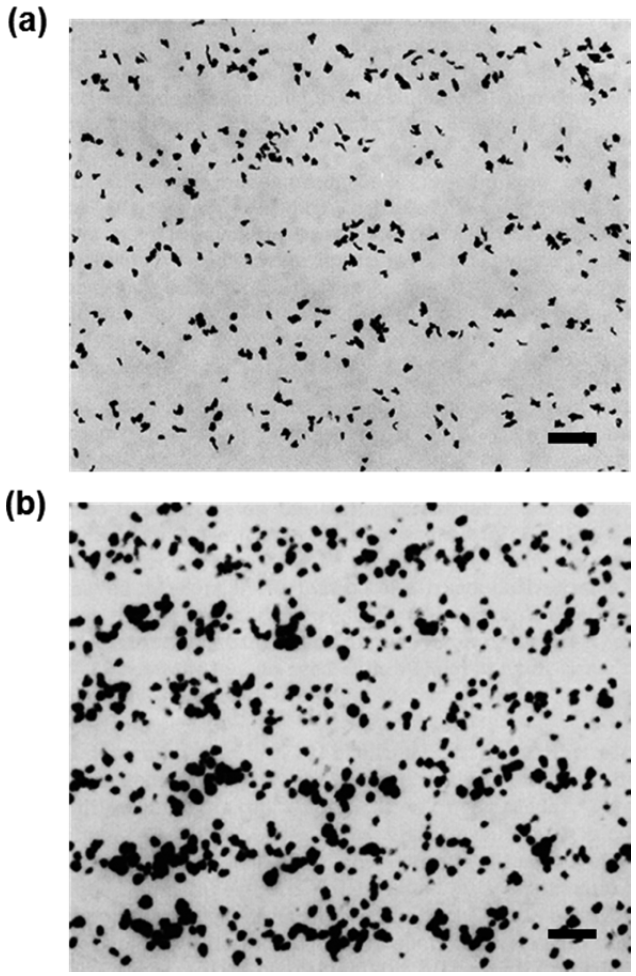

Figure 12. Increase in grain size due to bleaching of an emulsion shown by electron micrographs of hologram cross sections (a) An amplitude hologram produced by multibeam interference on Kodak 649F film, recorded with a HeNe laser (632.8 nm). (b) The hologram (amplitude) after bleaching. Scale bars = 500 nm. Reprinted with permission from ref 129. Copyright 1972 AIP Publishing, LLC.

$$\frac{V_{Ag^0}}{V_{AgX}} = \left(\frac{M_{Ag^0}}{S_{Ag^0}}\right)\left(\frac{M_{AgX}}{CS_{AgX}}\right)^{-1} \tag{7}$$

where M_{Ag^0} and M_{AgX} are the atomic weight and the molecular weight of silver metal and silver halide; S_{Ag^0} and S_{AgX} are the specific weights of silver atom and silver halide; and V_{Ag^0} and V_{AgX} are the atomic and molar volumes of silver atom and silver bromide. C (i.e., 2 for AgBr or AgCl) is the number of silver atoms required to form two molecules of silver halide by the bleaching reaction. The ratio of grain size can be obtained using the following expression:[129]

$$\sqrt[3]{\left(\frac{V_{Ag^0}}{V_{AgX}}\right)_{calc}} = \left(\frac{L_{Ag^0}}{L_{AgX}}\right)_{calc} \tag{8}$$

where L_{Ag^0} and L_{AgX} are the grain sizes of silver (Ag^0) and silver halide, respectively. The theoretical calculation of the grain sizes can be used to predict the degree of emulsion swelling after bleaching.

2.3.2. Laser Ablation. The formation of the amplitude and phase holograms in silver halide involves the use of photosensitizing dyes to increase the sensitivity to the laser light. However, the development of pulsed lasers with Q-switching (giant pulse formation) capabilities enabled production of light pulses with high peak power as compared to lasers operating in continuous wave mode.[118a] To reduce the complexity of the photochemical processing and allow the formation of holograms in hydrophobic materials, pulse lasers were employed.[92] In situ particle size reduction through laser ablation allows formation of diffraction gratings.[130] The first step in the preparation of the recording media involves doping the polymer with metallic nanoparticles or dyes that can absorb the laser light. To form a holographic grating, multibeam interference can be used with high-power (350 mJ, 6 ns) pulsed lasers, to selectively reduce the size of nanoparticles or dyes in the bright regions of the interference pattern[73] or form metal oxide shells on the nanoparticle surface,[131] which may create a refractive index contrast to produce a hologram. Factors such as power, laser wavelength, pulse duration, surface plasmon resonance of the nanoparticles, and their size influence the subsequent absorption of light by the nanoparticles, and the effectiveness of the laser-induced photochemical patterning.[132] In addition, the interaction between the laser light and the nanoparticles in situ may result in oxidation, particle diffusion within the emulsion, change in crystal structure, and particle redistribution.[130c,d,133] Although laser ablation offers practicality, holograms produced by this method have generally lower diffraction efficiencies than the holograms produced by silver halide-based photochemistry. Additionally, holograms formed through laser ablation are not compatible with a bleaching step. Holograms produced by this method are not limited to silver nanoparticles; other dyes or metallic nanoparticles such as gold, copper, tin, iron, nickel, and lead may be used.[134]

2.3.3. Photopolymerization. Although the silver halide-based hologram recording system is usually some 1−3 orders of magnitude more light sensitive than recording systems based on photopolymers, it does have some obvious disadvantages. Their major limitations include the cost of silver-based chemicals and the requirement for harsh postexposure chemical treatment to develop and stabilize or "fix" the holographic grating structure. To overcome these limitations, silver free systems have been developed.

dx.doi.org/10.1021/cr500116a | *Chem. Rev.* XXXX, XXX, XXX−XXX

Photopolymers are materials in which monomer molecules polymerize under the influence of light.[135] Typically, photopolymers are sensitized by adding a dye absorbing in the ultraviolet or visible region of the electromagnetic spectrum. After absorption of a photon, the excited dye molecule interacts with a free radical generator (initiator), which triggers polymerization. The conversion of monomer into polymer molecules leads to a change in the refractive index of the material. When the illuminating light field is spatially modulated, the photopolymerization is accompanied by a concentration gradient driven diffusion process. The final modulation of the optical refractive index n_1 is caused by (i) conversion of monomer into polymer; (ii) spatial density variation due to a concentration-driven monomer diffusion from dark to bright fringe areas; and (iii) spatial density variation due to concentration-driven short mobile polymer chains diffusing from bright to dark fringe areas. The diffusion of short polymer chains is particularly important at high spatial frequency of recording, because it leads to a nonlocal response in the material, and reduces its resolution.[136] In nanocomposite materials, there is a fourth process contributing to the final refractive index modulation: spatial redistribution of the nanoparticles.[137]

To record a hologram, the photopolymer coated glass or plastic substrate is located in the region where the object and the reference beams overlap in space. If these holograms are used in dry form, the recording is carried out in air. To achieve maximum brightness of the hologram, it is important to know the optimum intensity of the two recording beams. This is usually obtained by a study of the dependence of the diffraction efficiency of the hologram on recorded intensity.

To achieve high diffraction efficiency in photopolymers, it is necessary to find a fine balance between the monomer diffusion and polymerization rates. Recording in transmission mode requires using low intensity at low spatial frequencies, and increasing the intensity for recording at higher spatial frequencies. For example, when recording in acrylamide-based photopolymers at spatial frequency below 300 lines/mm, the optimum recording intensity is in the order of 1 mW/cm^2. For recording above 1000 lines/mm, the optimum recording intensity is in the range 5−10 mW/cm^2.[138] The intensities recommended above for recording in acrylamide-based photopolymer lead to close to 100% diffraction efficiency in layers with a thickness of 70 μm.

The spatial frequency in reflection mode of recording is in order of several thousands of lines (or cycles) mm^{-1}. This is a challenging regime of recording in photopolymers because of their nonlocal response to spatially modulated light. This means that the response of the material at one point in space and time depends on what happens at other points and times in the medium.[139] There are a number of models describing the behavior of photopolymers at high spatial frequency of recording. The nonlocal photopolymerization driven diffusion (NPDD) model[140] assumes that the chains grow away from their initiation point, resulting in "spreading" of the polymer. This model predicts that improvement at high spatial frequencies can be achieved if shorter polymer chains are created during the holographic recording. The use of chain transfer agents in the photopolymer mixture has been studied experimentally,[141] but the demonstrated improvement in diffraction efficiency is in order of few percent and the final diffraction efficiency is less than 20%. Alternatively, the two-way diffusion model,[136] which is also based on the nonlocal response of the materials, assumes that short polymer chains diffuse away from the bright fringes, thus reducing the refractive index modulation. Higher intensity of recording leads to a higher concentration of free radicals and a larger number of shorter polymer chains. Their migration from bright to dark regions leads to a lower refractive index modulation, and a lower diffraction efficiency of the recorded reflection hologram. Thus, high intensities of recording are not recommended in the reflection mode, unless an effective way of preventing the diffusion of the short polymer chains from bright to dark fringes can be implemented. To reduce the effect of short polymer chain diffusion, the permeability of the matrix should be controlled by choosing the appropriate concentration of the cross-linker, the initiator, and having a controlled amount of free radical inhibitors in the formulation. For acrylamide-based holograms, the optimum intensity of recording in reflection mode is 3−5 mW/cm^2, which leads to a diffraction efficiency in the order of 30%.[142] The final step in sensor fabrication is its exposure to UV light for up to 30 min, which is required to fully polymerize any remaining monomers and prevent further change of hologram's properties.

Photopolymerization can also be achieved using a UV laser to record a dry hologram in the UV region of the spectrum, and in aqueous solutions the same hologram diffracts light in the green region. This so-called double polymerization system allows the production of silver-free holographic sensors.[143] In this method, two polymerization steps are involved: (i) forming a polymer matrix (p1) and (ii) p1 must then allow the absorption of a highly photo-cross-linkable monomer (p2) such that the laser light can form a diffraction grating. First, a polymer film consisting of a cross-linker (~5 mol %) was free radical UV polymerized on a substrate. A concentrated cross-linker solution was then prepared and allowed to diffuse into the polymer. The resulting polymer/cross-linker system was exposed in a dry state to frequency tripled ND:YAG laser light of wavelength 355 nm. After the laser exposure, unpolymerized material in the dark fringes was washed away. This process allows the hologram to be visible, typically as a green light diffraction in aqueous solutions, in which the hologram expands.

Having a large proportion of cross-linking monomer in the second polymerization step results in a much harder and denser polymer; therefore, it has higher refractive index than that of the first polymer. Consequently, a bright holographic grating was obtained because the dark fringe regions still had the lower refractive index of the first polymer. However, this low refractive index in the nodes could only be achieved by preventing any additional cross-linking in the dark fringe regions due to free radicals migrating from the bright fringe regions. At 355 nm, one has the advantage also of the ease of production of particularly active free radicals. These active radicals not only polymerized the monomer in the antinodes, but also traveled into the dark fringe regions, where they were certainly not wanted. Addition of inhibitor or free radical scavenger to the monomer mixture effectively shortens the path length of the free radicals so that they would not travel beyond the bright fringe region.

The large refractive index modulation could produce highly diffraction efficient sensors.[143] If the recording material was in a relatively dry and unswollen state, the finished grating produced by exposing to a UV laser such as a frequency tripled Nd:YAG at 355 nm replayed the image at ~350 nm.[143] When placed in an aqueous solution at pH ~7.0, this hydrophilic hologram

replayed in a bright green color due to its capacity to swell when wet. Although this fabrication technique required the use of a high-cost (~$20−30k) frequency tripled Nd:YAG laser, continuous wave lasers operating in UV range could also be used.

Another photopolymerization technique involved the synthesis of a porphyrin derivative to record holograms with green laser light.[144] This study demonstrated a two-step process to fabricate holographic sensors. 5,10,15,20-Tetrakis[4″-(3‴-(acryloyloxy) propoxy)phenyl-4′-carboxyphenyl] porphyrin (TACPP) was synthesized with functional arms (acrylate groups) to covalently cross-link the porphyrin with the monomer (hydroxyethyl)methacrylate (HEMA) to form a recording medium. TACPP is a cross-linker and also serves as a light absorbing material. The sensors were fabricated in Denisyuk reflection mode using a single 6 ns Nd:YAG laser pulse (λ = 532 nm, 350 mJ) directed at the sample tilted at 5° from the surface plane of the recording medium. As the laser energy was absorbed by the TACPP molecules, pHEMA matrix was further cross-linked at the bright fringes. The final hologram had a diffraction grating, which was roughly one-half of the wavelength of the laser light.[144]

2.4. Readouts

2.4.1. Spectrophotometry. The most convenient way to interrogate a holographic sensor is through spectrophotometry, which allows quantification of the light diffracted or transmitted by the hologram as a function of wavelength (nm) or intensity (au). Most spectrophotometers are equipped with image sensors comprising a linear charge coupled device (CCD), and they are configured to measure the absorption profile.[145] In holographic sensing, specialized spectrophotometers, known as reflection spectrometers, are employed. Such detectors are capable of measuring the wavelength changes as well as the intensity of light, and convert it into an electrical signal. The interrogation of a holographic sensor through an absorption spectrophotometer is often not adequate because it can only measure the light that has not been diffracted by the hologram. This is less sensitive than measuring the diffracted light by the hologram as happens in the case of the reflection spectrophotometer. Therefore, a modified spectrophotometer setup was used, where both the angles of the incident light and the photodetector can be adjusted to interrogate the diffraction from the Bragg angle.[90] Hologram interrogation has been conducted with both flatbed and vertical sample placements. For vertical sample placement, the hologram is normally adhered to a supporting substrate, whereas a flatbed setup is preferred for free-standing thin films. Spectrophotometer setups generally include temperature and agitation control through a microflea stirring bar, and sample enclosure to prevent evaporation of the aqueous or gaseous analyte containing medium. Spectrophotometer measurements are performed in the dark or in controlled light conditions to avoid interference from the ambient light during measurements. For portable spectrophotometer setups, an enclosure is required so that the lighting conditions during readouts are consistent. Software packages for the spectrophotometric data acquisition of holographic readouts are capable of real-time measurements.

2.4.2. Determination of the Angle of Replay Wavelength. The holographic sensor can be recorded at different angles of the incident recording beams. For example, if the hologram is recorded from a mirror at ~5° with respect to the film plane in Denisyuk reflection mode, during the readouts when the hologram is illuminated perpendicular to the surface plane, the Bragg diffraction angle doubles (~10°) due to law of reflection (Figure 13). However, Snell's law also plays a role if

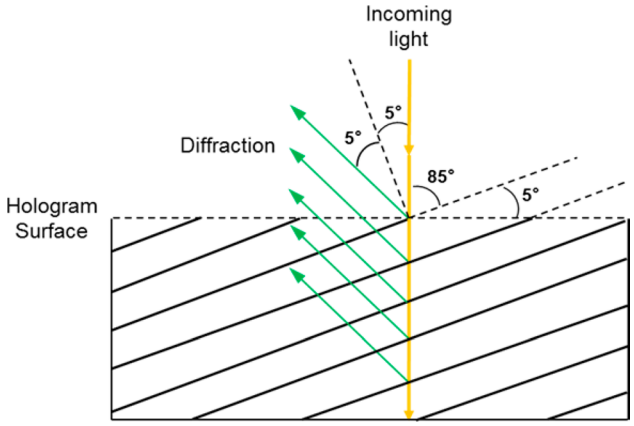

Figure 13. Proposed mechanism for the diffraction of light from a slanted grating. The hologram was illuminated with respect to the normal of the surface plane, resulting in diffraction with slanted angle doubling.

the hologram is illuminated with an angle with respect to the normal of the surface plane.[73] The angle of diffracted light with respect to the normal of the hologram depends on the quantity of the analyte measured because the uptake of the analyte will change the effective refractive index of the medium, and therefore it is important to know at what angle λ_{max} will be detected.

Traditionally, when a spectrophotometer is used to measure the diffracted wavelength from a hologram, it must be aligned with respect to the surface plane of the hologram. Adequate alignment of the spectrophotometer to obtain a holographic measurement can be tedious and time-consuming. This is the case even when the position of the hologram is well controlled on an optical bench in a laboratory setting. However, in practice, the hologram may be in a variety of possible orientations, where the position of the hologram or the diffraction angle of the Bragg peak is not well controlled. For these reasons, an optical system was developed to enable the measurement of the optical properties of a hologram, which is independent of the hologram's position and orientation.[146] The optical system allowed the viewing of light diffracted by the hologram in both image plane and focal plane of a lens. A combination of the images from the image plane and focal plane was used to determine the 3D position and the angular orientation of the holographic sensor.[146] Such a setup can enable the automated measurements of the diffracted light.

2.4.3. Digital Cameras. A digital photographic recording of the spatial distribution of light diffracted by the hologram when it is illuminated by white light at its Bragg angle can be used in analytical measurements.[147] If the digital camera utilized is appropriately calibrated, the wavelength measurement accuracy may be superior to 1 nm. If radiation from the hologram is spectrally narrow, spectrum over its surface can be determined by the colorimetric method. In digital photography, each pixel of a colored image corresponds to a specific color vector in the RGB (red, green, and blue) system. The average wavelength of the diffracted light could be determined from the photograph of a hologram. The digital camera is a colorimetric device that has

dx.doi.org/10.1021/cr500116a | Chem. Rev. XXXX, XXX, XXX−XXX

sufficient spatial resolution required for such measurements. The main limitations of using a commercial digital camera to measure the spectrum of a holographically diffracted light are that (i) the diffracted light must be narrow band and (ii) measurements must be performed in the spectral range in which at least two sensor types of the detecting array are simultaneously sensitive. In most digital cameras, the operating ranges are 470−540 and 570−600 nm for graphic output formats such as BMP, TIFF, and JPEG. For the unprocessed data obtained from the camera (i.e., RAW), data can be processed in the range between 455 and 625 nm. Depending on the wavelength and brightness of the image fragment, the mean square deviation of the wavelength can range from 0.3 to 3.0 nm.[147,148] Such readouts can also be achieved through smartphones, smartwatches, and other wearable technologies.[149]

2.4.4. Direct Readout. The advantages of holographic sensors are that they permit one to determine the presence/absence or concentrations of analytes both instrumentally and visually by direct readout.[150] Direct readout is particularly important in resource limited settings, where spectrophotometers are not readily available. Direct readout of holographic sensors is mainly utilized for yes/no or semiquantitative analyses. Visual inspection without the requirement for external equipment is an attractive attribute of holographic sensors. Such sensors can provide a response to a predetermined range of concentration of a substance or a group of substances to be sensed. Various holographic sensors have been designed that allow qualitative or quantitative measurement of analytes.[150] For example, when an alcohol sensor is breathed on, an existing image can disappear in the presence of alcohol, and a new image can indicate that the tested person should not drive.

2.4.5. Angular Tolerance. The use of a plane mirror with an offset angle allows the fabrication of holographic sensors that can be read from narrow ranges of viewing angle.[151] This limitation introduces a degree of complexity for the application that requires judging the position of the diffracted light with the eye. To overcome this challenge, optical components such as concave and convex mirrors and prisms were used to create lenses and diffusers that can prove improved control over the direction of the diffracted light.[152] This allows interrogation of the sensor from a wider range of angles and distances. For example, when a concave mirror is used as an object during laser light exposure, the hologram becomes a lens with a focusing effect on incident light. Such optical characteristics might allow the use of subcutaneous implants, which can be interrogated using a fiber optic bundle.

Holographers have long been familiar with the problem of recording the image of reflective objects with concave surfaces such as a polished silver teaspoon. A concave surface can focus the object beam, and its intensity may then exceed that of the reference beam at the focal point of the concave surface. This focusing causes overmodulation of the reference beam, so that the underlying standing wave pattern is no longer basically sinusoidal, but a square wave pattern in that focused region. Upon illumination with a white light source, this effect results in a broad selection of wavelengths occurring in that area, and the viewer typically sees a rainbow colored blob in that part of the image. In addition, convex mirror or beads allow creating lenses and diffusers that can enable the interrogation of the sensors from wide angles (30°).[152a] A problem with this approach is an unavoidable decrease in diffraction efficiency due to the dispersion of the object beam.

2.4.6. Lighting. Holography is a two-step process: recording of the interference pattern and the reconstruction of the image. To replay the image, the processed holographic plate should be illuminated by the reference beam to allow the reconstruction of the wavefront scattered by object during recording. This means that the characteristics of the reference recording and reconstruction beams must be identical in terms of spatial coherence, divergence, angle of incidence, and wavelength to construct a distortion-free holographic image.[61] For practical reasons, a conventional broadband white-light source is used to illuminate reflection holograms. This allows the use of the wavelength selective properties of the reflection hologram to filter out light with wavelength different from that of the recording light. When the holograms are illuminated with a white light source, which is diffuse and is not a point source, blurring will occur, which compromises the clarity and depth of the reconstructed image.

During the recording of the hologram, the laser light is usually spatially filtered using a pinhole with a diameter of 10−25 μm, which is several orders of magnitude smaller than the size of a white light source. This is to "clean the beam", which otherwise would usually be blemished by dust particles on the lenses, causing concentric ring patterns on the image. Halogen spotlights have source sizes of 1−2 cm. Such a low spatial coherence in the illumination source can cause source-size blurring, unless the source is at a sufficient distance from the hologram. To minimize source-size blurring, the reconstruction source size must be less than 1 mm in diameter for every 1 m of diagonal distance that separates from the illumination source and any point on the hologram.[44c] However, in the case of pulsed lasers, the high powers make spatial filtering a problem, and work is carried out satisfactorily despite the inevitable blemishes in the beam profile. Extremely high powers damage the pinhole of the spatial filter, whereas in the case of the continuous wave lasers, the energy is dissipated more readily.

2.5. Capabilities

2.5.1. Miniaturization. Holographic sensors can be miniaturized to construct arrays that may be used for multiplexing. Such approaches are possible through contact printing, microfluidics, and printing. It was previously shown that an array of 3 mm spot holographic sensors can be produced using contact printing.[153] In this study, a mask comprising fluorinated ethylene-polypropylene polymer was used to define the spot locations in which HEMA monomers were photopolymerized. The oxygen dissolved in fluoropolymer inhibited free radical polymerization in the masked regions, which eventually allowed the formation of holographic spots (circular regions). Another study involved the production of a polymer matrix, which later was spotted with amino-linked (10 base oligonucleotide).[153] In the constructed array, the spotted regions contained immobilized DNA.

Holographic sensors were also integrated into microfluidic devices to allow multiplexing and quantification of samples at low volumes. For example, cross-shaped channels (5 mm width × 75 μm depth) were micromachined to form a multiplex holographic assay, where each channel quantified 10−30 ppm water in hexane (5 mL).[154] In the same study, another hemispherical microfluidic channel−hologram system was configured to provide a semiquantitative readout of the sample concentration. As the water droplets traveled along the flow channel, the concentration of kerosene in water was measured from 30 to 120 ppm.[154] Such devices can be constructed with

dx.doi.org/10.1021/cr500116a | Chem. Rev. XXXX, XXX, XXX−XXX

multiple inlets or outlets for multiplex high-throughput applications.[155] Furthermore, holographic sensors can be integrated into a PDMS-based microfluidic bioreactor for continuous monitoring applications.[156]

2.5.2. Image Formation and Concealment. One of the most important attributes of holographic sensing includes image formation, which is not attainable by other Bragg grating-based optical sensing platforms. However, holographic sensors have the potential to go beyond this capability and display multiple images in response to analytes. This is particularly useful in applications in which an image needs to be revealed by a deliberate, chemically specific action to remove or alter the properties of an index matching layer. Such an optical characteristic can be useful in verifying the authenticity of a product to which the hologram is attached. The holographic sensor may comprise an image former, which allows the appearance of an image when the holographic matrix contacts with external stimuli.[107] On the other hand, an image concealer can act to attenuate the holographic image. The same hologram can also be programmed to replace an existing image with another image.

2.5.3. Formation of a Sensitivity Gradient. A sensor may comprise a heterogeneous structure, in which the degree of analyte sensitivity varies in a single holographic element. Such an approach may allow the sensor to exhibit a scale of responses due to the plurality of zones of different properties/reactivities. The heterogeneity may be formed by varying the degree of polymerization through the medium.[157] For example, the medium may comprise highly cross-linked or/and relatively less cross-linked regions. This may be accomplished by impregnating a preformed polymer matrix through pipetting with a cross-linker solution to form spots or by dipping specific regions of the polymer matrix into a cross-linker solution; the polymer matrix can be further polymerized to obtain a varying cross-linking density. Similarly, the functional groups attached to a polymer can be varied to form a gradient, where specific areas of the polymer are more responsive to the target analyte than other regions.[157] For example, a polymer comprising HEMA, aminoethyl methacrylate (AEMA), and EDMA monomers can be copolymerized, to obtain a medium with amino functional groups, which is readily modified. Next, the resulting polymer can be immersed incrementally into a buffered succinic anhydride solution (pH 7.0). The longer the medium is treated, the larger is the range of wavelengths attained for a given pH range.

3. SENSING APPLICATIONS

Holographic sensors consist of three-dimensional networks of functionalized polymers to quantify the concentration of various target analytes (Table 3). They can be utilized in two ways to act as a sensor: (i) altering the periodic spacing of the recorded lattice constant leading to a change in the spectral position of the Bragg peak in reflection holograms, and (ii) the alteration of diffraction efficiency due to a change in the refractive index modulation, which also leads to a spectral change, although significantly smaller than the one caused by volumetric change (see Bragg's law). Changes in lattice spacing and the refractive index modulation are induced due to a physical or chemical interaction between the chemical constituents of the polymer matrix and the target analyte. As the polymer swells, the angular position of the diffracted light also changes. On the basis of the recording mode, an image can appear, disappear, or be replaced by another image (i.e., superpositioning) as a consequence of the presence of a target analyte.

Table 3. Holographic Sensors and Their Target Analytes

category	analytes
ions	pH,[72,73,79,156,158] (Na^+, K^+),[120,159] divalent metal ions (Ni^{2+}, Zn^{2+}, Co^{2+}, Ca^{2+}, Mg^{2+}),[160] (Pb^{2+}, Co^{3+}),[158] periodate (IO_6^{5-}),[120] (Cu^{2+}, Fe^{2+})[144]
metabolites	glucose,[86a,c,d,158,161] lactate,[86b,162] urea,[163] acetylcholine,[99,100] testosterone[164]
enzymes	trypsin[70c,90] and amylase[120,134]
drugs	penicillin G[163,165]
physical parameters	pressure[166]
microorganisms	calcium dipicolinate[167]
gases	O_2,[161a] N_2,[95] alkanes, alkenes, alkynes,[92,94] and ammonia (NH_3)[168]
others	water activity in solvents,[70b] organic solvents,[144] alcohol,[85,120] humidity,[70a,74,169] temperature,[71,74] ionic strength,[170] anthraquinone-2 carboxylate,[161a] light,[166,171] magnetic field[166]

Transmission phase holograms require a monochromatic light source, a photodetector, and electronic circuitry to measure the diffraction efficiency or the direction of the diffracted light by using position sensitive photodetection. On the other hand, reflection holograms can be illuminated by a white light source, and a change in color can be monitored by the eye. The sensor can also be calibrated on the basis of the wavelength of the spectral peak of the diffracted light.

3.1. Organic Solvents

One of the earliest works on holographic sensors demonstrated the feasibility of measuring water in hydrocarbon solvents.[70b] This study involved forming a Denisyuk reflection hologram in a commercial gelatin-based holographic plate using a HeNe laser. In this work, the shrinking/swelling activity of the hologram in the presence of different mixtures of water and solvents was monitored using a spectrophotometer. The diffracted light from the sensor changed as a function of the water activity when the hologram was immersed in a wet hydrophobic liquid. The holographic sensor allowed the measurement of water content of hydrocarbon solvents at high sensitivities over a wide range of water concentrations. For example, a visual color change was observed when the water content in xylene was increased from 47 to 120 ppm.[70b] Similarly, 0−1% (w/w) ethanol in water was monitored, and visual color changes were observed. This study showed a proof of concept of holographic water sensor for hydrophobic liquids.

Quantification of alcohol content using a holographic sensor was also described. In this study, a diffraction grating was formed in a pHEMA film.[85,120] The performance of the sensor was demonstrated by measuring the alcohol contents of a range of alcoholic beverages including wines and beers, without sample pretreatment. The measured concentrations of the beverages were determined to be within ∼0.3 vol % of their stated values. It was also shown that the sensor was relatively insensitive to pH in the range 3−6.5 and highly stable, which is a requirement for use and in storage. Additionally, the sensor was unaffected by highly colored and turbid samples. Important contributions of this study to the literature were the employment of pHEMA, which is widely used in the contact lens industry, and the diffusion technique that allowed the formation of light-sensitive silver halide crystals in pHEMA matrix.[78]

dx.doi.org/10.1021/cr500116a | Chem. Rev. XXXX, XXX, XXX−XXX

Nanoparticle free holographic sensors were also used to quantify organic solvents.[144] In this study, a sensor was fabricated through dye-based photopolymerization, and its response to variation in organic solvent concentration was tested. The sensor responded within the visible region of the spectrum ($\lambda_{max} \approx 520-680$ nm) with a response time within 50 s. The tested organic solvents included ethanol, methanol, propan-2-ol, and dimethyl sulfoxide (DMSO) in DI water (0.0−10.0%, v/v). The recorded wavelength shifts were 100, 48, 162, and 56 nm for 10.0% (v/v) ethanol, methanol, propan-2-ol, and DMSO, respectively.[144] Response time and recovery times for 10.0% (v/v) ethanol, methanol, propan-2-ol, and DMSO were ∼50 s, ∼60 s; ∼30 s, ∼40 s; ∼50 s, ∼50 s; and ∼10 s, ∼20 s, respectively. Figure 14 illustrates the colorimetric response of the sensor to ethanol in DI water (0.0−10.0%, v/v).

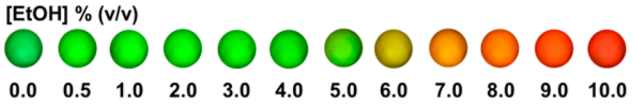

Figure 14. Nanoparticle free holographic sensor response to a variation in ethanol concentration (0.0−10.0%, v/v). Reprinted with permission from ref 144. Copyright 2014 Royal Society of Chemistry.

In comparison to holographic sensors, carbon nanotubes have been shown to respond to a variety of organic solvents. For example, carbon nanotube ethanol sensors were reported to operate at detection limits ranging from 1.1 to 300.0 ppm.[172] While these sensors provide ultrasensitivity to detect low concentrations of ethanol, they have a tendency to saturate at high concentrations of ethanol. Another drawback of the use of carbon nanotubes for sensing applications is that they exhibit hysteresis, and the sensor response is subject to drift.[172] However, holographic sensors can operate at concentrations up to 10% (v/v) ethanol in aqueous solutions, while the sensor response is reversible with no hysteresis.[85,144]

3.2. Humidity

The sensitivity of holographic recording materials to humidity has been known for many years.[67,173] In silver halide materials, for instance, humidity control has been used to achieve color control in reflection holograms.[67] Special care to avoid exposure to high humidity is required for other materials as it destroys the recorded hologram.[173] The design of a hologram-based humidity sensor requires a unique combination of properties of the holographic recording material, high sensitivity to humidity combined with resistance to damage by humidity. A humidity sensor using a wavelength-dependent holographic filter with fiber optic links has been reported.[70a] However, the sensor medium, gelatin-based (AGFA film), was characterized by a strong hysteresis in humidity response, temperature dependence, and variable sensitivity, and reported as unsuitable for use in a sensor.

The ability of reflection holograms recorded in acrylamide-based photopolymer to detect a change in the relative humidity of their environment has been demonstrated and characterized.[71,74,169] The material used in this study was a self-processing acrylamide-based photopolymer.[98b,174] Further studies reported humidity indicators comprising an optimized photopolymer composition for recording in reflection mode.[71,169a,175] The maximum diffraction efficiency of the reflection type sensors recorded with a standard two-beam holographic setup was 30%. Humidity indicators incorporating a holographic image of an object were recorded as Denisyuk type holograms.

A controlled environment chamber with humidity control system was used to characterize the response of the reflection holograms. The relative humidity (RH) in the chamber was maintained at a preset point in the range of 5−90% RH with an accuracy of ±1% RH. The probe light from a broad band light source was fiber guided into the humidity chamber. The light diffracted by the hologram was then coupled into a second fiber by a lens and guided to a spectral analyzer. Figure 15a shows the colorimetric response of the hologram at different humidity levels.

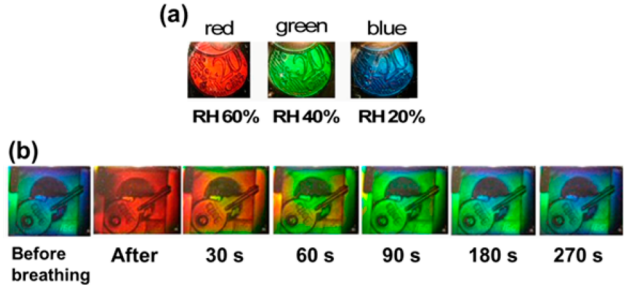

Figure 15. A holographic humidity sensor. Color appearance of a sensor (a) at different humidity levels (b) before and after breathing on it. Reprinted with permission from ref 169a. Copyright 2008 AIP Publishing, LLC.

It was observed that the indicator's response to humidity was completely reversible in the range from 5% to 80% RH. The response time of the indicators was found to depend on their matrix thickness. After thickness optimization, a response time in order of few seconds was achieved, and holograms that can change color after breathing on them were fabricated (Figure 15b). It was observed that the calibration curve of the sensor can be shifted by exposure to elevated temperature or by recording at a different relative humidity.[71]

Recent studies of transmission holograms exposed to relative humidity above 80% revealed that their response at high humidity strongly depends on temperature.[169b] The response is reversible at temperatures below 8 °C. Above this temperature, the diffraction efficiency of the gratings irreversibly decreases due to an irreversible change in grating's thickness, and due to up to a 75% decrease in refractive index modulation.

Zeolite was also employed in constructing holographic humidity sensors. The optical properties of zeolite AEI-($AlPO_4$-18)-doped photopolymer layers combined with the redistribution of the AEI nanoparticles during holographic recording have been used for fabrication of an irreversible humidity sensor based on a transmission holographic grating. It has been demonstrated that the diffraction efficiency of the sensor changes permanently after exposure to high humidity.[176] Achievement of higher nanoparticle concentration in the layer and improved redistribution is needed to increase the irreversible change of the diffraction efficiency.

3.3. Temperature

The sensitivity of reflection holograms to temperature has also been investigated.[71,74] A controlled environment chamber with humidity and temperature control system was used in this study. The temperature in the chamber was varied between 15 and 50 °C and maintained within 0.1 °C of the preset point.

dx.doi.org/10.1021/cr500116a | Chem. Rev. XXXX, XXX, XXX−XXX

Since the samples were also sensitive to humidity, the relative humidity in this experiment was kept constant. For relative humidity below 30% RH, there was little or no temperature dependence of the response. At 45% RH, a 25 nm shift of the spectral peak wavelength was reported for samples exposed to a temperature ranging between 15 and 50 °C. Obviously, for fabrication of practical devices, a material that is not sensitive to humidity should be sought, which may require the modification of the chemical composition of the holographic recording material.

3.4. Ionic Strength

The detection and monitoring of electrolytes and ionic strength are important in many medical, environmental, and biotechnological applications. Currently, low-cost, mass producible point-of-care diagnostic and environmental systems are needed for continuous and reusable electrolyte and ionic strength measurement. In addressing this need, holographic sensors were recorded in acrylamide-based thin films containing negatively and positively charged sulfonate and quaternary ammonium monomers, respectively.[170] The positively charged monomers contained (3-acrylamidopropyl)trimethylammonium chloride (ATMA) (20 mol %) (Figure 16a), and

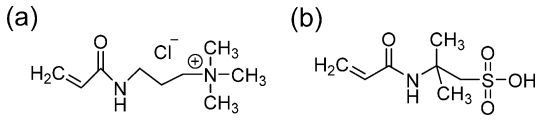

Figure 16. Monomers for the construction of a holographic ionic strength sensor: (a) 3-acrylamidopropyl)trimethylammonium chloride (ATMA) and (b) 2-acrylamido-2-methyl-1-propanesulfonic acid (AMPS).

the negatively charged monomers contained 2- acrylamido-2-methyl-1-propanesulfonic acid (AMPS) (Figure 16b). Hybrid mixtures containing both ATMA (10 mol %) and AMPS (10 mol %) were also prepared.

The diffracted peak wavelengths from these holograms allowed the measurement of variation in ionic strength of solutions based on the swelling and deswelling of the polymer matrix. For example, a change in the concentration of Na^+ from 1 to 500 mM caused a Bragg peak shift of 60 nm in a pAAm hologram containing MBA (5 mol %) as cross-linker, ATMA (10 mol %), and AMPS (10 mol %) at 30 °C. These acrylamide-based holograms containing equal molar concentrations of the negatively and positively charged monomers were capable of determining ionic strength independently of the ionic species present. These holographic sensors showed a diffraction wavelength of 1 and 7 nm to variation in pH in the range of 3−9 and temperature between 20 and 45 °C, respectively. Additionally, these sensors were fully reversible and free of hysteresis. For practical applications, the sensors displayed the capability of quantifying ionic strength in milk solutions, which are complex ionic biological mixtures.[170] In this application, when the ionic strength of the milk is decreased by serial dilutions of 1:1 and 1:9, the diffraction wavelength shifted about 12 and 23 nm from the original peak position.

3.5. Ions

3.5.1. H^+. The determination of pH is important in the biomedical, environmental, agricultural, food, beverage, and biotechnology industries. pH-sensitive holographic sensors comprise Bragg gratings and polymers that are functionalized with acidic and basic monomers within the polymeric backbone.[79,120] When these pendant functional groups are ionized (e.g., protonating carboxylic acid groups), the polymer swells or shrinks due to the electrostatic and Donnan osmotic pressure forces that can draw in or expel counterions along with water molecules, resulting in a change in the spatial period of the diffraction grating. This increase or decrease in the lattice spacing results in a shift of the Bragg peak to longer or shorter wavelengths. This systematic volume alteration consequently allows a quantitative readout through wavelength changes of the diffracted light, enabling spectroscopic measurement of color changes as a function of pH. There are a number of pH-sensitive holograms fabricated in pHEMA and pAAm systems. When ionizable groups are copolymerized with other monomers, their individual functions dictate the degree of pH-sensitivity of the holographic sensor. These sensors have been shown to produce a visually perceptible and reversible color change at either side of the apparent dissociation constant (pK_a) as a function of the pH. The range of the pH sensitivity can be adjusted by selecting the desired acidic and basic monomers to cover the pH range of the application of interest. The sensor can be calibrated on the basis of the Henderson−Hasselbalch equation.[177] A typical prepolymer solution consisted of the monomer (e.g., HEMA), cross-linker (e.g., EDMA), and the functional group (e.g., MAA), as well as DMPA in an appropriate solvent.[72] The functional groups can be chosen from methacrylic acid (MAA), trifluoromethyl propenoic acid (TFMPA), dimethylaminoethyl methacrylate (DMAEM), and vinyl imidazole to achieve the desired pH range from 2.0 to 9.0.[79] However, the pH-sensitive sensors can be affected by variation in ionic strength; therefore, they may be coupled with an ionic strength sensor.[170] Optimized pH sensors showed milli-pH resolution. Figure 17a illustrates pH sensors fabricated by silver halide chemistry, displaying visually perceptible and reversible color changes for different pH values.[72]

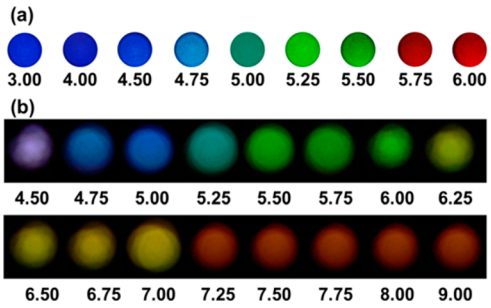

Figure 17. Photographic images of pH sensors. (a) The colorimetric response of sensors fabricated by silver halide chemistry to pH changes in phosphate buffers. Reprinted with permission from ref 72. Copyright 2014 Royal Society of Chemistry. (b) The colorimetric response of sensors fabricated by laser ablation to pH variations in artificial urine samples. Reprinted with permission from ref 73. Copyright 2014 Wiley-VCH Verlag GmbH&Co. KGaA, Weinheim.

Application of this sensor was demonstrated in quantifying the change in H^+ concentrations in real time in a milk sample undergoing homolactic fermentation in the presence of *Lactobacillus casei*. Because holographic pH sensors are amenable to miniaturization, they have been integrated into a PDMS-based microfluidic bioreactor to monitor the pH change caused by *Lactobacillus casei* in real time.[79,156] The accuracy of

dx.doi.org/10.1021/cr500116a | *Chem. Rev.* XXXX, XXX, XXX−XXX

the sensor was shown to be ±0.02 pH units, and the sensor response did not exhibit any hysteresis. Recently, pulsed laser ablation was used to produce pH-sensitive holographic sensors in Denisyuk reflection mode.[73] Clinical application was demonstrated through testing acid−base balance in artificial urine samples, which allowed the measurement of pH in the entire visible spectrum (Figure 17b).

3.5.2. Metal Ions. Complexation of metal ions with chelating agents is employed in separation, removal of specific species, ion-selective electrodes, biological mimics, and reaction catalysts.[178] Commonly used species of complexation agents are crown ethers, which consist of cyclic compounds that comprise ether groups. The field of crown ethers dates back to Pedersen's pioneering work in 1967.[179] These cyclic polyethers form stable complexes with cations selectively based on ion−dipole interaction between the cation and negatively charged oxygen atoms of the polyether ring.[180] These crown-metal complexes, also referred to as host−guest chemistry, are dictated by the chelate effect (entropy),[181] macrocyclic effect,[182] geometrical factors,[183] classification of donor atoms,[184] and ionic radius.[185] Crown ethers have different binding strengths and selectivities for metal cations. The multistep Eigen−Winkler mechanism[186] is an expression used to explain the complexation of metal cation and crown ethers.

$$M^+ + L \rightleftarrows M^+{-}L \rightleftarrows M^+L \rightleftarrows (ML)^+$$

where M^+ represents solvated metal ion, L is free macrocyclic ligand, $M^+{-}L$ is metal−macrocyclic ligand pair in solvent, M^+L is the contact pair, and $(ML)^+$ is the final complex. Although the complexation can be simplified by the multistep Eigen−Winkler mechanism, metal ion recognition and selectivity of the crown ethers are known to be more complex.

Holograms have been fabricated in the silver halide system, and incorporation of chelating agents was investigated to develop ion-selective sensors for applications in biomedical sensing and environmental monitoring.[120,159] To incorporate crown ethers in holographic sensors, functional groups allowing copolymerization of crown ether derivatives into the recording media were needed; hence, methacrylated crown ethers were synthesized.[159] These studies involved synthesis of methacrylate esters of homologous series of hydroxyether crown ethers and their copolymerization with hydroxyethyl methacrylate in the presence of a cross-linker (i.e., ethylene dimethacrylate) to form a chelating hydrogel film. The crown ether tests included 12-crown-4, 15-crown-5, and 18-crown-6 pendant functionalities, and were shown to respond to alkali and alkaline earth ions with varying specificity.[159] Table 4 shows the ionic radii of Li^+, Na^+, K^+, and Cs^+ cations, and the corresponding cavity diameters of crown ethers. For example, holograms comprising 18-crown-6 were shown to respond linearly to K^+ ions over the physiological range (3.5−5.0 mmol/L for blood, 25−100 mmol/24 h for urine),[187] while the sensor response was not affected by physiological variations in background Na^+ ion concentrations (∼130−150 mM).[159] The optimized hologram containing 18-crown-6 (50 mol %) showed swelling behavior as a function of complexation in the presence of ≤30 mM metal ions, exhibiting ≤200 nm of Bragg peak shift within 30 s, highlighting its potential to be used in the quantification of electrolytes in biological samples. However, the selectivity of the other crown ethers was shown to be limited. The feasibility of functionalizing hydrogels with crown ether derivatives has been demonstrated previously in CCAs.[7,188] 4-Acryloylamino-benzo-18-crown-6 and acrylamide were copolymerized to form CCA matrixes, which allowed selectively sensing Pb^{2+}, Ba^{2+}, and K^+ ions. For example, a ∼13 mM K^+ ions produced a red Bragg peak shift of ∼100 nm.[188] The Bragg shifts obtained in holographic sensors showed a 34 nm shift for the same concentration of K^+ ions in CCA.[159] Another CCA-based sensor displayed 125 and 200 nm of red Bragg peak shifts in the presence of 13 and 40 mM K^+ ions, respectively.[189] The differences in Bragg peak shifts may be attributed to the employment of different polymer matrixes, pHEMA and pAAm in holographic sensors and CCA, as well as variation in cross-linking densities. Another study showed that holographic recording media based on copolymers of acrylamide with ionogen comonomers are sensitive to Pb^{2+} and Co^{2+} ions (10^{-5} M), whereas the sensor's sensitivity to Mn^{2+} and Sr^{2+} ions was 2 orders of magnitude lower.[158] Additionally, the response to alkali metal ions (Na^+, K^+) was an order of magnitude lower than Pb^{2+}. CCA system was also used in sensing Pb^{2+} ion concentration of 10 mM, displaying a red Bragg shift of ∼160−215 nm.[190]

Further studies in holographic sensing with chelating agents investigated incorporation of a methacrylated analogue of iminodiacetic acid (IDA), which was copolymerized with HEMA to form a pHEMA-based recording medium for the detection of divalent metal ions such as Ca^{2+}, Mg^{2+}, Ni^{2+}, Co^{2+}, and Zn^{2+}.[160a] This study involved the use of silver halide chemistry and the diffusion method. The effects of varying the active monomer, concentration of cross-linker, pH, and ionic strength on the sensor response were studied. Polymers containing >10 mol % chelating monomer and 6 mol % cross-linker showed a Bragg peak shift of up to 46.3 nm within 30 s at an ion concentration of 0−40 mM. The relative Bragg peak shifts of the holograms toward different ions tested were Ni^{2+} (46.3 nm) > Zn^{2+} (35 nm) > Co^{2+} (33 nm) > Ca^{2+} (15 nm) > Mg^{2+} (12 nm). The real-time reversible response of the sensor was demonstrated in monitoring Ca^+ ion efflux during the early stages of germination of *Bacillus megaterium* spores.[160a]

Porphyrin was also used as a chelating agent for sensing metal ions.[144] The sensor was used to quantify variation in Cu^{2+} and Fe^{2+} cations in the concentration range of 0.05−1.00 mM and produced blue Bragg shifts of 5.24 and 4.66 nm, respectively.[144] The sensor required ∼30 s to equilibrate (±subnanometer), and the mechanism was reversible without hysteresis. However, the system was found to be insensitive to low concentrations (<10 mM) of metal ions because the amount of porphyrin molecule in the polymer matrix serves as the chelating agent as well as the cross-linker, which limits the swelling of the polymer matrix. Hence, the design of pendant chelating agents may increase its sensitivity.

3.5.3. Periodate. Periodate (IO_6^-) is an anion consisting of iodine and oxygen, and it is widely used in redox reactions

Table 4. Cations, Cationic Diameters, and Crown Ether Cavities

cation	cation diameter (Å)[a]	crown ether	cavity diameter (Å)[b,c]
Li^+	1.36	12-crown-4	1.2−1.5
Na^+	1.94	15-crown-5	1.7−2.2
K^+	2.66	18-crown-6	2.6−3.2
Cs^+	3.34	21-crown-7	3.4−4.3

[a]Cation diameters were obtained from ref 191. [b]Corey−Pauling−Koltun atomic models.[192] [c]Fisher−Hirschfelder−Taylor models.[193]

dx.doi.org/10.1021/cr500116a | Chem. Rev. XXXX, XXX, XXX−XXX

involving organic and inorganic compounds, as an indicator for catalytic-kinetic analysis.[194] A holographic sensor consisting of methacrylamide, acylamide, *N*,*N*′-(1,2-dihydroxyethylene) bis-(acrylamide), and thioindigo vat dye in its leuco form was copolymerized.[120] The samples were treated with silver nitrate, and then dipped in a bromide bath for a minute, followed by exposure to the laser light, development, and fixation. The resulting holograms responded to $NaIO_4$ (0.1 M) in 30 min through swelling by the cleavage of the vicinal diol functionality in the cross-linker by the periodate anion.[120]

3.6. Glucose

Early diagnosis and monitoring of diabetes allows treatment and self-monitoring through quantification of glucose concentrations in biological fluids.[195] Most diabetics exhibit hypo/hyperglycaemia requiring tight control of blood glucose concentration.[196] However, diabetics are required to take regular blood glucose measurements by finger pricking, up to five times a day. This invasive practice reduces the rate of patient compliance and results in less effective glycaemic control. According to the International Diabetes Federation, there are 175 million undiagnosed diabetic patients, 80% of which live in low- and middle-income countries.[197] Currently, there is an ever increasing need for noninvasive glucose monitoring.

3-(Acrylamido)phenylboronic acid (3-APB) forms reversible covalent bonds with *cis*-diol units of lactate, glucose, fructose, and other carbohydrates.[86a] Boronic acid (pK_a = ~8.8) at low pH values is in an uncharged and trigonal planar configuration (1), while at higher pH values (pH > pK_a) the trigonal form can react with OH^- to form the more stable negatively charged tetrahedral state (2), which can bind to *cis*-diol groups more readily (3−4) (Figure 18).[198] Early studies in a colloidal crystal

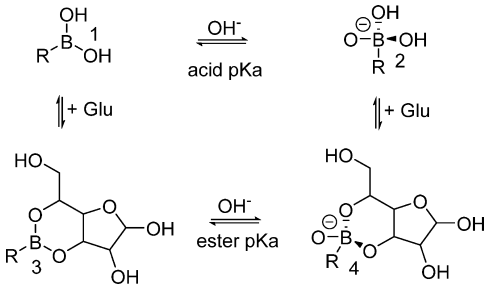

Figure 18. Simplified illustration of the complexation equilibrium between the boronic acid derivatives and glucose. Glu = glucose. Reprinted with permission from ref 199. Copyright 2003 American Chemical Society.

array platform showed that the binding of *cis*-diol results in the formation of boronate anions and subsequent swelling of the hydrogel through a Donnan osmotic pressure increase.[199] This swelling increases the recorded grating spacing, which shifts the narrow-band diffraction peak to longer wavelengths. However, the requirement for conventional boronates posed a challenge at physiological pH values.

Holographic sensors comprising pAAm matrixes functionalized with 3-acrylamidophenylboronic acid (3-APB) have been fabricated, and their sensitivity was optimized for glucose detection using reflection holograms.[161a] The maximal sensitivity at a 3-APB concentration of ~20 mol % was observed.[86a,161c] The hologram displayed a monochromatic red shift in diffraction peak wavelength as a function of glucose concentration (2−10 mM) across the physiological range.[158] When the glucose molecules perfuse into the holographic matrix, the pK_a of the boronic acid−glucose complex decreases systematically through the stabilization of the charged tetrahedral phenylboronate anion. As a result of producing charged groups, the Donnan osmotic pressure of the polymer increases, causing the hologram to absorb more water. Subsequently, the hologram swells, and its Bragg peak shifts to longer wavelengths (Figure 19a−c).

The glucose and *cis*-diol binding is reversible due to the formation of the covalent bond in aqueous media. When the hologram is rinsed with glucose-free solution, the hologram contracts and the Bragg peak wavelength returns to its original value. Such a capability allows the sensor to be used in continuous real-time sensing of dynamic changes in glucose concentration. However, a serious challenge with 3-APB is that it also binds to other *cis*-diol containing species (e.g., fructose) and lactate in the biological fluids.[86b] For example, the interaction of fructose or lactate with the phenylboronic acid may lead to an artificially elevated glucose readout. An additional limitation of hydrogel-based holographic sensors is the dependency on ionic strength; solutions with higher ionic strength cause contraction of the polymer matrix.[158]

To overcome the specificity and pH-sensitivity issues, holographic sensors incorporating new boronic acid derivatives that bind to glucose in physiological pH values have been developed. For example, 2-acrylamidophenylboronate (2-APB) was synthesized, and its mechanism for binding to glucose was investigated.[161d,h] This study has shown that 2-APB predominantly adopts a zwitterionic tetrahedral form at physiological pH values, and it has a tendency to complex with glucose rather than lactate. The same study also showed that the binding mechanism of 2-APB to glucose was unaffected by the pH variation within the physiological range. Further studies investigated circumventing fructose interference. For example, the incorporation of tertiary amine monomer or quaternary monomer (i.e., (3-acrylamidopropyl)trimethylammonium chloride (ATMA)) into holographic sensors containing phenylboronic acids resulted in improved selectivity for glucose.[161i,200] In a follow-up investigation, the concentration of blood glucose was quantified in vitro.[86c] This study involved a hologram comprising acrylamidophenylboronic acid and ATMA to measure human blood plasma samples at concentrations of 3−33 mmol/L over an extended period for application in real-time continuous monitoring (Figure 20). The results showed that the sensors have a performance comparable to that of electrochemical sensors, without lag or hysteresis. Additionally, the measurement accuracy was not affected in the presence of common antibiotics, diabetic drugs, pain killers, and endogenous substances.[161l]

Another study investigated the use of holographic glucose sensors in urinalysis.[86d] Laser ablation in Denisyuk reflection mode was used to fabricate the diffraction gratings in acrylamide-based holograms. Holographic sensors comprising 3-APB (10−20 mol %) were initially shown to work in artificial urine samples, then tested with human urine samples. These holographic sensors exhibited reversible Bragg peak shifts within the range of 510−1100 nm. In using a sensor with 3-APB (20 mol %), the base Bragg peak was ~565 nm for glucose-free artificial urine, and additions of up to 10.0 mM glucose red-shifted the peak by 21, 81, 356, 379, and 420 nm at pH values of 7.00, 7.25, 7.40, 7.75, and 8.00.[86d] The diffracted light was visible by eye, and it shifted from green to yellow to

dx.doi.org/10.1021/cr500116a | *Chem. Rev.* XXXX, XXX, XXX−XXX

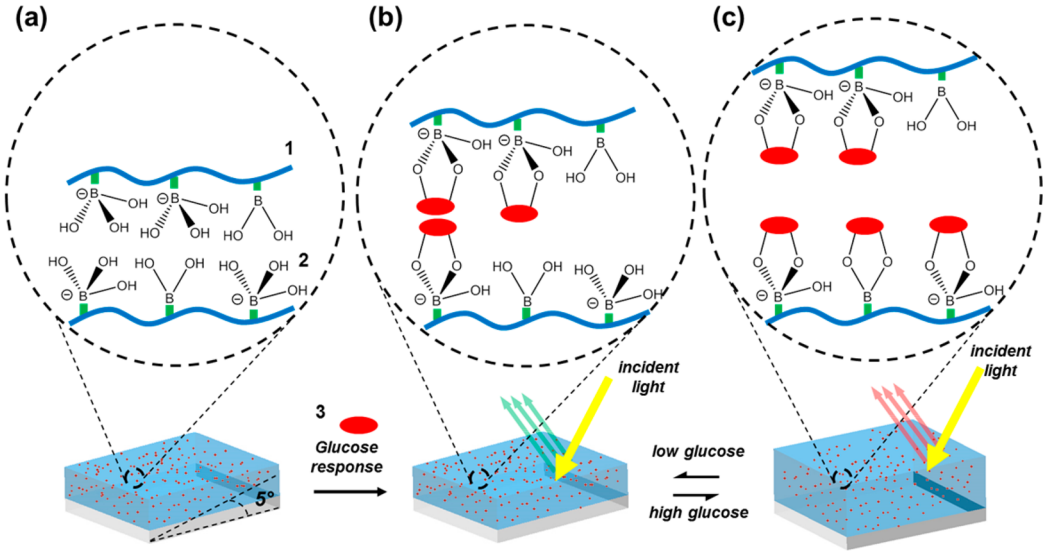

Figure 19. Principle of operation of the holographic glucose sensor. The device consists of pAAm-based hydrogel (**1**) functionalized with 3-APB (**2**) for sensing glucose (**3**). (a–c) Reversible swelling and shrinking of the holographic sensor by glucose changes the Ag^0 NP lattice spacing, and shifts the diffracted light from short to longer wavelengths as the pAAm matrix swells in the direction normal to the underlying substrate. Reprinted with permission from ref 86d. Copyright 2014 American Chemical Society.

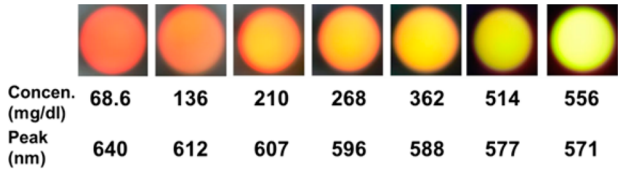

Figure 20. Readout of a holographic glucose sensor comprising 3 mol % MBA, 12 mol % 3-APB, 12 mol % ATMA hologram in human blood plasma, as a function of glucose concentration (pH 7.4 and 37 °C). Reprinted with permission from ref 86c. Copyright 2007 American Association for Clinical Chemistry.

orange to red before moving into near-infrared. At pH 8.00, a minimum detection limit of 90 μm was achieved. The control experiments were conducted by varying the concentrations of lactate and fructose to assess the potential interference. For example, in the presence of 1.0 and 10.0 mM lactate, the sensor (20 mol % 3-APB) produced Bragg peak shifts of 15 and 125 nm, respectively. Sensors comprising 20 mol % 3-APB produced Bragg peak shifts of ~115 and ~260 nm in the presence of 1.0 and 2.0 mM fructose, respectively.[86d] The experimental sensitivity of the sensor (10 mol % 3-APB) allowed diagnosis of glucosuria in the urine samples of diabetic patients. The sensor performance (R^2 = 0.79) showed improved accuracy as compared to commercial colorimetric dipsticks (R^2 = 0.28) read by automated readers and comparable accuracy with fully automated clinical chemistry systems. It was also found that the average concentrations of lactate and fructose in urine were 0.27 mM and 23.18 μM, respectively; this corresponds to lactate and fructose interference of 1.57% and 0.32%.[86d] In these experiments, the sensor response was achieved within 5 min using a kinetics theory. This approach allows the estimation of the concentration of glucose based on the slope of a Bragg peak shift. With time, the rate of Bragg peak shift decreases due to the reduction of tetrahedral form of *cis*-diol groups, and the binding mechanism transforms to trigonal planar form. Hence, the Bragg peak shift is proportional to the amount of binding of *cis*-diol groups to glucose molecules; this relationship can be expressed as the following:

$$\frac{d\lambda(t)}{dt} \propto (C_g - \Delta\lambda(t))(C_f - \Delta\lambda(t)) = a(C_g - \Delta\lambda(t))(C_f - \Delta\lambda(t)) \quad (9)$$

where C_g and C_f are constants with proportionality to *cis*-diol and glucose groups present. Hence, this relationship can be used to calculate the expected saturation point of Bragg peak in the sensor. Other factors such as a potential decrease in the elasticity of the polymer matrix might influence the projected decrease of the Bragg peak shift. This approach can be applied to other hydrogel-based sensing mechanisms to reduce the measurement time. In terms of reusability, the sensor was reset to baseline (519 ± 5.8 nm) in ~10 s using acetic acid (10 mol %, v/v). As the pH decreases, the *cis*-diol groups transform from tetrahedral state to trigonal form, and they release the glucose molecules. Such sensors might be useful in the development of reusable point-of-care diagnostics devices.

The need for minimally invasive, easy to use glucose sensors has motivated the investigation of ophthalmic glucose sensors, allowing the detection of glucose in ocular fluid (tears). A proof-of-concept study involved the incorporation of a 3-APB-based holographic sensor operated at near-infrared into a contact lens, and the feasibility of noninvasive monitoring of glucose concentration was investigated.[161e,j] Another experiment was conducted in which the hologram was implanted subcutaneously just below the eye of a rabbit, followed by anesthesis using an xylazine-based protocol, which increased the concentration of glucose in the blood.[161f] A 25 nm shift in Bragg wavelength was achieved in ~3 min, which was correlated with simultaneous measurement of glucose (~10 mg %) in the blood. Such a sensor can also be fabricated to semiquantitatively indicate the concentrations of glucose by displaying different colors or images.[161m] However, controversy still remains whether the concentrations of glucose in tear fluid and in blood are correlated.[201] Table 5 summarizes the

dx.doi.org/10.1021/cr500116a | *Chem. Rev.* XXXX, XXX, XXX–XXX

holographic glucose sensors, the experimental conditions, and the respective wavelength shifts.

Table 5. Tested Boronic Acid Derivatives in Holographic Sensors and Their Respective Bragg Peak Shifts at Saturation Points[a]

ligand (mol %)	pH	concentration (mM) (wavelength shift (nm))	ref
3-APB (12)	7.4	2 (20), 11 (70)	161c
3-APB (20)	7.4	2 (50), 11 (220)	161c
3-APB (25)	7.4	2 (40), 7.4 (120)	86a
3-APB (12)	7.4	2 (20), 11 (70)	86a
3-APB (20)	7.4	2 (60), 11 (220)	86a
5-F 2MAPB (15)	7.4	2 (30), 11 (120)	86a
2-APB (20)	7.1	2 (0), 12 (0)	161h
2-APB (20)	5.8	2 (−5), 12 (−23)	161h
2-APB (20)	6.5	2 (−5), 12 (−23)	161h
2-APB (20)	7.0	2 (−5), 12 (−23)	161h
2-APB (20)	7.8	2 (−5), 12 (−23)	161h
3-APB (12)	5.8	2 (−3), 12 (−6)	161h
3-APB (12)	6.5	2 (−5), 12 (−12)	161h
3-APB (12)	7.0	2 (−15), 12 (−35)	161h
3-APB (12)	7.4	2 (−17), 12 (−45)	161h
3-APB (12)	7.8	2 (−10), 12 (−25)	161h
3-APB (12)	7.4	2 (20), 9 (70)	200
3-APB (20)[c]	6.5	1 (0), 10 (1)	86d
3-APB (20)[c]	7.0	1 (2), 10 (3)	86d
3-APB (20)[c]	7.25	1 (20), 10 (90)	86d
3-APB (20)[c]	7.4	1 (90), 10 (350)	86d
3-APB (20)[c]	7.75	1 (100), 10 (375)	86d
3-APB (20)[c]	8.0	1 (120), 10 (410)	86d
3-APB (12) + DAPA (16)	7.4	2 (−30), 11 (−60)	200
3-APB (12) + ATMA (12)[b]	7.4	4.9 (−60), 8.9 (−70)	86c
2-APB (20) + ATMA (3)	7.4	2 (8), 9 (30)	161k
2-APB (20) + PEG (3)	7.4	2 (6), 9 (20)	161k
2-APB (20) + AETA (3)	7.4	2 (4), 9 (17)	161k
2-APB (20)	7.4	2 (3), 9 (15)	161k
2-APB (20) + ATMA (9)	6.5	2 (−4), 11 (−7)	161k
2-APB (20) + ATMA (9)	7.0	2 (−4), 11 (−7)	161k
2-APB (20) + ATMA (9)	7.4	2 (−4), 11 (−7)	161k
2-APB (20) + ATMA (9)	7.8	2 (−4), 11 (−7)	161k

[a]Ionic strength of 150 mM at 30−37 °C. [b]Blood. [c]Artificial urine.

3.7. L-Lactate

L-Lactate is a metabolite produced by organisms as a result of anaerobic metabolism, and its quantification has applications within clinical diagnostics, the food industry, fermentation, and exercise performance in sports medicine. Phenylboronic acid derivatives are known to bind with bidentate chelating ligands to form five- and six-membered cyclic esters.[161j] For example, the boronates have a tendency to bind with saccharides, carbohydrates, *o*-diphenols, *o*-hydroxy acids, dicarboxylic acids, and α-hydroxy acids (e.g., L-lactate).[202] Holographic sensors comprising boronic acid-based receptors have been optimized to improve the selectivity for L-lactate.[86b] The same study also investigated the effects of hydrogel composition, fluctuating L-lactate concentrations, and the response of potential interfering agents. Incorporation of 3-acrylamidophenyl boronic acid (15 mol %) into acrylamide showed the largest response to L-lactate, and 3-APB (5 mol %) exhibited improved sensitivity to lactate over glucose.[86b] Table 6 shows the composition of the tested L-lactate-responsive sensors and their respective Bragg peak shifts. A follow-up study demonstrated that the binding mechanism of L-lactate to the trigonal form of 3-APB involves a nucleophilic attack on the boron atom by the more acidic carboxyl group followed by ring closure with the less acidic hydroxyl.[162] Specifically, it is thought that the lactate binds to the boron atom via the negatively charged $-C(=O)O^-$ group, and then rotates so that the α-hydroxy group also binds to the boron atom (Figure 21).[203] Therefore, it was proposed that boronic acid compounds such as (5-amino-2-hydroxymethylphenyl)boronic acid do not bind to glucose but do bind to α-hydroxy carboxylic acids such as lactic acid and lactate. To improve the selectivity, a number of compounds and polymers bearing similar boronic acid groups have been prepared.[203] For example, *N*-(1-hydroxy-1,3-dihydro-benzo[*c*][1,2]oxaborol-6-yl)-acrylamide (~10 mol %) was copolymerized with acrylamide (~88 mol %) and *N*,*N*′-methylenebis(acrylamide) (~1.7 mol %), which was followed by hologram formation using photopolymerization. When six increments of 20 μL per aliquot of 0.1 M lactate were applied to the hologram, the Bragg peak shifted by 25 nm toward longer wavelengths.[203] Although these studies have shown the feasibility of sensing lactate in buffer solutions, no evidence was provided about the selectivity of the sensor in the presence of any interfering species.

Table 6. Holographic Sensors Tested with L-Lactate[a]

ligand (mol %)	pH	concentration (mM) (Bragg peak shift (nm))	ref
3-APB (12)	7.4	2 (0), 11 (5)	161c
3-APB (12)	7.4	2 (20), 11 (100)	86a
3-APB (20)	7.4	2 (20), 11 (90)	86a
5-F 2MAPB (15)	7.4	2 (10), 11 (50)	86a
2-APB (12)	7.4	2 (0), 11 (0)	86b
3-APB (12)	7.4	2 (18), 11 (90)	86b
4-APB (12)	7.4	2 (10), 11 (65)	86b
3-APB (15)	7.4	2 (20), 11 (115)	86b
3-APB (20)	7.4	2 (15), 11 (100)	86b
2-APB (20)	7.1	2 (−5), 12 (−25)	161h
3-APB (20)	7.4	1 (15), 10 (130)	86d

[a]Ionic strength of 150 mM at 30 °C.

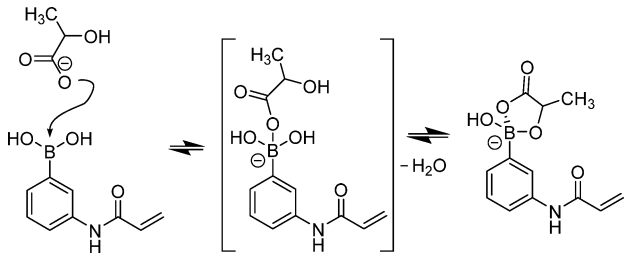

Figure 21. Proposed binding mechanism of the lactate to a *cis*-diol group.

3.8. Enzymes and Metabolites

Holographic sensors can be used to quantitatively measure or detect the presence of enzyme activity. For example, enzymes present in solution, on, or in a polymer matrix where a hologram is recorded cause changes in parameters such as pH, which may be detected by the hologram. Alternatively the holograms can be prepared with degradable materials, which are broken down by enzymes, resulting in changes that can be detected by measuring the shift in Bragg peak and/or the diffraction efficiency. For example, the degradation of a gelatin-

dx.doi.org/10.1021/cr500116a | Chem. Rev. XXXX, XXX, XXX−XXX

based hologram by an enzyme reduces the cross-linking of the gelatin matrix by digesting the collagen, resulting in the expansion of the hologram, and a shift of the Bragg peak to longer wavelengths.

3.8.1. Trypsin. The earliest use of a holographic sensor was to monitor serine proteases such as trypsin in biological media.[70c] In this study, gelatin-based holograms were prepared and exposed to trypsin and chymotrypsin. The enzymatic degradation of the gelatin holograms was used as a screening test to detect the concentrations of proteases, which may indicate clinically related conditions such as pancreatic disorders.[70c] In the pancreas, proteolytic cleavage of trypsinogen may activate trypsin, which may cause pancreatic self-digestion, also known as pancreatitis (inflammation of pancreas).[204] The holographic sensor was capable of quantifying trypsin and chymotrypsin concentrations down to 20 and 23 μg/mL, respectively. For example, the sensor took 20 min to exhibit a reduction in peak diffraction efficiency ~90%, confirming the presence of trypsin. This study demonstrated a proof-of-concept for a general protease sensor, which had a sensitivity to trypsin down to 0.04 μg/mL. Further studies have explored incorporation of poly(amino acid) poly(L-lysine) into PVA, which was degraded in a concentration-dependent manner by trypsin.[90] Reflection spectra of a PVA/poly(L-lysine) (95:5 (w/w)) hologram treated with 2.5, 20, 25, and 50 μg/mL trypsin in Tris-HBr buffer (50 mM, pH 8.1) were recorded at 60 s intervals, which showed a reduction in Bragg peak wavelengths by approximately 20, 30, 40, and 40%, respectively.[90]

3.8.2. Urea. The quantification of the concentration of urea in biological fluids is an important analytical test to assess renal function.[205] For example, when the concentration of urea is outside the normal range of 3.6−7.1 mmol/L in human serum and 214−607 mmol/24 h in urine, the abnormality may indicate kidney dysfunction.[187] An enzymatic assay-based holographic sensor was prepared to quantify urea concentrations in biological solutions.[163] The sensor comprised comonomers of HEMA, dimethylaminoethyl methacrylate (DMAEM), and EDMA. The hologram was subsequently exposed to a urease solution (100 U/mg, 25 mg/mL in PBS), which was allowed to evaporate for 2 h to concentrate the enzyme on the surface of the hologram. Enzyme immobilization was achieved with a glutaraldehyde solution (25% (v/v) solution in water, diluted to 1.25% (v/v) with PBS), which was allowed to evaporate over 2 h. The urease modified holograms were incubated in a MES buffer solution with a pH of 7 at 30 °C, and the shift in Bragg peak was measured. Urease (EC 3.5.1.5) catalyzes the hydrolysis of urea into ammonium and bicarbonate ions, $(NH_2)_2CO + 2H_2O + H^+ \rightarrow 2NH_4^+ + HCO_3^-$. Hence, the indirect measurement of urea was achieved by monitoring changes in pH. For example, 20 mM urea resulted in a Bragg shift of ~90 nm after ~17 min. This study has demonstrated that an enzyme-based holographic assay can be used to quantify urea.[163]

3.8.3. Penicillin. The measurement of penicillin can find applications in the control of bioprocesses as well as in quality control of antibiotic preparations. A hologram comprised of HEMA, EDMA (5 mol %), and MAA (6 mol %) was prepared. *N*-Succinimidyl *S*-acetylthioacetate (SATA) possesses an active *N*-hydroxysuccinimide ester moiety, which can react with protein amino groups of penicillinase to form stable amide linkages.[163] Hence, penicillinase was modified with protected sulfydryl groups (1.8 mol per mole of penicillinase), which may be deprotected with the use of excess hydroxylamine. The enzyme immobilization protocol was based on the direct attachment of the thiolated enzyme to the silver grains within the hologram via the sulfydryl group. The pencillinase functionalized holographic sensor responded to a 20 mM penicillin G with a ~200 nm red Bragg wavelength shift in ~5 min. The holographic sensor is of interest in the monitoring of natural and industrial fermentation processes.[163]

In another study, a holographic ELISA-type sensor comprising HEMA (89 mol %), EDMA (5 mol %), and MAA (6 mol %) was prepared, and antibodies were immobilized on its surface.[165] Next, a sample containing hemoglobin was washed over the immobilized antibodies, resulting in the binding of hemoglobin to the antibodies. In the following step, a second antibody, labeled with a protein penicillinase, was washed over the system, which caused the second antibody to bind to the immobilized hemoglobin, eventually forming an antibody−hemoglobin−antibody sandwich. A solution containing penicillin was flowed over the surface of the holographic system. Hence, the second antibody containing the protein penicillinase converted the penicillin to penicilloic acid. Finally, the change of pH due to the presence of penicilloic acid was monitored through Bragg peak shifts. The peak shifted from near-infrared to the red region of the electromagnetic spectrum as the pH decreased as a result of the production of penicilloic acid.[165]

3.8.4. Amylase. To attach starch to a substrate, the substrate was coated with a mixture that comprised potato starch hydrolyzed for electrophoresis, agarose (Type A 0169), and ammonium dichromate crystals dissolved in deionized water.[120] The resulting solution was spin-coated on a glass microscope slide, under yellow safelighting. The spin-coated slides were subsequently exposed to a UV light source to promote the cross-linking of ammonium dichromate. Next, a recording medium was prepared, which comprised potato starch hydrolyzed for electrophoresis and glutaraldehyde in water deposited over the presubbed substrate. Silver halide chemistry was used to form the holographic diffraction gratings in the recording medium. Using this hologram, the concentration of the digestive enzyme α-amylase was measured from the rate of reduction of diffraction efficiency at a certain wavelength over a 15 min.[120] The study showed that as the peak at one wavelength collapsed a second peak at a shorter wavelength built up to at least one-half the amplitude of the original peak. Neither β amylase nor maltase showed these effects on holograms in potato starch. A Bragg peak shift of 30 nm was observed after 30 min.[120] However, the mechanism of action is not well understood.

Recently, holographic amylase sensors were also fabricated using laser ablation.[134] This study involved preparation of a hybrid polymer matrix consisting of starch, acrylamide, and methacrylamide, which were copolymerized using the UV free radical initiator 2,2′-azobis (2-methylpropionamidine) dihydrochloride on a substrate previously presubbed with 3-(trimethoxysilyl) propyl methacrylate. A solution was prepared by mixing (1:1, v/v) silver nitrate solution (0.2 M) with a hydroquinone (0.25 M) solution containing 0.5% acetic acid, followed by dispensing an array of 0.2 mL droplets of this solution on a glass substrate. The hybrid polymer matrix was placed over the array of solution droplets to allow diffusion for a minute, followed by an exposure to alkaline triethylamine vapor to achieve a chemical reduction of silver ions to metallic silver. The final colloidal silver dispersion had an optical density

of ~0.7−1.2. Next, the recording medium was fixed with sodium thiosulfate ($Na_2S_2O_3$) (20%, w/v) to remove any excess silver salts, which may inhibit the activity of amylase. The moist recording medium was exposed to a pulse of laser light (~350 mJ at 532 nm) to form a diffraction grating. While the resulting hologram irreversibly underwent a Bragg shift of 8 nm in the presence of α-amylase in 20 min, it was irresponsive to β-amylase.[134]

3.8.5. Acetylcholine. One of the primary biological functions of acetylcholinesterase (EC 3.1.1.7, AChE) is the termination of impulse transmission at the cholinergic synapses via hydrolysis of the neurotransmitter acetylcholine into two products, choline and acetic acid.[206] The acetic acid can cause a local decrease in pH. Acetylcholine is known to bind with specific serine residues in AChE's active site, forming a covalent acetyl-enzyme intermediate. To prevent the binding of acetylcholine, certain organophosphates that form stable covalent bonds with serine present in the active site of acetylcholinesterase may be used.[100]

The incorporation of enzymes in holographic sensors is promising, in particular, to enhance the sensors' selectivity toward biological targets of interest. For this, a holographic enzyme inhibition assay was developed for drug discovery.[99] This study described an enzyme inhibition-based holographic sensor as a potential label-free detection system. To construct a holographic array, a mask was prepared to form four spots with diameters of 8 mm. This mask was used to produce polymer matrixes as an array, which consisted of copolymerized HEMA (6 mol % MAA, 5 mol % EDMA). Silver−halide chemistry was used to form diffraction gratings in the polymer matrix array. AChE (50 U/mL, predissolved in 10 mM phosphate buffer, pH 7.0 containing 1 mg/mL BSA), lactitol (8%, w/v), and dextran sulfate (0.1%, w/v) were added to a solution of gelatin (2.5%, w/v) and mixed.[99] This mixture was coated over the hologram surfaces and left to dry. Subsequently, the array was placed in a sealed chamber containing formaldehyde vapor (37% (w/v) formalin) for 45 min at room temperature. The sensor was washed and stored in assay buffer (1 mM Tris-HCl, 154 mM NaCl, pH 8.0) at 4 °C prior to testing. This sensor, based on a pH-sensitive hologram, was capable of sensing the effect of acetic acid produced from the hydrolysis of acetylcholine by the enzyme acetocholinesterase. Upon addition of the AChE with concentrations of 3.13, 6.25, 25, 50, 100, and 200 U/mL, the sensor produced Bragg peak shifts of 45, 55, 80, 95, 120, and 145 nm, respectively.[99] In addition, the sensor was used in determining apparent inhibition parameters of several drug inhibitors (e.g., chlorpyriphos, edrophonium, parathion methyl, galanthamine, eserine, neostigmine, and tacrine) of the enzyme. Holographic sensors in an array format might find applications in high throughput drug screening.[99]

3.8.6. Testosterone. Holographic molecularly imprinted polymer (MIP) films have been synthesized by using interference photolithography (Figure 22a).[164] MIPs can be prepared by templating at the molecular level.[207] Figure 22b shows the surface topography of a holographic MIP film fabricated by photopolymerization. Polymerization was performed in the presence of a template molecule (target), and the cross-linked polymer matrix consisted of cavities that were complementary to the template molecule in terms of shape, size, and position of functional groups (Figure 22c,d). Hence, MIPs had the capability to bind to target molecules with high affinity and specificity. These MIPs were used as sensors with the capability of detecting steroid testosterone.[164a] In these studies, MAA was chosen as the complexing functional monomer and EDMA as the cross-linker. The optimal solvent to monomer ratio was 133% (v/v), which provided sufficient porosity of polymer network to yield a leveled film. The polymer with 50% (functional monomer mol % to cross-linker mol %) cross-linking density was chosen because it allowed formation of MIPs. However, the highly cross-linked polymer severely limited the elasticity of the holographic system. For example, 3.6 and 2.8 nm Bragg shifts were achieved for 10 and 1 μM testosterone, while the control samples showed 2.4 and 1.4 nm wavelength shifts, which might be due to changes in ionic strength of the test samples.[164a] The need for a very high degree of cross-linking to obtain enough rigidity in the imprinted cavities in the polymer matrix to maintain specificity conflicts with the fundamental need for flexibility, and hence there are no large Bragg peak shifts in the holographic grating. Current efforts in this area are in the direction of rendering these holographic sensors capable of changing their physicochemical structure and/or signal amplification to design practical sensors.

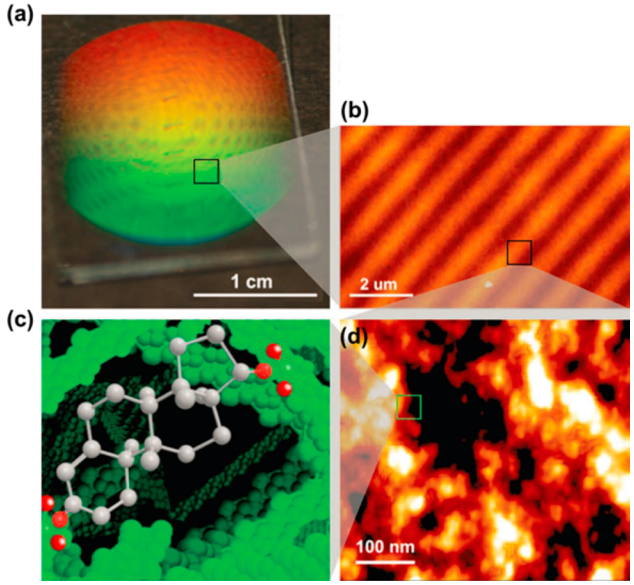

Figure 22. Holographic molecularly imprinted polymers (MIPs). (a) The hologram recorded by photopolymerization with two interfering laser beams at 532 nm. (b) AFM image of the surface topography of the holographic film (10 × 10 μm). (c) An imprinted molecular cavity specific for testosterone. (d) AFM image of the porosity of the MIP film (0.7 × 0.7 μm). Reprinted with permission from ref 164b. Copyright 2013 Wiley-VCH Verlag GmbH&Co. KGaA, Weinheim.

3.8.7. Anthraquinone-2 Carboxylate. Holographic sensors comprising methacrylated α-, β-, and γ-cyclodextrins incorporated in polymer matrixes were used to quantify anthraquinone-2 carboxylate.[161a] The α-, β-, and γ-cyclodextrin-based holographic sensors exhibited approximately 10, 14, and 19 nm of Bragg peak shift, respectively, in the presence of 1.0 mM anthraquinone-2 carboxylate, in pH 7.5 at 30 °C. Additionally, α- and γ-cyclodextrins were used to quantify the concentration of 4-nitrophenol, which yielded approximately 8.5 and 2.0 nm shifts, respectively, for 1 mM of the target molecule.[161a]

3.9. Microorganisms and Their Metabolites

Sensors to detect and monitor cells are essential in clinical, environmental, security, and safety applications. Gelatin

dx.doi.org/10.1021/cr500116a | Chem. Rev. XXXX, XXX, XXX−XXX

holograms are known to degrade in the presence of protease, which is a metabolic product of the bacterium. For example, *Bacillus subtilis* can produce protease and allow the hologram to become softer and hence expand the polymer in the direction normal to the underlying substrate. For this study, mid-exponential phase culture (in nutrient broth) was inoculated in a cuvette containing the gelatin-based hologram, and the diffracted light was measured at 10 min intervals over 15 h at 30 °C. In 5 h, a ∼20 nm red Bragg shift was reported.[208] Additionally, holographic sensors have been developed for the detection of viable bacterial *Bacillus* species spore germination and vegetative growth.[160b] These holograms, fabricated by the silver halide chemistry, were utilized to study the response to various extracellular products of bacterial spore germination and vegetative metabolism. Functionalization of a pHEMA-based holographic matrix was accomplished by incorporating a methacrylated analogue of nitrilotriacetic acid as the chelating monomer, thus rendering the polymer sensitive to divalent metal ions. The holographic sensors were capable of monitoring Ca^{2+} ions released during *B. subtilis* spore germination in real-time, where a 16 nm blue shift in Bragg wavelength was reported.[160b] Additionally, pH-sensitive holograms functionalized with methacrylic acid as the ionizable monomer were able to detect pH changes due to early vegetative metabolism following germination of *B. megaterium*, by displaying a 75 nm blue shift of the Bragg peak. Additionally, casein and starch-based holographic matrixes containing acrylamide were able to detect exoenzymes released during late-stage vegetative bacterial cell growth of both *B. megaterium* and *B. subtilis* spores. The exoenzymes caused enzymatic cleavage of the holographic matrix, resulting in reduction in diffraction intensity.[160b] Holographic sensors have also been developed to detect spore-specific calcium diplicolinate (Ca-DPA).[167] These sensors were functionalized with acid-soluble spore proteins (SASPs) extracted from dormant spores. The structural integrity of SASP-based matrixes in response to proteolytic enzymatic degradation by recombinant germination protease, followed by activation with Ca-DPA, was characterized by changes in the diffraction efficiency of the hologram. As a result of SASP degradation, an irreversible reduction in diffraction efficiency was measured. In this work, SASPs were extracted from mature *B. megaterium* spores that were cross-linked with formaldehyde to form hydrogel films on a substrate. A peptidoglycan-based hologram was fabricated in the hydrogel and SASP-based matrixes by the silver halide chemistry. The effect of Ca^{2+}-dipicolinic acid (DPA) activated germination protease (GPR) on the diffraction characteristics of the SASP-based hologram was monitored. After an initial 10 min delay, a steady and gradual irreversible reduction in peak intensity was measured over 1.5−2 h.[167b] Therefore, a proof-of-principle for a Ca-DPA-activated enzyme-linked holographic sensor was demonstrated, showing the potential of a system whereby Ca-DPA released from germinating spores can result in the activation of GPR in close proximity to an SASP-based hologram.[167a] These holograms represent a potential platform for the label-free detection of cells and their byproducts. For practical applications, such sensors can be integrated in rapid testing devices to determine the effectiveness of sterilization processes.[209]

3.10. Gases

The development of gas sensors to detect and monitor volatile organic compounds or hydrocarbons is important because these substances are potentially harmful to human health and the environment.[210] Holographic sensors have been developed to provide real-time monitoring of a variety of volatile organic compounds.[92,94] The holograms for volatile organic compound detection were based on PDMS matrixes. Concentrations of 100% (v/v) at 22 °C for 1-butyne, butane, 1-butene, isobutane, propane, propene, acetylene, and ethane resulted in Bragg shifts of approximately 77, 63, 51, 43, 13, 11, 4, and 3 nm, respectively.[92] While tests performed at higher temperatures (40 °C) resulted in larger Bragg shifts with respect to the tests performed at 22 °C, lower temperatures (8 °C) led to smaller Bragg shifts. The wavelength shifts may be correlated with the van der Waals surface areas of the hydrocarbon gases.[94] In these studies, PDMS-based hydrophobic matrixes on glass substrates were impregnated with a silver pentafluoropropionate (AgPFP) in THF (0.1 M). The AgPFP was reduced to colloidal silver in PDMS using a vapor mixture (1:3, v/v) of triethylamine (TEA) in dichloromethane (DCM). The excess reactants were removed from the PDMS matrix by rinsing with acetone. Next, the PDMS−glass system was exposed to a single 6 ns laser pulse from a Nd:YAG laser operating at 532 nm (Q-switch: 258 μs, ∼350 mJ) with a collimated (5−10 mm) beam in Denisyuk reflection mode. In a closed chamber, the responses of the PDMS-based holographic sensor to ethane, propane, and butane were obtained. The holographic sensor showed red Bragg shifts of approximately 4, 15, and 63 nm for 100% (v/v) ethane, propane, and butane, respectively.[92] A gas mixture comprising 65% butane and 35% propane by volume resulted in a red Bragg shift of ∼25 nm.[134] Another PDMS-based hologram was fabricated, and the red Bragg shift of the sensor was monitored in the presence of chlorobenzene vapor, resulting in a red Bragg shift of ∼55 nm within ∼10 min, followed by a gradual blue Bragg shift as a result of the evaporation of chlorobenzene from the hologram's interior. This PDMS-based hologram containing hydroquinone was also tested in the presence of hexane vapor, hexane saturated water, and camping gas (6:4 (v/v), butane:propane).[134] After the holographic sensor was spiked with 20 mL of hexane vapor, a red Bragg shift of approximately 27 nm was measured after ∼15 s. The Bragg peak returned to its initial wavelength after ∼30 s. Poly(vinyl dichloride) (PVDC)-based holograms have also been produced to measure the presence of chlorobenzene; however, weak Bragg peaks were observed, limiting the use of such sensor for the detection of this particular analyte.

Another follow-up study involved the preparation of a clear polystyrene film, which was subsequently immersed in a solution of AgPFP in THF. The film was then exposed to ethanolamine vapor, resulting in a dispersion of colloidal silver throughout the polystyrene film. The recording medium was exposed to a single pulse of laser light (532 nm, 350 mJ) in Denisyuk reflection mode. The resulting hologram's response was tested using chlorobenzene vapor showing a wavelength shift of ∼65 nm in 10 s.[134] It was also found that low-density polyethylene-based holograms, prepared with AgPFP in THF (0.3 M) followed by an immersion in a solution of hydroquinone (0.5 M), were unresponsive to water, alcohols, acetone, and their respective vapors. However, in the presence of chlorobenzene vapor, these polyethylene-based holograms showed a ∼36 nm Bragg shift. In a subsequent study, these sensors were shown to be sensitive to standard lead-free petroleum vapor (100%), with a ∼29 nm Bragg shift at 24 °C.[134] The fabrication of diffraction gratings in hydrophobic

matrixes allows holographic sensors that are capable of operating without interference from water.

Holographic ammonia (NH_3) sensors were also demonstrated.[168] The recording media consisted of proton exchange membranes such as perfluorosulfonic acid/polytetrafluoroethylene (PTFE) copolymer (Nafion), which can form reversible interactions with charged molecules of gaseous ammonia.[211] Nafion membranes were used to construct holographic matrixes that can respond to ammonia in the 0.19−12.50% concentration range. The holograms were recorded by laser ablation in Denisyuk reflection mode, which produced diffraction gratings consisting of Ag^0 NPs with an average diameter of ∼17 nm. In the presence of 3.12%, 6.25%, 9.37%, and 12.5% ammonia gas, the sensor produced blue Bragg shifts of approximately 15, 25, 55, and 70 nm, respectively.[168] This contraction is based on the interaction between ammonia and sulfonates in the polymer matrix. The Nafion-based holographic sensor's response time was 1 min in the presence of 12.5% ammonia gas under controlled ambient conditions (23.5 °C, 40% RH).[168]

The detection and monitoring of oxygen and nitrogen are important in many biological, medical, and industrial processes. In an effort to monitor oxygen, holographic sensors have been prepared by immobilizing oxygen protein carriers, such as hemoglobin and myoglobin, in polymer matrixes.[161a] Hemoglobin (Hb), found in red blood cells, acts as the oxygen carrier in blood, binding with up to four oxygen molecules. For example, hemoglobin A (MW ∼64 kDa) is composed of four globular protein subunits each containing an embedded heme group (iron-containing porphyrin) that has an iron atom with oxygen binding capability.[212] On the other hand, myoglobin (Mb) is located in muscle tissue facilitating oxygen movement and acting as an oxygen reservoir. Mb is a single chain globular protein (MW ∼16.7 kDa) also containing a heme, responsible for oxygen binding, with the capability to bind to only one oxygen molecule.[213] Hb is pH sensitive while Mb is not.[161a] Recording media have been produced by immobilizing hemoglobin and myoglobin onto porous pHEMA polymer matrixes.[161a] Initially, the pHEMA matrixes were immersed in solutions containing hemoglobin or myoglobin in water (50 mg/mL) for 2 h, followed by drying and subsequent exposure to acidified glutaraldehyde in water (1.5%, v/v) for 3 min. The resulting Hb- and Mb-based holograms were sparged with oxygen for ∼5 min, and both showed comparable Bragg shifts of ∼8−9 nm.[161a]

Oxygen may also be monitored utilizing Vaska's complex, which refers to the chemical compound *trans*-chlorocarbonylbis(triphenylphosphine)iridium(I) ($IrCl(CO)[P(C_6H_5)_3]_2$, MW: 780.25 g/mol).[214] Vaska's complex contains a central iridium atom with oxygen binding capability. It can undergo oxidative addition and bind to O_2 reversibly. Oxygen-sensitive holograms were prepared by immersing a pHEMA-based hologram in a solution consisting of Vaska's complex (5 mg/mL) in chloroform, followed by solvent evaporation.[161a] The hologram was subsequently sparged with oxygen in a nitrogen saturated buffer at pH 7.0, resulting in a 13 nm Bragg shift within 3 min. After sparging ceased, a proportion of the bound oxygen molecules underwent a reverse reaction, and the Bragg peak blue-shifted by 3 nm.[161a] Other compounds such as ruthenium-tris(4,7-diphenyl-1,10-phenanthroline) dichloride (Ru(dpp)) may be used for the quantification of oxygen.[215]

In efforts to monitor nitrogen, biologically active silk optical gratings were doped with hemoglobin.[95] In this study, a mixture of hematocrit human red blood cells and silk fibroin was prepared, and cast on a 600 lines/mm optical grating and dried overnight. The absorbance curves showed two peaks typical of oxyhemoglobin absorption. When the system was exposed to nitrogen, the immobilized hemoglobin underwent a transition from the oxygenated to the deoxygenated state, monitored through variations in the absorption curve. The sensing was reversible; hence when the nitrogen flow was stopped, the oxyhemoglobin peaks were recovered.[95]

3.11. Gas/Liquid-Phase Organic Components

The use of zeolite-doped photopolymers for the design of holographic sensors has been proposed for sensing toluene.[216] Theoretical modeling has demonstrated that both reflection and transmission holographic gratings can change optical properties upon exposure to an analyte to which the zeolite nanoparticles are sensitive. The basic concept is that adsorption/absorption of the targeted analyte will lead to a change in the refractive index of the nanoparticles, and thus to a change in the optical properties of the hologram. The contribution of the zeolite nanodopants to the refractive index modulation created during holographic recording is given by

$$n_1^{\,n} = f_{\text{nanodopants}}(n_{\text{nanodopants}} - n_{\text{host}}) \tag{10}$$

where $f_{\text{nanodopants}}$ is the volume fraction of nanoparticles in the nanoparticle-rich region, $n_{\text{nanodopant}}$ is the refractive index of the zeolite nanoparticles, and n_{host} is the refractive index of the host polymer matrix. A change of the refractive index of the zeolite nanoparticles will lead to a change of the overall refractive index modulation and to a change of the diffraction efficiency or the spectral characteristics of the hologram. The operation of a sensor based on a transmission hologram requires a spatial redistribution of the analyte-sensitive zeolite nanoparticles, while sensors based on reflection holograms do not necessarily require such redistribution (Figure 23).

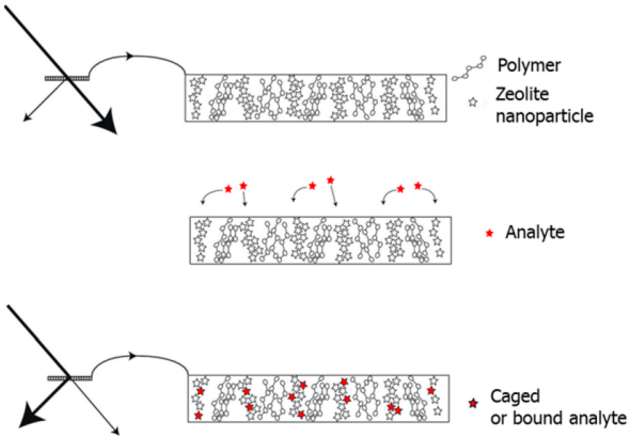

Figure 23. Principle of operation of transmission holograms recorded in zeolite-based nanocomposites. Reprinted with permission from ref 1b. Copyright 2011 Taylor and Francis Group LLC Books.

Zeolite β polymorph A (BEA) doped photopolymer has been used for fabrication of holographic gratings sensitive to toluene. These sensors were fabricated in PVA/pAAm-based photopolymer and colloidal zeolite nanoparticles of zeolite BEA and zeolite A. The zeolite BEA nanoparticles (up to 5 wt %) produced an effective increase in nanoparticle-doped polymer

dx.doi.org/10.1021/cr500116a | *Chem. Rev.* XXXX, XXX, XXX−XXX

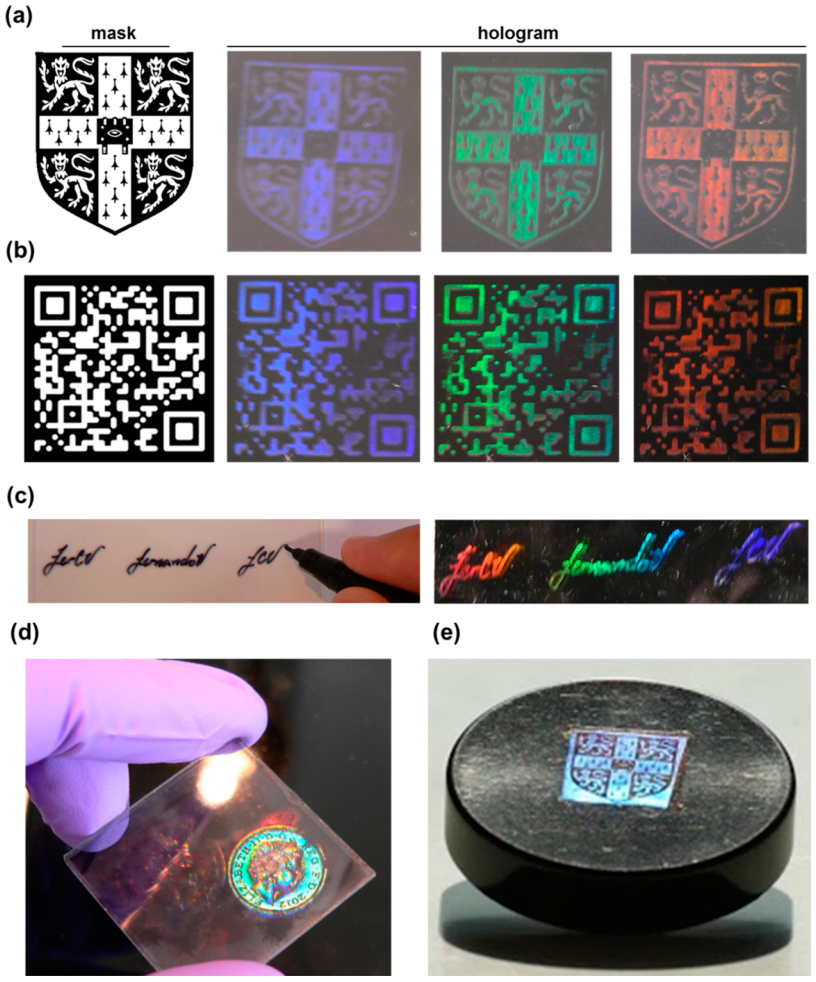

Figure 24. Surface holograms fabricated via printing and laser ablation in Denisyuk reflection and transmission modes. Holographic (a) logo, (b) QR code, (c) signature, (d) 3D coin on a transparent surface, and (e) image on an opaque plastic surface. Images illustrate diffractions of the surface holograms as a function of the angle of incident light. Reprinted with permission from ref 221. Copyright 2014 American Chemical Society.

thickness, which doubled the diffraction efficiency of the hologram with respect to undoped photopolymer.[176,216] However, the nanocomposite containing zeolite A nanoparticles did not interact with the polymer matrix, which had comparable diffraction efficiency with the undoped photopolymer. The addition of BEA-type zeolite to the polymer matrixes increased the sensitivity to toluene.[216]

PDMS-based films were also used to sense toluene. They comprised a solution (1:1, v/v) of hydroquinone (0.2 M) in a solution of AgPFP in THF (0.1 M), which was coated on glass slides, dried, and subsequently recorded in Denisyuk reflection mode using laser ablation.[134] Spiking these PDMS-based holograms with toluene saturated water (400 μL) produced a ~80 nm Bragg shift within 5 s. The Bragg peak returned to its original wavelength after 50 s. These PDMS-based holograms were also shown to respond to hexane saturated water with a ~67 nm Bragg shift within 10 s.[134]

3.12. Security Applications

Counterfeiting of branded consumer products is a pressing issue for high- as well as low-value products; existing technologies are ultimately copied or compromised by criminals. Such technologies may include taggants, specialized inks, dyes, barcodes, or embossed holograms. These verification devices have a wide application in consumer products including subscription and over the counter pharmaceuticals, food (e.g., baby formula), and cosmetics, which continue to be subject to counterfeiting and tampering. In addition, counterfeit products and products subjected to tampering are generally detectable by trained personnel in the field, often using specialized and expensive devices, which are not available to the consumer. Currently, there is a need for the consumers to verify the authenticity and safety of the products prior to consumption and use.

Bio-optical, interactive visual sensors can enable consumers to "self-validate" their purchases prior to consumption or use to ensure the product is genuine and tamper-free. Such responsive sensors showing a visual holographic image/color can display a different image/color upon detection of human breath or a drop of water.[217] Such security holograms may display multiple images observed at different angles of view, and new images can be seen after an external stimulus has been applied.[218] Additionally, these sensors can be combined with other security features such as papers with green fluorescent fibers or printable color-shifting pigments (e.g., Securalic Blue-Lilac from Merck).[219] Such advanced and secure devices may also be fabricated using different laser wavelengths and multiple angles of recording to produce unique holograms, whose superpositioned multicolored images are observed from different angles.[220]

dx.doi.org/10.1021/cr500116a | *Chem. Rev.* XXXX, XXX, XXX−XXX

Printable surface holograms have also been developed for storing information for personalized security and sensing applications.[221] The first step in their fabrication is to deposit ink on various transparent or opaque materials by inkjet printing, spin coating, mask printing, or handwriting. The surface holograms were fabricated with the use of a 6 ns (~10 mJ) Nd:YAG laser pulse in Denisyuk reflection (transparent materials) and transmission (opaque materials) modes. The samples ablated in reflection mode at 20° with respect to surface plane produced surface gratings with a skewed wave, which had a periodicity of ~750 nm observed parallel to the surface of the substrate.[221] The topographic characterization of the device showed that the average grating surface had a depth of ~117 nm. The surface holograms displayed visible-light Bragg diffraction and monochromatic color corresponding to the angle of view. These holograms can be printed on a variety of material surfaces to produce holographic QR (Quick Response) codes, logos, barcodes, signatures, and 3D images (Figure 24). For example, holographic QR codes can be used to identify counterfeit medications and other high-value products. The printable holograms can be combined with other authentication methods such as microprinting, security threads, intaglio printing, magnetic/color changing inks, taggants, and watermarks. Printing holograms is a scalable technology for producing custom images and signatures. In the future, it may be possible to integrate this technology in desktop printers for easy-to-fabricate holograms for applications in data storage to optical displays and devices.

3.13. Light

Light sensors have been produced from gelatin-based holograms.[166] First, the hologram was fabricated through silver halide chemistry in Denisyuk reflection mode, followed by bleaching with Fe(III)-based formulation with KBr to form light-sensitive nanoparticles. The resulting hologram was exposed to white light, and the intensity of the Bragg peak was monitored. The spectroscopic measurements showed that the intensity (brightness) of the diffracted light decreased by 15% in ~3 h.[171] However, the intensity of the light source was not reported in these studies. In comparison with holographic light sensors, avalanche photodiodes are widely used semiconductor-based sensors.[222] They operate through photoelectric effect, which allows the conversion of light to electricity. A single-photon avalanche photodiode running in Geiger-mode has detection efficiencies up to 85% in the visible range.[222] While avalanche photodiodes are a sensitive technology for the detection of light, they require a circuitry and a readout device. On the other hand, holographic sensors offer an equipment free and low-cost approach for the measurements of broad band light intensity.[171] However, systematic studies need to be conducted to justify the feasibility of holographic light sensors for use in equipment free technologies.

3.14. Pressure

A holographic sensor that responded to pressure was also reported.[166] A monomer mixture consisting of acrylamide:methacrylamide (2:1, v/v) with cross-linker MBA (5 mol %) was prepared, followed by a free radical polymersation to create a 10 μm film on a substrate. Using silver−halide chemistry, a hologram was recorded by a frequency doubled Nd:YAG laser (λ = 532 nm) while the polymer matrix was soaking in a water bath. The hologram was sandwiched using another transparent substrate, and pressure was applied onto the polymer matrix using a pair of G-clamps spaced approximately 15 mm apart. As the G-clamps were tightened, the hologram contracted, and the Bragg peak shifted by 3 nm to shorter wavelengths.[166] Analogous to the development of holographic pressure sensors, pressure-sensitive porous elastomeric photonic crystals (EPCs) with 350 nm void size have been developed.[223] EPCs underwent a series of 30 compression−decompression cycles with an applied compressive pressure of ~15 kPa, which produced a blue Bragg peak shift of 60 nm.[223] The difference in the wavelength shifts produced by holographic sensors and EPCs may be attributed to the variation in the cross-linking densities of these polymers. However, systematic studies are required to examine a range of elastic polymers and quantitatively measure the resulting contraction upon applied pressure.

3.15. Magnetic Field

Holographic sensors responding to magnetic field have been designed.[166] For example, a recording medium can consist of PANiCNQ produced from poly(PANi) and an acceptor molecule, tetracyanoquinodimethane (TCNQ).[224] Such polymers exhibit magnetic properties at room temperature (24 °C). A hologram may be formed in this recording medium through silver halide chemistry, laser ablation, or photopolymerization.[166] In addition to holographic sensors, superparamagnetic CCAs have also been fabricated.[225] Photonic crystals were fabricated from highly charged, monodisperse superparamagnetic ~134 nm polystyrene (shell) and iron oxide (core) composite colloidal spheres. Superparamagnetic CCA film exposed to a 2.4 kOe magnetic field with a 3.2 kOe/cm gradient produced a reversible 10 nm blue Bragg peak shift.[225b] Magnetic field-sensitive CCAs were also developed from polyacrylate-capped superparamagnetic magnetite (Fe_3O_4) colloidal nanocrystal clusters.[225a] As the external magnetic field was varied by decreasing the magnet−sample distance from 3.1 to 1.8 cm, Fe_3O_4 colloidal (d = 93 nm) photonic crystals showed a blue Bragg peak shift of ~250 nm.[225a] While hydrogel-based magnetic field sensors are in their early stages, microelectromechanical system (MEMS)-based sensors made substantial progress.[226] Semiconductor device fabrication techniques render MEMS-based sensors amenable to miniaturization and manufacturing. For example, a resonant magnetic field sensor was constructed from a seesaw plate, two torsional beams, four flexural beams, and a Wheatstone bridge with four p-type piezoresistors.[227] The sensor was based on the Lorentz force principle and operated at its first resonant frequency (136.52 kHz). The sensor had a maximum magnetic sensitivity of 40.3 μV G^{-1} (magnetic fields < 70 G) and power consumption less than 10.0 mW.[227] In contrast to holographic sensors and photonic crystal-based magnetic sensors, MEMS-based sensors offer established manufacturing mechanisms; however, they require electricity and a dedicated readout device. Recently, there were also advances in the modulation of fluorescence brightness of negatively charged nitrogen-vacancy centers in nanodiamonds.[228] These nanodiamonds were arbitrarily located on a substrate, which led to a wide range of nondegenerate spin transitions associated with individually oriented nitrogen vacancy centers. The number of addressable centers were dependent on the number of nanoverlapping Lorentzian resonances over the maximum frequency splitting based on an applied magnetic field. Because each center had a splitting of 2.8 MHz/G for the magnetic field magnitude parallel to the axis of the nitrogen vacancy center, for an applied field of 200 G, a resolution up to 55 addressable classes of

dx.doi.org/10.1021/cr500116a | Chem. Rev. XXXX, XXX, XXX−XXX

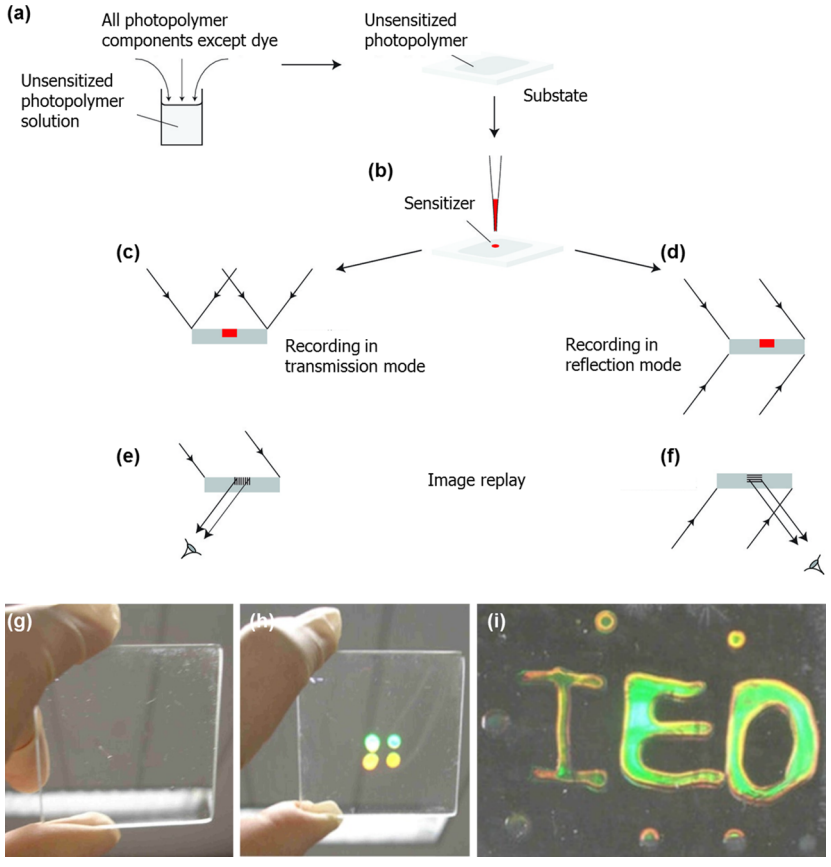

Figure 25. Holographic recording by dye deposition lithography. Addition of (a) all photopolymer components except dye sensitizer and (b) sensitizer. Recording the image in (c) transmission and (d) Denisyuk reflection modes. Readouts in (e) transmission and (f) reflection modes. Reprinted with permission from ref 1b. Copyright 2011 Taylor and Francis Group LLC Books. (g) A sensitized photopolymer sample prior to exposure to laser light. (h) A transmission and (i) a reflection grating recorded in the areas, where the dye was deposited. Reprinted with permission from ref 229a. Copyright 2009 European Optical Society.

nitrogen vacancy centers was achieved within a diffraction limited spot.[228] For example, using a CCD camera, this technique enabled superresolution imaging with subwavelength localization down to 12 nm with a frame rate of 0.7 Hz. This approach also allowed multispectral particle tracking because fluorescence nanodiamonds were cytocompatible and did not bleach in biological applications.[228]

3.16. Sensing by Hologram Formation

The formation of a hologram could itself be a sensing action.[1b,229] This approach is based on the composition of certain photopolymer systems used in holography, and it utilizes a new approach to their sensitization. Most photopolymer materials for holographic recording using visible light include a dye photosensitizer. The role of the dye is to absorb visible light, and transfer the absorbed energy to a cosensitizer so that polymerization can begin. The dye is normally included in the photopolymer composition at the preparation stage to ensure its uniform distribution throughout the photopolymer, so that the holographic response can be spatially uniform. However, the sensitizer can be added at a later stage, and a hologram can still be recorded, providing that the unsensitized dry layer is sufficiently permeable to facilitate diffusion of externally deposited sensitizer into the bulk photopolymer layer. In this strategy, the photopolymerization process can be used to detect dye labeled analytes, and it offers visual, easily interpreted information, providing an alternative to fluorescence detection methods.

Figure 25 illustrates the principle of holographic recording utilizing dye deposition. A hologram recorded by dye deposition lithography was prepared by initially coating a glass substrate with an unsensitized photopolymer solution containing all of the required components, except for the dye sensitizer; this followed drying the layer (Figure 25a).[229a] The dye sensitizer in liquid form was deposited on the dry film, which became locally sensitized as the dye diffused into it (Figure 25b,g). The film was subsequently illuminated by an interference pattern produced by two coherent laser beams to record a holographic diffraction grating, but only in the bulk photopolymer directly underneath the deposited dye, although some lateral diffusion also occurred. Depending on the illumination geometry, a transmission (Figure 25c) or a reflection grating (Figure 25d) was recorded. A rainbow effect produced by a transmission diffraction grating (Figure 25e,h) or a single color produced by a reflection grating (Figure 25f,i) was observed in white light illumination. In either case, examination in white light revealed the presence and the exact location of the dye. Dyes such as erythrosine B, eosin Y, and eosin 5-isothiocyanate in concentrations as low as 10^{-8} M have been visually detected by recording holographic transmission and reflection diffraction gratings.[229a]

Dye deposition lithography can be utilized in a detection scheme, in which a dye labeled chemical or biochemical analyte may be used to photoactivate an unsensitized photopolymer film. The presence of the analyte and its location can be

dx.doi.org/10.1021/cr500116a | *Chem. Rev.* XXXX, XXX, XXX−XXX

revealed by diffraction of light as a result of the formation of a holographic grating. The scheme can potentially offer detection of dye-labeled analytes by providing a visual and easily interpreted signal. Figure 26 shows the fabrication and the principle of operation of a sensor that can detect the presence of a DNA sequence. Dye deposition lithography involves an amplification process in the form of a polymerization chain reaction, triggered by a single excited dye molecule. In addition, diffraction by the recorded grating produces an optical signal in a direction in which no light was previously detected, so that the signal-to-noise ratio is intrinsically high.[1b]

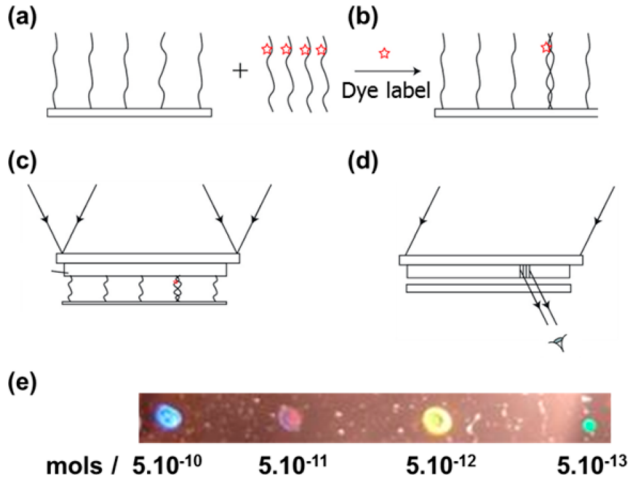

Figure 26. A holographic DNA sensor by dye deposition lithography. (a) Preparation of a substrate for depositing dye labeled DNA, (b) the addition of a dye labeled DNA sequence, (c) a separately prepared unsensitized dry photopolymer layer was placed on top of the immobilized dye labeled DNA, and subsequent formation of a diffraction grating in transmission mode, and (d) optical readout of the transmission hologram. Reprinted with permission from ref 1b. Copyright 2011 Taylor and Francis Group LLC Books. (e) Transmission holograms recorded in photopolymer layer deposited on top of dye-labeled DNA molecules immobilized on a substrate. Color dots indicate areas in contact with dye-labeled DNA exposed to holographic recording. Colors depend on the angle of view and are not correlated with the concentration of the analyte. Reprinted with permission from ref 229a. Copyright 2009 European Optical Society.

In commercial systems, a dye-labeled analyte is detected by the fluorescent light, in which the dye emits a specific wavelength when it is illuminated by light of appropriate wavelength.[230] This is a well-established method, but fluorescent emission is isotropic, necessitating the use of an optical system to ensure that as much of the fluorescence as possible reaches the detector.[231] Dye labels for biological molecules usually have high fluorescence yield and are not suitable as sensitizers for photopolymerization, for which high triplet yield and long-lived triplet states are required. However, a number of suitable commercial dyes such as eosin-5-isothiocyanate are available. This dye was used at a concentration of 10 mM as a label for 17-mer single stranded DNA. 0.05 μL solutions containing dye-labeled DNA in concentrations from 10^{-3} to 10^{-9} M were deposited on a microarray substrate so that the amount of DNA at each location varied between 0.5 fmol and 0.5 nmol (Figure 26a,b).[229a] A separately prepared unsensitized dry photopolymer layer was peeled from its substrate and placed on top of the immobilized, dye labeled DNA. Holographic transmission diffraction gratings were recorded in the photopolymer layer in only those areas in contact with the dye labeled DNA (Figure 26c). The lowest concentration detected by this method was 50 fmol (Figure 26d,e).[229a] Further optimization of the dye label, photopolymer composition, and the recording geometry are necessary to achieve sensitivity comparable to that of the fluorescent methods. This holographic detection method has potential applications in point-of-care diagnostic devices, bioassays and biosensors, and environmental monitoring devices.

4. CONCLUSION

Holographic sensors are still in an early development stage. As compared to other diffraction grating-based sensors, holographic sensing offers distinct advantages involving three-dimensional image capability and compatibility with laser manufacturing. Nevertheless, like other hydrogel-based optical sensors, they suffer from low selectivity, which stands out as an issue for the development of products that can compete with molecular dye-based and electrochemical sensing platforms. Therefore, the emphasis on selectivity should be increased so that holographic sensors become a mature platform to create real-world products.

Investigations regarding the functionalization and optimization of holographic recording media need to be accelerated. In this aspect, although humidity and solvent sensors have a fast response time, slow sensor response often stands out as a significant limitation in biomolecular sensing applications as compared to other sensing mechanisms such as electrochemical sensing. This requires further investigations in polymer chemistry involving the design of hydrogel characteristics. Understanding the fundamentals of binding kinetics and reversibility will allow construction of assays with improved control for real-time continuous monitoring applications. Studies on polymer system dynamics and characteristics including expansion, shrinkage, diffraction efficiency, control over nanoparticle size distribution, polymer−analyte interactions, surface energy, release characteristics, reversibility, control of pore size, polymer decay, and effect of porous and solid nanodopants will contribute to the development of holographic sensors. The quality and shelf life of the sensor after long-term storage also require further investigations.

Nanoparticle-free methods (templating, photopolymerization) and development of new deposition methods will play greater roles in the optimization of the overall performance of the sensor, along with a reduction of batch to batch variability. For example, Aztec gratings may be adopted for the development of holographic sensors, where mass production by embossing is desired.[232] Similarly, printing techniques or the use of photomasks during laser exposure can introduce more user-friendly fool proof text/quantity-reporting capabilities. Digital printing in particular can be used to fabricate individualized holographic sensors that can also be used as security devices. Additionally, digital holography (no real object requirement) may lead to image multiplexing techniques.[233]

Issues relating to angular tolerance and readouts should also be addressed. Currently, at least for silver nanoparticle-based systems, holographic sensor fabrication is based on the use of a plane mirror. This method produces low-diffraction efficiency (<1%) gratings in pHEMA and pAAm matrixes, and it also results in diffraction at a narrow angle range (0−5°), making it difficult to find the hologram by eye. To address these issues, studies on improving brightness by optimization of the

dx.doi.org/10.1021/cr500116a | Chem. Rev. XXXX, XXX, XXX−XXX

recording materials and chemical composition and the use of lenses and diffusers should gain momentum. Future investigations involving data processing strategies on automated capabilities to mitigate errors due to variation in ambient light will be valuable contributions to the field. Such studies may lead to solutions for reducing interference from the background color of the samples (e.g., blood). Quantitative data processing on mobile devices such as smartphones, tablets, smart watches, or other wearable devices should enhance the standardization and feasibility of integrated holographic diagnostic devices.[149] Although significant time has been devoted to spectrophotometric detection, the colorimetric readout capability of holographic sensing must not be overlooked. The use of external readers is a barrier for the existing assays, yet holographic sensing can offer semiquantitative as well as quantitative readouts in the same assay. This attribute is an advantage for commercial applications.

All of these advances will lead to multiplexed assays that are capable of moderately sensitive detection or quantitation of a wide array of analytes. Adoption of microfluidic technology can allow miniaturization, reduce the reagent consumption, and enable high-throughput low-cost devices.[234] Development of holograms sensitive to environmental stressors will allow for fabrication of disposable devices for environmental monitoring. Novel approaches toward instrument-free detection of amplicons and whole cells will be other important contributions to the field. Such sensors can be used in screening for genetic predisposition to diseases. Intensive effort is required to transform the sensing mechanism into a highly reproducible platform. Possible trials must demonstrate the feasibility and cost-effectiveness of scaling up.

The sensing mechanisms for point-of-care tests are primarily based on gold colloids with antibody/antigen interactions, molecular-dye-based sensors, and electrochemistry.[235] These mechanisms are readily available and standard for simple, qualitative, and low-cost point-of-care devices, while also having enough capability to be utilized in highly sensitive, fully quantitative, and multiplex assays. Therefore, efforts should focus on sensing applications that are not currently feasible with existing sensing platforms and explore areas in great need. Niche technologies include reusable, wearable, implantable, wireless, and powerless devices. The ultimate challenge will be to justify the holographic sensor performance and the cost to attain a "killer" application, such as the urine molecular dye-based dipsticks, nanoparticle-based pregnancy tests, electrochemical glucometers for monitoring glucose in blood, and low-cost embossed holograms in security applications. Unless holographic sensors provide significant competitive advantage over existing technologies in design and operational requirements such as sensitivity, selectivity, response time, and user-friendliness, while still offering low-cost solutions to address practical problems, it will be clearly challenging to replace established platforms in point-of-care and security applications.

The engagement of multidisciplinary research and commercial awareness is imperative in achieving the performance requirements for a wide array of applications in point-of-care diagnostics and security. Only then will holographic sensors be able to fulfill ultimately their commercial potential and create a social impact.

AUTHOR INFORMATION

Corresponding Author

*E-mail: ay283@cam.ac.uk.

Author Contributions

A.K.Y. designed the review. I.N. wrote sections 2.1.3, 2.2, 2.3.3, 3.2, 3.3, 3.11, and 3.16. F.C.V. partially wrote sections 3.8, 3.9, and 3.10. J.B. wrote sections 1.4, 2.3.1, 2.3.3, and 3.8.4. A.K.Y. wrote the rest of the manuscript. A.K.Y., J.B., and C.R.L. edited the manuscript.

Notes

The authors declare no competing financial interest.

Biographies

Ali Yetisen is a Ph.D. candidate in the Department of Chemical Engineering & Biotechnology at the University of Cambridge. He received a B.Sc. degree in Mechanical Engineering from the University of Arizona in 2010. His research interests are nanotechnology, diagnostics, drug delivery, and biomimicry. He has taught entrepreneurship and commercialization courses at the Judge Business School in Cambridge. Ali has published 20 journal articles and has a patent licensed to Hoffmann-La Roche. He has been the recipient of The Ann & Norman Hilberry Scholarship, Roche Continents Award, and Cambridge Infectious Diseases Fellowship. Currently, Ali serves as an ad-hoc reviewer for 10 journals in nanotechnology, photonics, and microfluidics.

Izabela Naydenova was awarded her M.Sc. in Applied Optics from the University of Sofia and her Ph.D. in Physics from the Bulgarian Academy of Sciences, in 1999. After postdoctoral work at the Institute for Physical and Theoretical Chemistry, Technical University of Munich, and the Centre for Industrial and Engineering Optics, Dublin Institute of Technology (DIT), she took up her current academic position in the School of Physics, DIT, in 2008. Her research interests

dx.doi.org/10.1021/cr500116a | Chem. Rev. XXXX, XXX, XXX−XXX

are in photopolymers for holographic sensing, optical devices fabricated by digital printing, and holographic actuators. She has over 100 publications and is cofounder of a spin-out company for holographic security devices.

Fernando da Cruz Vasconcellos obtained a B.Sc. degree in chemical engineering from the University of California - Santa Barbara (UCSB), in 2000. From the State University of Campinas (UNICAMP), he received M.Sc. (2007) and Ph.D. (2011) degrees in chemical engineering. Part of his Ph.D. was performed at the Department of Materials Science and Engineering at the Massachusetts Institute of Technology (MIT) (2008−2009). Fernando is currently a postdoctoral research fellow in the Department of Chemical Engineering and Biotechnology at the University of Cambridge. His current research interests include functional biomaterials, micro/nanofabrication, photonics and holographic devices for security, data storage, and sensing applications.

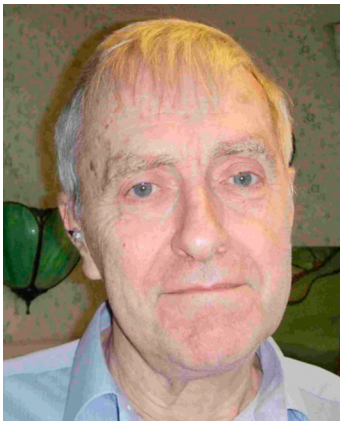

Jeff Blyth is a Senior Research Associate at the University of Cambridge, born in 1938. By his early 30s he did an Applied Chemistry degree as a mature student. While working for startup companies and as a science teacher, he pioneered new methods of making and processing holograms and simultaneously did an M.Phil. degree on developing photopolymers to record holograms with laser light sponsored by the Ilford film company. In the 1980s he was a consultant for MasterCard, Fiat, and Rohm (Plexiglas). In 1992, with a grant from the Leverhulme Trust he joined the University of Cambridge to develop holographic biosensors. He has helped many Ph.D. students and postdocs to produce holographic sensors and coauthored 30 articles.

Professor Christopher R. Lowe is in the Institute of Biotechnology at the Department of Chemical Engineering & Biotechnology at the University of Cambridge and researches in both diagnostics and therapeutics in the healthcare biotechnology sector. He is a fellow of the Royal Academy of Engineering, the Institute of Physics, and the Royal Society of Chemistry. He has 360 publications, 8 books and monographs, >100 patents, and has supervised >95 Ph.D. students and has a number of national and international prizes: "Queen's Award for Technological Achievement"; "Queen's Anniversary Prize for Higher and Further Education"; "Most Entrepreneurial Scientist of the UK"; OBE in the Queen's New Year Honours; and BBSRC Commercial Innovator of the Year in 2011. He has been the driving force for the establishment of 11 spin-out companies. He is active in various government committees and in various legal and entrepreneurial roles.

REFERENCES

(1) (a) Lowe, C. R.; Millington, R. B.; Blyth, J.; Mayes, A. G. Hologram used as a sensor. WO Patent Application 1995026499 A1, October 5, 1995. (b) Toal, V. *Introduction to Holography*; CRC Press: Boca Raton, FL, 2011; p 441.

(2) Postnikov, V. A.; Kraiskii, A. V.; Sergienko, V. I. In *Holography - Basic Principles and Contemporary Applications*; Mihaylova, E., Ed.; InTech: Rijeka, 2013; p 103.

(3) Mihaylova, E.; Cody, D.; Naydenova, I.; Martin, S.; Toal, V. In *Holography - Basic Principles and Contemporary Applications*; Mihaylova, E., Ed.; InTech: Rijeka, 2013; p 89.

(4) Sidharta, R.; Hiyama, A.; Tanikawa, T.; Hirose, M. *16th International Conference on Artificial Reality and Telexistence*; ICAT: Hangzhou, China, 2006; p 115.

(5) Chen, R. H. *Liquid Crystal Displays: Fundamental Physics and Technology*; John Wiley & Sons: Hoboken, 2011; p 75.

(6) Zhao, Y.; Xie, Z.; Gu, H.; Zhu, C.; Gu, Z. *Chem. Soc. Rev.* **2012**, *41*, 3297.

(7) Ge, J.; Yin, Y. *Angew. Chem., Int. Ed.* **2011**, *50*, 1492.

(8) Zhao, Y. J.; Zhao, X. W.; Gu, Z. Z. *Adv. Funct. Mater.* **2010**, *20*, 2970.

(9) Citartan, M.; Gopinath, S. C.; Tominaga, J.; Tang, T. H. *Analyst* **2013**, *138*, 3576.

(10) Directive 2008/50/EC of the European Parliament and of the Council of 21 May 2008 on ambient air quality and cleaner air for Europe, European Commission, *Off. J. Eur. Union L.*, 2008; Vol. *152*.

(11) Ho, C. K.; Robinson, A.; Miller, D. R.; Davis, M. J. Sandia Report: Sensors for Environmental Monitoring and Long-Term Environmental Stewardship, Sandia National Laboratories, 2004.

(12) Aldhous, P. *Nature* **2005**, *434*, 132.

(13) Havocscope LLC, Market Report: Value of Counterfeit Goods Worldwide, 2014.

(14) Newton, P.; Proux, S.; Green, M.; Smithuis, F.; Rozendaal, J.; Prakongpan, S.; Chotivanich, K.; Mayxay, M.; Looareesuwan, S.; Farrar, J.; Nosten, F.; White, N. J. *Lancet* **2001**, *357*, 1948.

(15) Bate, R.; Hess, K. *Malar. J.* **2010**, *9*, 157.

dx.doi.org/10.1021/cr500116a | *Chem. Rev.* XXXX, XXX, XXX−XXX

(16) Newton, P. N.; Green, M. D.; Fernandez, F. M.; Day, N. P.; White, N. J. *Lancet Infect. Dis.* **2006**, *6*, 602.
(17) (a) Tay, S.; Blanche, P. A.; Voorakaranam, R.; Tunc, A. V.; Lin, W.; Rokutanda, S.; Gu, T.; Flores, D.; Wang, P.; Li, G.; St Hilaire, P.; Thomas, J.; Norwood, R. A.; Yamamoto, M.; Peyghambarian, N. *Nature* **2008**, *451*, 694. (b) Blanche, P. A.; Bablumian, A.; Voorakaranam, R.; Christenson, C.; Lin, W.; Gu, T.; Flores, D.; Wang, P.; Hsieh, W. Y.; Kathaperumal, M.; Rachwal, B.; Siddiqui, O.; Thomas, J.; Norwood, R. A.; Yamamoto, M.; Peyghambarian, N. *Nature* **2010**, *468*, 80.
(18) Llordes, A.; Garcia, G.; Gazquez, J.; Milliron, D. J. *Nature* **2013**, *500*, 323.
(19) (a) Comiskey, B.; Albert, J. D.; Yoshizawa, H.; Jacobson, J. *Nature* **1998**, *394*, 253. (b) Chen, Y.; Au, J.; Kazlas, P.; Ritenour, A.; Gates, H.; McCreary, M. *Nature* **2003**, *423*, 136.
(20) (a) Yablonovitch, E. *Sci. Am.* **2001**, *285*, 47. (b) Krauss, T. F. *Nat. Mater.* **2003**, *2*, 777. (c) Akahane, Y.; Asano, T.; Song, B. S.; Noda, S. *Nature* **2003**, *425*, 944. (d) Norris, D. J. *Nat. Mater.* **2007**, *6*, 177.
(21) (a) Li, Y.; Wang, X.; Sun, J. Q. *Chem. Soc. Rev.* **2012**, *41*, 5998. (b) Noda, S.; Tomoda, K.; Yamamoto, N.; Chutinan, A. *Science* **2000**, *289*, 604. (c) Lin, S. Y.; Fleming, J. G.; Hetherington, D. L.; Smith, B. K.; Biswas, R.; Ho, K. M.; Sigalas, M. M.; Zubrzycki, W.; Kurtz, S. R.; Bur, J. *Nature* **1998**, *394*, 251.
(22) (a) Gruning, U.; Lehmann, V.; Ottow, S.; Busch, K. *Appl. Phys. Lett.* **1996**, *68*, 747. (b) Birner, A.; Wehrspohn, R. B.; Gosele, U. M.; Busch, K. *Adv. Mater.* **2001**, *13*, 377.
(23) (a) Butt, H.; Montelongo, Y.; Butler, T.; Rajesekharan, R.; Dai, Q.; Shiva-Reddy, S. G.; Wilkinson, T. D.; Amaratunga, G. A. *Adv. Mater.* **2012**, *24*, OP331. (b) Butt, H.; Kidambi, P. R.; Dlubak, B.; Montelongo, Y.; Palani, A.; Amaratunga, G. A. J.; Hofmann, S.; Wilkinson, T. D. *Adv. Opt. Mater.* **2013**, *1*, 869.
(24) Wanke, M. C.; Lehmann, O.; Muller, K.; Wen, Q.; Stuke, M. *Science* **1997**, *275*, 1284.
(25) (a) Buenger, D.; Topuz, F.; Groll, J. *Prog. Polym. Sci.* **2012**, *37*, 1678. (b) Galisteo-Lopez, J. F.; Ibisate, M.; Sapienza, R.; Froufe-Perez, L. S.; Blanco, A.; Lopez, C. *Adv. Mater.* **2011**, *23*, 30.
(26) Aguirre, C. I.; Reguera, E.; Stein, A. *Adv. Funct. Mater.* **2010**, *20*, 2565.
(27) Schacher, F. H.; Rupar, P. A.; Manners, I. *Angew. Chem., Int. Ed.* **2012**, *51*, 7898.
(28) Bonifacio, L. D.; Lotsch, B. V.; Puzzo, D. P.; Scotognella, F.; Ozin, G. A. *Adv. Mater.* **2009**, *21*, 1641.
(29) (a) Matsushita, S. I.; Yagi, Y.; Miwa, T.; Tryk, D. A.; Koda, T.; Fujishima, A. *Langmuir* **2000**, *16*, 636. (b) Rogach, A.; Susha, A.; Caruso, F.; Sukhorukov, G.; Kornowski, A.; Kershaw, S.; Mohwald, H.; Eychmuller, A.; Weller, H. *Adv. Mater.* **2000**, *12*, 333. (c) Yin, Y. D.; Lu, Y.; Xia, Y. N. *J. Mater. Chem.* **2001**, *11*, 987.
(30) Urbas, A.; Fink, Y.; Thomas, E. L. *Macromolecules* **1999**, *32*, 4748.
(31) (a) Montelongo, Y.; Tenorio-Pearl, J. O.; Williams, C.; Zhang, S.; Milne, W. I.; Wilkinson, T. D. *Proc. Natl. Acad. Sci. U.S.A.* **2014**. (b) Butt, H.; Butler, T.; Montelongo, Y.; Rajesekharan, R.; Wilkinson, T. D.; Amaratunga, G. A. J. *Appl. Phys. Lett.* **2012**, *101*, 251102. (c) Montelongo, Y.; Chen, B. A.; Butt, H.; Robertson, J.; Wilkinson, T. D. *Appl. Phys. Lett.* **2013**, *103*, 111104. (d) Kong, X.-T.; Butt, H.; Yetisen, A. K.; Kangwanwatana, C.; Montelongo, Y.; Deng, S.; Cruz Vasconcellos, F.d.; Qasim, M. M.; Wilkinson, T. D.; Dai, Q. *Appl. Phys. Lett.* **2014**, *105*, 053108. (e) Montelongo, Y.; Butt, H.; Butler, T.; Wilkinson, T. D.; Amaratunga, G. A. *Nanoscale* **2013**, *5*, 4217.
(32) Bruening, M.; Dotzauer, D. *Nat. Mater.* **2009**, *8*, 449.
(33) Asher, S. A.; Peteu, S. F.; Reese, C. E.; Lin, M. X.; Finegold, D. *Anal. Bioanal. Chem.* **2002**, *373*, 632.
(34) Hatton, B.; Mishchenko, L.; Davis, S.; Sandhage, K. H.; Aizenberg, J. *Proc. Natl. Acad. Sci. U.S.A.* **2010**, *107*, 10354.
(35) Khandpur, A. K.; Foerster, S.; Bates, F. S.; Hamley, I. W.; Ryan, A. J.; Bras, W.; Almdal, K.; Mortensen, K. *Macromolecules* **1995**, *28*, 8796.
(36) Moon, J. H.; Yang, S. *Chem. Rev.* **2010**, *110*, 547.
(37) Ganesh, N.; Zhang, W.; Mathias, P. C.; Chow, E.; Soares, J. A.; Malyarchuk, V.; Smith, A. D.; Cunningham, B. T. *Nat. Nanotechnol.* **2007**, *2*, 515.
(38) Di Falco, A.; O'Faolain, L.; Krauss, T. F. *Appl. Phys. Lett.* **2009**, *94*, 063503.
(39) Yanik, A. A.; Cetin, A. E.; Huang, M.; Artar, A.; Mousavi, S. H.; Khanikaev, A.; Connor, J. H.; Shvets, G.; Altug, H. *Proc. Natl. Acad. Sci. U.S.A.* **2011**, *108*, 11784.
(40) Kravets, V. G.; Schedin, F.; Jalil, R.; Britnell, L.; Gorbachev, R. V.; Ansell, D.; Thackray, B.; Novoselov, K. S.; Geim, A. K.; Kabashin, A. V.; Grigorenko, A. N. *Nat. Mater.* **2013**, *12*, 304.
(41) (a) Zhou, J.; Sun, C. Q.; Pita, K.; Lam, Y. L.; Zhou, Y.; Ng, S. L.; Kam, C. H.; Li, L. T.; Gui, Z. L. *Appl. Phys. Lett.* **2001**, *78*, 661. (b) Kuai, S. L.; Bader, G.; Ashrit, P. V. *Appl. Phys. Lett.* **2005**, *86*, 221110. (c) Pevtsov, A. B.; Kurdyukov, D. A.; Golubev, V. G.; Akimov, A. V.; Meluchev, A. A.; Sel'kin, A. V.; Kaplyanskii, A. A.; Yakovlev, D. R.; Bayer, M. *Phys. Rev. B: Condens. Matter Mater. Phys.* **2007**, *75*, 153101.
(42) (a) Leonard, S. W.; Mondia, J. P.; van Driel, H. M.; Toader, O.; John, S.; Busch, K.; Birner, A.; Gosele, U.; Lehmann, V. *Phys. Rev. B: Condens. Matter Mater. Phys.* **2000**, *61*, R2389. (b) Kang, D.; Maclennan, J. E.; Clark, N. A.; Zakhidov, A. A.; Baughman, R. H. *Phys. Rev. Lett.* **2001**, *86*, 4052. (c) Mach, P.; Wiltzius, P.; Megens, M.; Weitz, D. A.; Lin, K. H.; Lubensky, T. C.; Yodh, A. G. *Europhys. Lett.* **2002**, *58*, 679.
(43) (a) Gu, Z. Z.; Fujishima, A.; Sato, O. *J. Am. Chem. Soc.* **2000**, *122*, 12387. (b) Sumioka, K.; Kayashima, H.; Tsutsui, T. *Adv. Mater.* **2002**, *14*, 1284. (c) Lumsdon, S. O.; Kaler, E. W.; Williams, J. P.; Velev, O. D. *Appl. Phys. Lett.* **2003**, *82*, 949. (d) Fleischhaker, F.; Arsenault, A. C.; Kitaev, V.; Peiris, F. C.; von Freymann, G.; Manners, I.; Zentel, R.; Ozin, G. A. *J. Am. Chem. Soc.* **2005**, *127*, 9318. (e) Xia, J. Q.; Ying, Y. R.; Foulger, S. H. *Adv. Mater.* **2005**, *17*, 2463. (f) Jeong, U.; Xia, Y. *Angew. Chem., Int. Ed.* **2005**, *44*, 3099. (g) Maurer, M. K.; Lednev, I. K.; Asher, S. A. *Adv. Funct. Mater.* **2005**, *15*, 1401. (h) Barry, R. A.; Wiltzius, P. *Langmuir* **2006**, *22*, 1369. (i) Snoswell, D. R. E.; Bower, C. L.; Ivanov, P.; Cryan, M. J.; Rarity, J. G.; Vincent, B. *New J. Phys.* **2006**, *8*, 267.
(44) (a) Bjelkhagen, H. I. *Silver-Halide Recording Materials for Holography and Their Processing*, 2nd ed.; Springer: Heidelberg, 1995; p 13. (b) Saxby, G. *Practical Holography*, 3rd ed.; Institute of Physics Publishing: London, 2004; p 46. (c) Bjelkhagen, H.; Brotherton-Ratcliffe, D. *Ultra-Realistic Imaging: Advanced Techniques in Analogue and Digital Colour Holography*; Taylor & Francis: Boca Raton, FL, 2013; p 89.
(45) Maxwell, J. C. *Philos. Trans. R. Soc. London* **1865**, *155*, 459.
(46) (a) Zenker, W. *Lehrbuch der Photochromie (Textbook on Photochromism)*; F. Viewag und Suhn: Berlin, 1868; p 88. (b) Guther, R. *Proc. Soc. Photo-Opt. Instrum. Eng.* **1999**, *3738*, 20.
(47) Hertz, H. *Electric Waves: Being Researches on the Propagation of Electric Action with Finite Velocity Through Space*; Macmillan Publishers: London, 1893; p 278.
(48) Wiener, O. *Ann. Phys. (Berlin, Ger.)* **1890**, *276*, 203.
(49) Lippmann, G. *J. Phys. (Paris)* **1894**, *3*, 97.
(50) Bjelkhagen, H. I. *Lippman Photographs Recorded in DuPont Color Photopolymer Material, Practical Holography XI and Holographic Materials III*; SPIE: San Jose, CA, 1997.
(51) Bragg, W. L. *Proc. Cambridge Philos. Soc.* **1912**, *17*, 43.
(52) Wolfke, M. *Phys. Z.* **1920**, *21*.
(53) (a) Gabor, D. *Nature* **1948**, *161*, 777. (b) Gabor, D. *Proc. R. Soc. A* **1949**, *197*, 454.
(54) Einstein, A. *Phys. Z.* **1917**, *18*, 121.
(55) (a) Gould, R. G. *The Ann Arbor Conference on Optical Pumping*; University of Michigan: Ann Arbor, MI, 1959; p 128. (b) Maiman, T. H. *Nature* **1960**, *187*, 493.
(56) (a) Denisyuk, Y. N. *Dokl. Akad. Nauk SSSR* **1962**, *144*, 1275. (b) Leith, E. N.; Upatnieks, J. *J. Opt. Soc. Am.* **1962**, *52*, 1123.
(57) Benton, S. A. Method for making reduced bandwidth holograms. U.S. Patent 3,633,989 A, January 11, 1972.

(58) (a) Cowan, J. J. *J. Opt. Soc. Am. A* **1990**, *7*, 1529. (b) Cowan, J. J. Proceedings of the 7th International Symposium on Display Holography, Wales, UK, 2006; p 263. (c) Hobbs, D. S. Laser-Induced Damage in Optical Materials: 2008, Boulder, CO, 2008; p 71321K. (d) Cowan, J. J. Optical Security and Counterfeit Deterrence Techniques VI, San Jose, CA, 2006; p 60750Q.
(59) Hariharan, P. *Basics of Interferometry*; Academic Press: San Diego, CA, 2010; p 111.
(60) Born, M.; Wolf, E. *Principles of Optics: Electromagnetic Theory of Propagation, Interference and Diffraction of Light*, 7th ed.; Cambridge University Press: Cambridge, 1999; p 296.
(61) Collier, R. J.; Burckhardt, C. B.; Lin, L. H. *Optical Holography*; Academic Press: New York, 1971; p 152.
(62) Benton, S. A.; Bove, V. M. *Holographic Imaging*; John Wiley & Sons: Hoboken, 2007; p 173.
(63) Kubota, T. *Appl. Opt.* **1988**, *27*, 4358.
(64) Walker, J. L. In Situ Color Control for Reflection Holography, M.S., MIT, Cambridge, MA, 1987.
(65) Hariharan, P. *Appl. Opt.* **1990**, *29*, 2983.
(66) (a) Blyth, J. *Holosphere* **1979**, *8*, 5. (b) Hariharan, P. *Opt. Commun.* **1980**, *35*, 42. (c) Kaufman, J. A. *Proc. Int'l Symp. on Display Holography*; Lake Forest College, IL, 1983; p 195. (d) Moore, L. *Proc. Int'l Symp. on Display Holography*; Lake Forest College, IL, 1983; p 163.
(67) Wuest, D. R.; Lakes, R. S. *Appl. Opt.* **1991**, *30*, 2363.
(68) Walker, J. L.; Benton, S. A. *Practical Holography III*; Los Angeles, CA, 1989; p 192.
(69) Benton, S. A.; Walker, J. L. Holographic Color Control Systems. U.S. Patent 4,986,619 A, January 22, 1991.
(70) (a) Spooncer, R. C.; Al-Ramadhan, F. A. S.; Jones, B. E. *Int. J. Optoelectron.* **1992**, *7*, 449. (b) Blyth, J.; Millington, R. B.; Mayes, A. G.; Frears, E. R.; Lowe, C. R. *Anal. Chem.* **1996**, *68*, 1089. (c) Millington, R. B.; Mayes, A. G.; Blyth, J.; Lowe, C. R. *Sens. Actuators, B* **1996**, *33*, 55.
(71) Naydenova, I.; Jallapuram, R.; Martin, S.; Toal, V. In *Humidity Sensors: Types, Nanomaterials and Environmental Monitoring*; Okada, C. T., Ed.; Nova Science Publishers: Hauppauge, 2011; p 117.
(72) Tsangarides, C. P.; Yetisen, A. K.; Vasconcellos, F. D.; Montelongo, Y.; Qasim, M. M.; Wilkinson, T. D.; Lowe, C. R.; Butt, H. *RSC Adv.* **2014**, *4*, 10454.
(73) Yetisen, A. K.; Butt, H.; Vasconcellos, F. D.; Montelongo, Y.; Davidson, C. A. B.; Blyth, J.; Chan, L.; Carmody, J. B.; Vignolini, S.; Steiner, U.; Baumberg, J. J.; Wilkinson, T. D.; Lowe, C. R. *Adv. Opt. Mater.* **2014**, *2*, 250.
(74) Naydenova, I.; Jallapuram, R.; Toal, V.; Martin, S. *Sens. Actuators, B* **2009**, *139*, 35.
(75) Kogelnik, H. *Bell Syst. Technol. J.* **1969**, *48*, 2909.
(76) Zaarour, M.; Dong, B.; Naydenova, I.; Retoux, R.; Mintova, S. *Microporous Mesoporous Mater.* **2014**, *189*, 11.
(77) Matisons, J. G. In *Silanes and Other Coupling Agents*; Mittal, K. L., Ed.; Brill Publishers: Leiden, 2009; Vol. *5*, p 3.
(78) Blyth, J.; Millington, R. B.; Mayes, A. G.; Lowe, C. R. *Imaging Sci. J.* **1999**, *47*, 87.
(79) Marshall, A. J.; Blyth, J.; Davidson, C. A.; Lowe, C. R. *Anal. Chem.* **2003**, *75*, 4423.
(80) Cariou, J. M.; Dugas, J.; Martin, L.; Michel, P. *Appl. Opt.* **1986**, *25*, 334.
(81) Ozawa, T. *Hist. Photogr.* **1981**, *5*, 285.
(82) Maddox, R. L. *Br. J. Photogr.* **1871**, *18*, 422.
(83) *Gelatin Handbook, Gelatin Manufacturers Institute of America*, 2012.
(84) Lowe, C. R. In *Handbook of Biosensors and Biochips*; Marks, R. S., Cullen, D. C., Karube, I., Lowe, C. R., Weetall, H. H., Eds.; John Wiley & Sons: Chichester, 2008; Vol. *1*, p 587.
(85) Mayes, A. G.; Blyth, J.; Kyröläinen-Reay, M.; Millington, R. B.; Lowe, C. R. *Anal. Chem.* **1999**, *71*, 3390.
(86) (a) Kabilan, S.; Marshall, A. J.; Sartain, F. K.; Lee, M. C.; Hussain, A.; Yang, X. P.; Blyth, J.; Karangu, N.; James, K.; Zeng, J.; Smith, D.; Domschke, A.; Lowe, C. R. *Biosens. Bioelectron.* **2005**, *20*, 1602. (b) Sartain, F. K.; Yang, X. P.; Lowe, C. R. *Anal. Chem.* **2006**, *78*, 5664. (c) Worsley, G. J.; Tourniaire, G. A.; Medlock, K. E.; Sartain, F. K.; Harmer, H. E.; Thatcher, M.; Horgan, A. M.; Pritchard, J. *Clin. Chem.* **2007**, *53*, 1820. (d) Yetisen, A. K.; Montelongo, Y.; da Cruz Vasconcellos, F.; Martinez-Hurtado, J. L.; Neupane, S.; Butt, H.; Qasim, M. M.; Blyth, J.; Burling, K.; Carmody, J. B.; Evans, M.; Wilkinson, T. D.; Kubota, L. T.; Monteiro, M. J.; Lowe, C. R. *Nano Lett.* **2014**, *14*, 3587.
(87) Hochstrasser, D. F.; Patchornik, A.; Merril, C. R. *Anal. Biochem.* **1988**, *173*, 412.
(88) Kabilan, S.; Marshall, A. J. Holographic sensor. WO Patent Application 2006027575 A1, March 16, 2006.
(89) (a) Lelièvre, S.; Couture, J. J. A. *Appl. Opt.* **1990**, *29*, 4384. (b) García, C.; Pascual, I.; Fimia, A. *Appl. Opt.* **1999**, *38*, 5548.
(90) Mayes, A. G.; Blyth, J.; Millington, R. B.; Lowe, C. R. *J. Mol. Recognit.* **1998**, *11*, 168.
(91) Todorov, T.; Nikolova, L.; Tomova, N. *Appl. Opt.* **1984**, *23*, 4309.
(92) Martinez-Hurtado, J. L.; Davidson, C. A.; Blyth, J.; Lowe, C. R. *Langmuir* **2010**, *26*, 15694.
(93) (a) Sackmann, E. K.; Fulton, A. L.; Beebe, D. J. *Nature* **2014**, *507*, 181. (b) Yetisen, A. K.; Jiang, L.; Cooper, J. R.; Qin, Y.; Palanivelu, R.; Zohar, Y. *J. Micromech. Microeng.* **2011**, *21*, 054018.
(94) Martinez-Hurtado, J. L.; Davidson, C. A. B.; Lowe, C. R. *Proc. SPIE*; Orlando, FL, 2011; p 80240Y.
(95) Lawrence, B. D.; Cronin-Golomb, M.; Georgakoudi, I.; Kaplan, D. L.; Omenetto, F. G. *Biomacromolecules* **2008**, *9*, 1214.
(96) Jin, H. J.; Park, J.; Karageorgiou, V.; Kim, U. J.; Valluzzi, R.; Cebe, P.; Kaplan, D. L. *Adv. Funct. Mater.* **2005**, *15*, 1241.
(97) Kabilan, S.; Blyth, J. Sensor. WO Patent Application 2006120426 A1, November 16, 2006.
(98) (a) Naydenova, I.; Jallapuram, R.; Howard, R.; Martin, S.; Toal, V. *Appl. Opt.* **2004**, *43*, 2900. (b) Martin, S.; Leclere, P.; Renotte, Y.; Toal, V.; Lion, Y. *Opt. Eng. (Bellingham)* **1992**, *33*, 3942.
(99) Tan, E. V.; Lowe, C. R. *Anal. Chem.* **2009**, *81*, 7579.
(100) Lowe, C. R.; Davidson, C. A.; Tan, E. V. Holographic sensor and its use in the detection of enzyme inhibition. WO Patent Application 2010041078 A1, April 15, 2010.
(101) Baker, T. T. *Photographic Emulsion Technique*; American Photographic Publishing Co.: Boston, MA, 1948; p 49.
(102) Zelikman, V. L.; Levi, S. M. *Making and Coating Photographic Emulsions*; Focal Press: Waltham, 1964; p 312.
(103) Blyth, J. *Appl. Opt.* **1991**, *30*, 1598.
(104) Lowe, C. R.; Davidson, C. A. B.; Blyth, J.; Kabilan, S.; Marshall, A. J.; Madrigal Gonzalez, B.; James, A. P. Holographic Sensor Based on a Volume Hologram in Porous Medium. WO Patent Application 2003087789 A1, October 23, 2003.
(105) Ben-Moshe, M.; Alexeev, V. L.; Asher, S. A. *Anal. Chem.* **2006**, *78*, 5149.
(106) Naydenova, I.; Toal, V. In *Ordered Porous Solids*; Valtchev, V., Mintova, S., Tsapatsis, M., Eds.; Elsevier: Amsterdam, 2009; p 559.
(107) Lowe, C. R.; Davidson, C. A. B.; Blyth, J.; Kabilan, S.; Marshall, A. J. Holographic or Diffraction Devices. WO Patent Application 2005122099 A2, December 22, 2005.
(108) McCusker, L. B.; Baerlocher, C. In *Introduction to Zeolite Science and Practice*; Čejka, J., van Bekkum, H., Corma, A., Schüth, F., Eds.; Elsevier: Amsterdam, 2007; Vol. *168*, p 13.
(109) Dyer, A. *An Introduction to Zeolite Molecular Sieves*; Wiley: New York, 1988; p 12.
(110) Bu, X.; Feng, P. In *The Chemistry of Nanostructured Materials*; Yang, P., Ed.; World Scientific: Singapore, 2003; p 1.
(111) Kallus, S.; Condre, J. M.; Hahn, A.; Golemme, G.; Algieri, C.; Dieudonne, P.; Timmins, P.; Ramsay, J. D. F. *J. Mater. Chem.* **2002**, *12*, 3343.
(112) (a) McCusker, L. B.; Baerlocher, C. In *Introduction to Zeolite Science and Practice*; van Bekkum, H., Flanigen, E. M., Jacobs, P. A., Jansen, J. C., Eds.; Elsevier: Amsterdam, 2001; Vol. *137*, p 37. (b) Gilson, J. P.; Marie, O.; Mintova, S.; Valtchev, V., III. *FEZA School on Zeolites: Fundamentals and Applications*; Valencia, 2011; p 245.

(113) (a) Babeva, T.; Todorov, R.; Gospodinov, B.; Malinowski, N.; El Fallah, J.; Mintova, S. *J. Mater. Chem.* **2012**, *22*, 18136. (b) Gospodinov, B.; Dikova, J.; Mintova, S.; Babeva, T. *J. Phys.: Conf. Ser.* **2012**, *398*.
(114) Javan, A.; Bennett, W. R., Jr.; Herriott, D. R. *Phys. Rev. Lett.* **1961**, *6*, 106.
(115) Bridges, W. B. *Appl. Phys. Lett.* **1964**, *4*, 128.
(116) Fowles, G.; Silfvast, W. *IEEE J. Quantum Electron.* **1965**, *1*, 131.
(117) Duarte, F. J. *Tunable Lasers Handbook*; Academic Press: San Diego, CA, 1996; p 33.
(118) (a) Svelto, O. *Principles of Lasers*; Springer: Heidelberg, 2010; p 397. (b) Hänsch, T. W. *Appl. Opt.* **1972**, *11*, 895.
(119) Geusic, J. E.; Marcos, H. M.; Van Uitert, L. G. *Appl. Phys. Lett.* **1964**, *4*, 182.
(120) Blyth, J.; Lowe, C. R.; Mayes, A. G.; Millington, R. B. Holographic sensors and their production. WO Patent Application 1999063408 A1, December 9, 1999.
(121) Bjelkhagen, H. I. New recording materials for holography. Conference of Holography, Art and Design (Holography and Three-Dimensional Displays), London, 1998; p 72330K.
(122) (a) Ackermann, G. K.; Eichler, J. *Holography: A Practical Approach*; Wiley: Darmstadt, 2007; p 29. (b) Yaroslavsky, L. In *The Art and Science of Holography: A Tribute to Emmett Leith and Yuri Denisyuk*; Caulfield, H. J., Ed.; The Society of Photo-Optical Instrumentation Engineers: Bellingham, 2004; p 45.
(123) Mehta, P. C.; Rampal, V. V. *Lasers and Holography*; World Scientific: Singapore, 1993; p 322.
(124) Gurney, R. W.; Mott, N. F. *Proc. R. Soc. A* **1938**, *164*, 151.
(125) (a) Mott, N. F.; Gurney, R. W. *Electronic Processes in Ionic Crystals*; Clarendon Press: Oxford, 1948; p 275. (b) Hamilton, J. F. *The Mechanism of Formation of the Latent Image in The Theory of the Photographic Process*, 4th ed.; Macmillan: New York, 1977; p 105.
(126) Jacobson, R. E.; Ray, S. F.; Attridge, G. G.; Axford, N. R. *The Manual of Photography: Photographic and Digital Imaging*, 9th ed.; Focal Press: Oxford, 2000; p 273.
(127) Jeong, T. H.; Aumiller, R. W.; Ro, R. J.; Blyth, J. Practical Holography XVI and Holographic Materials VIII, San Jose, CA, 2002; p 103.
(128) Salvaggio, N. *Basic Photographic Materials and Processes*, 3rd ed.; Focal Press: Boston, MA, 2008; p 403.
(129) Akagi, M.; Ishiba, T.; Kaneko, T. *Appl. Phys. Lett.* **1972**, *21*, 93.
(130) (a) Kaneko, K.; Sun, H. B.; Duan, X. M.; Kawata, S. *Appl. Phys. Lett.* **2003**, *83*, 1426. (b) Smirnova, T. N.; Kokhtych, L. M.; Kutsenko, A. S.; Sakhno, O. V.; Stumpe, J. *Nanotechnology* **2009**, *20*, 405301. (c) Rybaltovskii, A. O.; Gerasimova, V. I.; Minaev, N. V.; Sokolov, V. I.; Timashev, P. S.; Troitskaya, E. A.; Firsov, V. V.; Yusupov, V. I.; Bagratashvili, V. N. *Nanotechnol. Russ.* **2010**, *5*, 435. (d) Bagratashvili, V. N.; Rybaltovsky, A. O.; Minaev, N. V.; Timashev, P. S.; Firsov, V. V.; Yusupov, V. I. *Laser Phys. Lett.* **2010**, *7*, 401.
(131) Kapinus, E.; Meir, M. Photosensitive Material. WO Patent Application 2006040772 A1, April 20, 2006.
(132) (a) Dell'Aglio, M.; Gaudiuso, R.; ElRashedy, R.; De Pascale, O.; Palazzo, G.; De Giacomo, A. *Phys. Chem. Chem. Phys.* **2013**, *15*, 20868. (b) Wagener, P.; Ibrahimkutty, S.; Menzel, A.; Plech, A.; Barcikowski, S. *Phys. Chem. Chem. Phys.* **2013**, *15*, 3068. (c) Toftmann, B.; Doggett, B.; Rgensen, C. B. J.; Schou, J.; Lunney, J. G. *J. Appl. Phys.* **2013**, *113*, 083304. (d) Montelongo, Y.; Tenorio-Pearl, J. O.; Milne, W. I.; Wilkinson, T. D. *Nano Lett.* **2014**, *14*, 294.
(133) Chung, J.; Han, S.; Lee, D.; Ahn, S.; Grigoropoulos, C. P.; Moon, J.; Ko, S. H. *Opt. Eng.* **2013**, *52*, 024302.
(134) Davidson, C. A.; Blyth, J.; Lowe, C. R. Method of production of a holographic sensor. WO Patent Application 2010041079 A1, April 15, 2010.
(135) Smothers, W. K.; Monroe, B. M.; Weber, A. M.; Keys, D. E. *Practical Holography IV Proc. SPIE 1212*, 1990; p 20.
(136) Babeva, T.; Naydenova, I.; Mackey, D.; Martin, S.; Toal, V. *J. Opt. Soc. Am. B* **2010**, *27*, 197.
(137) (a) Tomita, Y.; Nishibiraki, H. *Appl. Phys. Lett.* **2003**, *83*, 410. (b) Sánchez, C.; Escuti, M. J.; van Heesch, C.; Bastiaansen, C. W. M.; Broer, D. J.; Loos, J.; Nussbaumer, R. *Adv. Funct. Mater.* **2005**, *15*, 1623.. (c) Smirnova, T. N.; Sakhno, O. V.; Bezrodnyj, V. I.; Stumpe, J. *Appl. Phys. B: Laser Opt.* **2005**, *80*, 947. (d) Naydenova, I.; Leite, E.; Babeva, T.; Pandey, N.; Baron, T.; Yovcheva, T.; Sainov, S.; Martin, S.; Mintova, S.; Toal, V. *J. Opt.* **2011**, *13*, 044019.
(138) Martin, S.; Naydenova, I.; Jallapuram, R.; Howard, R. G.; Toal, V. Holography 2005: International Conference on Holography, Optical Recording, and Processing of Information, 2006; p 625205.
(139) Sheridan, J. T.; Lawrence, J. R. *J. Opt. Soc. Am. A* **2000**, *17*, 1108.
(140) Sheridan, J. T.; Downey, M.; O'Neill, F. T. *J. Opt.* **2001**, *3*, 477.
(141) (a) Guo, J. X.; Gleeson, M. R.; Liu, S.; Sheridan, J. T. *J. Opt.* **2011**, *13*, 095601. (b) Fernandez, E.; Fuentes, R.; Ortuno, M.; Belendez, A.; Pascual, I. *Appl. Opt.* **2013**, *52*, 6322.
(142) (a) Naydenova, I.; Sherif, H.; Martin, S.; Jallapuram, R.; Toal, V. Holographic sensor. U.S. Patent 8,263,291 B2, September 11, 2012. (b) Naydenova, I.; Sherif, H.; Martin, S.; Jallapuram, R.; Toal, V. Holographic sensor. U.S. Patent 8,535,853 B2, September 17, 2013.
(143) Davidson, C. A. B.; Blyth, J.; Madrigal Gonzalez, B. Holographic Sensors and Their Production. WO Patent Application 2004081676 A1, September 23, 2004.
(144) Yetisen, A. K.; Qasim, M. M.; Nosheen, S.; Wilkinson, T. D.; Lowe, C. R. *J. Mater. Chem. C* **2014**, *2*, 3569.
(145) Poole, R. K.; Kalnenieks, U. *Introduction to Light Absorption: Visible and Ultraviolet Spectra*; Oxford University Press: Oxford, 2000; p 9.
(146) Creasey, C. D. Holographic sensors and their uses. WO Patent Application 2007010241 A2, January 25, 2007.
(147) Kraiskii, A. V.; Mironova, T. V.; Sultanov, T. T. *IEEE J. Quantum Electron.* **2010**, *40*, 652.
(148) Kraiskii, A. V.; Mironova, T. V.; Sultanov, T. T. *Quantum Electron.* **2012**, *42*, 1137.
(149) (a) Yetisen, A. K.; Martinez-Hurtado, J. L.; Garcia-Melendrez, A.; Vasconcellos, F. D.; Lowe, C. R. *Sens. Actuators, B* **2014**, *196*, 156. (b) Yetisen, A. K.; Martinez-Hurtado, J. L.; da Cruz Vasconcellos, F.; Simsekler, M. C.; Akram, M. S.; Lowe, C. R. *Lab Chip* **2014**, *14*, 833.
(150) Millington, R. B. Sensor with Holographic Multiplexed Image Display. WO Patent Application 2001050113 A1, July 12, 2001.
(151) Dobson, C. A. Design, Fabrication and Characterization of Holographic Optical Elements. Ph.D., The University of Cambridge, Cambridge, UK, 2007.
(152) (a) Blyth, J.; Lowe, C. R.; Davidson, C. A. B.; Kabilan, S.; Dobson, C. A. Holographic sensor. WO Patent Application 2005012884 A1, February 10, 2005. (b) Butt, H.; Knowles, K. M.; Montelongo, Y.; Amaratunga, G. A.; Wilkinson, T. D. *ACS Nano* **2014**, *8*, 2929. (c) Deng, S.; Yetisen, A. K.; Jiang, K.; Butt, H. *RSC Adv.* **2014**, *4*, 30050.
(153) Lowe, C. R.; Davidson, C. A. B.; Blyth, J.; Marshall, A. J.; James, A. P. Holographic sensors and their production. WO Patent Application 2004081546 A1, September 23, 2004.
(154) Marshall, A. J.; Kew, S. Use of holographic sensors. WO Patent Application 2007039717 A1, April 12, 2007.
(155) Marshall, A. J.; Creasey, C. D.; Kew, S.; Cane, M. R.; Clements, J. P. Sensor housing. WO Patent Application 2008119962 A2, October 9, 2008.
(156) Bell, L. L.; Seshia, A. A.; Davidson, C. A. B.; Lowe, C. R. *Procedia Eng.* **2010**, *5*, 1352.
(157) Lowe, C. R.; James, A. P.; Rayne, E.; Kabilan, S.; Marshall, A. J. Holographic sensor having heterogeneous properties. WO Patent Application 2006008524 A1, January 26, 2006.
(158) Kraiskii, A. V.; Postnikov, V. A.; Sultanov, T. T.; Khamidulin, A. V. *IEEE J. Quantum Electron.* **2010**, *40*, 178.
(159) Mayes, A. G.; Blyth, J.; Millington, R. B.; Lowe, C. R. *Anal. Chem.* **2002**, *74*, 3649.
(160) (a) Gonzalez, B. M.; Christie, G.; Davidson, C. A. B.; Blyth, J.; Lowe, C. R. *Anal. Chim. Acta* **2005**, *528*, 219. (b) Bhatta, D.; Christie, G.; Madrigal-Gonzalez, B.; Blyth, J.; Lowe, C. R. *Biosens. Bioelectron.* **2007**, *23*, 520.

(161) (a) Lowe, C. R.; Davidson, C. A. B.; Blyth, J.; Kabilan, S.; Marshall, A. J.; Madrigal Gonzalez, B.; James, A. P. Method of Detecting an Analyte in a Fluid. WO Patent Application 2003087899 A1, October 23, 2003. (b) Kabilan, S.; Blyth, J.; Lee, M. C.; Marshall, A. J.; Hussain, A.; Yang, X. P.; Lowe, C. R. *J. Mol. Recognit.* **2004**, *17*, 162. (c) Lee, M. C.; Kabilan, S.; Hussain, A.; Yang, X.; Blyth, J.; Lowe, C. R. *Anal. Chem.* **2004**, *76*, 5748. (d) Lowe, C. R.; Blyth, J.; Kabilan, S.; Hussain, A.; Yang, X. P.; Sartain, F. K.; Lee, M. C. Holographic Sensor. WO Patent Application 2004081624 A1, September 23, 2004. (e) Domschke, A.; Kabilan, S.; Anand, R.; Caines, M.; Fetter, D.; Griffith, P.; James, K.; Karangu, N.; Smith, D.; Vargas, M.; Zeng, J.; Hussain, A.; Xiaoping, Y.; Blyth, J.; Mueller, A.; Herbrechtsmeier, P.; Lowe, C. R. Sensors. *Proc. IEEE* **2004**; p 1320. (f) Lowe, C. R.; Kabilan, S.; Blyth, J.; Domschke, A.; Smith, D.; Karangu, N. Ophthalmic device comprising a holographic sensor. WO Patent Application 2005031442 A1, April 7, 2005. (g) Horgan, A. M.; Marshall, A. J.; Kew, S. J.; Dean, K. E. S.; Creasey, C. D.; Kabilan, S. *Biosens. Bioelectron.* **2006**, *21*, 1838. (h) Yang, X.; Lee, M. C.; Sartain, F.; Pan, X.; Lowe, C. R. *Chemistry* **2006**, *12*, 8491. (i) Kabilan, S.; Lee, M. C.; Horgan, A. M.; Medlock, K. E. S. Novel boronate complex and its use in a glucose sensor. WO Patent Application 2007054689 A1, May 18, 2007. (j) Domschke, A.; March, W. F.; Kabilan, S.; Lowe, C. *Diabetes Technol. Ther.* **2006**, *8*, 89. (k) Yang, X. P.; Pan, X. H.; Blyth, J.; Lowe, C. R. *Biosens. Bioelectron.* **2008**, *23*, 899. (l) Worsley, G. J.; Tourniaire, G. A.; Medlock, K. E.; Sartain, F. K.; Harmer, H. E.; Thatcher, M.; Horgan, A. M.; Pritchard, J. *J. Diabetes Sci. Technol.* **2008**, *2*, 213. (m) Burles, B.; Millington, R. B.; Lowe, C. R.; Kabilan, S.; Blyth, J. Ophthalmic device comprising a holographic sensor. US Patent 8,241,574 B2, August 14, 2012.

(162) Sartain, F. K.; Yang, X. P.; Lowe, C. R. *Chem.—Eur. J.* **2008**, *14*, 4060.

(163) Marshall, A. J.; Young, D. S.; Blyth, J.; Kabilan, S.; Lowe, C. R. *Anal. Chem.* **2004**, *76*, 1518.

(164) (a) Fuchs, Y.; Kunath, S.; Soppera, O.; Haupt, K.; Mayes, A. G. *Adv. Funct. Mater.* **2014**, *24*, 688. (b) Fuchs, Y.; Soppera, O.; Mayes, A. G.; Haupt, K. *Adv. Mater.* **2013**, *25*, 566.

(165) Lowe, C. R.; Marshall, A. J. Use of holographic sensor. WO Patent Application 2007023282 A1, March 1, 2007.

(166) Lowe, C. R.; Blyth, J.; James, A. P. Interrogation of a sensor. WO Patent Application 2006008531 A1, January 26, 2006.

(167) (a) Bhatta, D.; Christie, G.; Blyth, J.; Lowe, C. R. *Sens. Actuators, B* **2008**, *134*, 356. (b) Christie, G.; Lowe, C. R. Sensor for spores. WO Patent Application 2008087407 A1, July 24, 2008.

(168) Hurtado, J. L.; Lowe, C. R. *ACS Appl. Mater. Interfaces* **2014**, *6*, 8903.

(169) (a) Naydenova, I.; Jallapuram, R.; Toal, V.; Martin, S. *Appl. Phys. Lett.* **2008**, *92*, 031109. (b) Mikulchyk, T.; Martin, S.; Naydenova, I. *J. Opt.* **2013**, *15*, 105301.

(170) Marshall, A. J.; Young, D. S.; Kabilan, S.; Hussain, A.; Blyth, J.; Lowe, C. R. *Anal. Chim. Acta* **2004**, *527*, 13.

(171) Kabilan, S.; Marshall, A. J. Interrogation of a light-sensitive sensor. WO Patent Application 2007010244 A1, January 25, 2007.

(172) Kauffman, D. R.; Star, A. *Angew. Chem., Int. Ed.* **2008**, *47*, 6550.

(173) (a) Fielding, H. L.; Ingwall, R. T. *Photopolymerizable Compositions Used in Holograms*; Polaroid Corp.: 1986. (b) Naik, G. M.; Mathur, A.; Pappu, S. V. *Appl. Opt.* **1990**, *29*, 5292.

(174) Jallapuram, R. Optimisation of an acrylamide-based photopolymer for reflection holographic recording. Ph.D., Dublin Institute of Technology, Dublin, 2005.

(175) Jallapuram, R.; Martin, S.; Naydenova, I.; Sherif, H.; Toal, V. A holographic sensor. WO Patent Application 2007060648 A3, September 27, 2007.

(176) Leite, E.; Babeva, T.; Ng, E. P.; Toal, V.; Mintova, S.; Naydenova, I. *J. Phys. Chem. C* **2010**, *114*, 16767.

(177) Po, H. N.; Senozan, N. M. *J. Chem. Educ.* **2001**, *78*, 1499.

(178) Hancock, R. D.; Martell, A. E. *Chem. Rev.* **1989**, *89*, 1875.

(179) (a) Pedersen, C. J. *J. Am. Chem. Soc.* **1967**, *89*, 7017. (b) Pedersen, C. J. *J. Am. Chem. Soc.* **1967**, *89*, 2495.

(180) Gokel, G. W. *Crown Ethers and Cryptands*; Royal Society of Chemistry: Cambridge, 1994; p 197.

(181) Schwarzenbach, G. *Helv. Chim. Acta* **1952**, *35*, 2344.

(182) Cabbiness, D. K.; Margerum, D. W. *J. Am. Chem. Soc.* **1969**, *91*, 6540.

(183) Lundeen, M.; Hugus, Z. Z. *Thermochim. Acta* **1992**, *196*, 93.

(184) Ahrland, S.; Chatt, J.; Davies, N. R. *Q. Rev. Chem. Soc.* **1958**, *12*, 265.

(185) Irving, H.; Williams, R. J. P. *J. Chem. Soc. (Resumed)* **1953**, 3192.

(186) Eigen, M.; Wilkins Ralph, G. In *Mechanisms of Inorganic Reactions*; Kleinberg, J., Murmann, R. K., Fraser, R. T. M., Bauman, J., Eds.; American Chemical Society: Washington, DC, 1965; Vol. *49*, p 55.

(187) Kratz, A. *N. Engl. J. Med.* **2004**, *351*, 2461.

(188) Holtz, J. H.; Asher, S. A. *Nature* **1997**, *389*, 829.

(189) Saito, H.; Takeoka, Y.; Watanabe, M. *Chem. Commun. (Cambridge, U. K.)* **2003**, 2126.

(190) (a) Reese, C. E.; Asher, S. A. *Anal. Chem.* **2003**, *75*, 3915. (b) Reese, E.; Baltusavich, M. E.; Keim, J. P.; Asher, S. A. *Anal. Chem.* **2001**, *73*, 5038.

(191) Steed, J. W.; Atwood, J. L. *Supramolecular Chemistry*; John Wiley & Sons: Chichester, 2000; p 87.

(192) (a) Corey, R. B.; Pauling, L. *Rev. Sci. Instrum.* **1953**, *24*, 621. (b) Koltun, W. L. Space filling atomic units and connectors for molecular models. U.S. Patent 3170246 A, February 23, 1965.

(193) *Fisher-Hirschfelder-Taylor Metal-Coordination Atom Model Kit*; Fisher Scientific Co.: Pittsburgh, PA, 1970.

(194) Othman, A. M. *J. Anal. Chem.* **2010**, *65*, 1191.

(195) (a) Polonsky, K. S. *N. Engl. J. Med.* **2012**, *367*, 1332. (b) Inzucchi, S. E. *N. Engl. J. Med.* **2012**, *367*, 542.

(196) Report: Screening for Type 2 Diabetes; World Health Organization, 2003.

(197) "Diabetes Atlas", International Diabetes Federation, 2013.

(198) (a) Hisamitsu, I.; Kataoka, K.; Okano, T.; Sakurai, Y. *Pharm. Res.* **1997**, *14*, 289. (b) Springsteen, G.; Wang, B. H. *Tetrahedron* **2002**, *58*, 5291.

(199) Asher, S. A.; Alexeev, V. L.; Goponenko, A. V.; Sharma, A. C.; Lednev, I. K.; Wilcox, C. S.; Finegold, D. N. *J. Am. Chem. Soc.* **2003**, *125*, 3322.

(200) Dean, K. E. S.; Horgan, A. M.; Marshall, A. J.; Kabilan, S.; Pritchard, J. *Chem. Commun.* **2006**, 3507.

(201) Baca, J. T.; Finegold, D. N.; Asher, S. A. *Ocul. Surf.* **2007**, *5*, 280.

(202) (a) Pizer, R.; Babcock, L. *Inorg. Chem.* **1977**, *16*, 1677. (b) Friedman, S.; Pace, B.; Pizer, R. *J. Am. Chem. Soc.* **1974**, *96*, 5381. (c) Babcock, L.; Pizer, R. *Inorg. Chem.* **1980**, *19*, 56. (d) Pizer, R.; Selzer, R. *Inorg. Chem.* **1984**, *23*, 3023. (e) Ishihara, K.; Mouri, Y.; Funahashi, S.; Tanaka, M. *Inorg. Chem.* **1991**, *30*, 2356. (f) Pizer, R.; Tihal, C. *Inorg. Chem.* **1992**, *31*, 3243.

(203) Lowe, C. R.; Sartain, F. K.; Yang, X. Sensor molecules incorporating a boronic acid sensor group. WO Patent Application 2006079843 A1, August 3, 2006.

(204) Banks, P. A.; Freeman, M. L. *Am. J. Gastroenterol.* **2006**, *101*, 2379.

(205) Carvounis, C. P.; Nisar, S.; Guro-Razuman, S. *Kidney Int.* **2002**, *62*, 2223.

(206) Sussman, J.; Harel, M.; Frolow, F.; Oefner, C.; Goldman, A.; Toker, L.; Silman, I. *Science* **1991**, *253*, 872.

(207) (a) Chen, L. X.; Xu, S. F.; Li, J. H. *Chem. Soc. Rev.* **2011**, *40*, 2922. (b) Xu, S. F.; Lu, H. Z.; Zheng, X. W.; Chen, L. X. *J. Mater. Chem. C* **2013**, *1*, 4406.

(208) Lowe, C. R.; Davidson, C. A. B. Detection of microorganisms with holographic sensors. WO Patent Application 2004005537 A1, January 15, 2004.

(209) Horgan, A.; Marshall, A. J. Use of holographic sensor to determine sterilisation. WO Patent Application 2007010245 A1, January 25, 2007.

(210) (a) Kesselmeier, J.; Staudt, M. *J. Atmos. Chem.* **1999**, *33*, 23. (b) Brown, S. K.; Sim, M. R.; Abramson, M. J.; Gray, C. N. *Indoor Air* **1994**, *4*, 123.
(211) Kreuer, K. D.; Paddison, S. J.; Spohr, E.; Schuster, M. *Chem. Rev.* **2004**, *104*, 4637.
(212) Eaton, W. A.; Henry, E. R.; Hofrichter, J.; Mozzarelli, A. *Nat. Struct. Biol.* **1999**, *6*, 351.
(213) Nagao, S.; Osuka, H.; Yamada, T.; Uni, T.; Shomura, Y.; Imai, K.; Higuchi, Y.; Hirota, S. *Dalton Trans.* **2012**, *41*, 11378.
(214) Vaska, L.; DiLuzio, J. W. *J. Am. Chem. Soc.* **1961**, *83*, 2784.
(215) Rumsey, W. L.; Vanderkooi, J. M.; Wilson, D. F. *Science* **1988**, *241*, 1649.
(216) Leite, E.; Naydenova, I.; Mintova, S.; Leclercq, L.; Toal, V. *Appl. Opt.* **2010**, *49*, 3652.
(217) Kabilan, S.; Marshall, A. J.; Horgan, A.; Creasey, C. D.; Kew, S. J.; Dean, K. E. S.; Terrell, S. F.; Affleck, L. J. Technical Proceedings of the 2006 NSTI Nanotechnology Conference and Trade Show, 2006; p 467.
(218) Riddle, R.; Weiden, M. Interactive Holographic Security Element. WO Patent Application 2007042176 A1, April 19, 2007.
(219) Riddle, R.; Weiden, M. Multiple Security Means Comprising an Interactive Security Element. WO Patent Application 2007042177 A1, April 19, 2007.
(220) Cox, T.; Creasey, C. D. Method of making multicoloured holograms. WO Patent Application 2009027739 A1, March 5, 2009.
(221) Vasconcellos, F.d.C.; Yetisen, A. K.; Montelongo, Y.; Butt, H.; Grigore, A.; Davidson, C. A. B.; Blyth, J.; Monteiro, M. J.; Wilkinson, T. D.; Lowe, C. R. *ACS Photonics* **2014**, *1*, 489.
(222) Eisaman, M. D.; Fan, J.; Migdall, A.; Polyakov, S. V. *Rev. Sci. Instrum.* **2011**, *82*, 071101.
(223) Arsenault, A. C.; Clark, T. J.; Von Freymann, G.; Cademartiri, L.; Sapienza, R.; Bertolotti, J.; Vekris, E.; Wong, S.; Kitaev, V.; Manners, I.; Wang, R. Z.; John, S.; Wiersma, D.; Ozin, G. A. *Nat. Mater.* **2006**, *5*, 179.
(224) Zaidi, N. A.; Giblin, S. R.; Terry, I.; Monkman, A. P. *Polymer* **2004**, *45*, 5683.
(225) (a) Ge, J. P.; Hu, Y. X.; Yin, Y. D. *Angew. Chem., Int. Ed.* **2007**, *46*, 7428. (b) Xu, X. L.; Friedman, G.; Humfeld, K. D.; Majetich, S. A.; Asher, S. A. *Adv. Mater.* **2001**, *13*, 1681.
(226) Lenz, J.; Edelstein, A. S. *IEEE Sens. J.* **2006**, *6*, 631.
(227) Herrera-May, A. L.; Garcia-Ramirez, P. J.; Aguilera-Cortes, L. A.; Martinez-Castillo, J.; Sauceda-Carvajal, A.; Garcia-Gonzalez, L.; Figueras-Costa, E. *J. Micromech. Microeng.* **2009**, *19*, 015016.
(228) Chen, E. H.; Gaathon, O.; Trusheim, M. E.; Englund, D. *Nano Lett.* **2013**, *13*, 2073.
(229) (a) Naydenova, I. G.; Martin, S.; Toal, V. *J. Eur. Opt. Soc., Rapid Publ.* **2009**, *4*, 09042. (b) Farrelly, V.; Martin, S.; Naydenova, I.; Toal, V. A holographic method and product. EP Patent Application 2054779 A2, May 6, 2009. (c) Martin, S.; Naydenova, I.; Toal, V. Selective hologram formation. U.S. Patent 8,383,294 B2, February 26, 2013.
(230) Lakowicz, J. R. *Principles of Fluorescence Spectroscopy*, 3rd ed.; Springer: New York, 2007; p 1.
(231) Chaudhery, V.; George, S.; Lu, M.; Pokhriyal, A.; Cunningham, B. T. *Sensors* **2013**, *13*, 5561.
(232) Hobbs, D. S.; Cowan, J. J. Optical wavelength resonant device for chemical sensing. U.S. Patent 6,870,624 B2, March 22, 2005.
(233) (a) Schnars, U.; Jueptner, W. *Digital Holography: Digital Hologram Recording, Numerical Reconstruction, and Related Techniques*; Springer: Heidelberg, 2005; p 41. (b) Picart, P.; Li, J. *Digital Holography*; ISTE/John Wiley & Sons: London, 2013; p 165.
(234) (a) Yetisen, A. K.; Akram, M. S.; Lowe, C. R. *Lab Chip* **2013**, *13*, 2210. (b) Volpatti, L. R.; Yetisen, A. K. *Trends Biotechnol.* **2014**, *32*, 347. (c) Yetisen, A. K.; Volpatti, L. R. *Lab Chip* **2014**, *14*, 2217. (d) Akram, M. S.; Daly, R.; Vasconcellos, F. C.; Yetisen, A. K.; Hutchings, I.; Hall, E. A. H. In *Lab-on-a-Chip Devices and Micro-Total Analysis Systems*; Castillo-Leon, J., Svendsen, W. E., Eds.; Springer: New York, 2014.
(235) Chin, C. D.; Linder, V.; Sia, S. K. *Lab Chip* **2012**, *12*, 2118.